Measurement and Filtration of Virus Aerosols

A DISSERTATION
SUBMITTED TO THE FACULTY OF
UNIVERSITY OF MINNESOTA
BY

Zhili Zuo

IN PARTIAL FULFILLMENT OF THE REQUIREMENTS
FOR THE DEGREE OF
DOCTOR OF PHILOSOPHY

Dr. Thomas H. Kuehn, advisor
Dr. David Y.H. Pui, co-advisor

June 2014

Acknowledgements

I would like to express my sincere gratitude to my advisor Prof. Thomas Kuehn and my co-advisor Prof. David Pui for their continuous guidance and mentoring throughout my graduate study. It is them who initiated me into the study of aerosols and they have created numerous opportunities for me. Their instruction, advice, inspiration, encouragement, and patience have made the past six years the most memorable learning experience in my life.

I heartily thank my committee members: Prof. Peter Raynor, Prof. Chris Hogan, and Prof. McMurry for reviewing my dissertation and offering valuable comments and suggestions. I enjoyed each conversation with Prof. Chris Hogan, which was always full of energy, enthusiasm, and motivation.

I am also deeply grateful to the former NIOSH group members: Prof. Thomas Kuehn, Prof. Peter Raynor, Prof. Sagar Goyal, Sunil Kamar, Harsha Verma, Aschalew Bekele, Martha Abin, Yogesh Chander, Song Ge, Jessica Appert, and Seung Won Kim for the wonderful multidisciplinary experience they brought me. I still remember the distinct ways of thinking from people with different background during our biweekly NIOSH meeting. My special thanks go to the virologists on St. Paul campus, who introduced me to the world of microbiology and offered valuable advice and assistance in virus sample analysis. Special thanks also to Prof. Peter Raynor for permission to use lab equipment in

the Industrial Hygiene Laboratory, especially the aerosol test tunnel, on which almost all my research projects relied.

My sincere thanks also go to my current and former colleagues in the Particle Technology Laboratory: Leo Cao, Qingfeng Cao, Sheng-Chieh Chen, Chang Hyuk Kim, Seong Chan Kim, Kyoungtae Kim, Shigeru Kimoto, Lin Li, Tsz Yan Ling, Gus Lindquist, Zhun Liu, Bernard Olsen, Qisheng Ou, Chenxing Pei, Nickhil Ramash, Swathi Satish, Weon Gyu Shin, Nick Stanley, Jake Swanson, Drew Thompson, Jing Wang, and Kai Xiao as well as my Indian friends, Pulkit Agarwal, Saket Gupta, and Srijan Aggarwal. Their company, discussion, and assistance have been invaluable.

The financial support from the Center for Filtration Research (CFR) at the University of Minnesota is greatly appreciated. In particular, I would like to thank Stan Kaufman from TSI Inc. for his unreserved mentoring during the AMC project, Dan Japuntich, John Sebastian, and Caroline Ylitalo from 3M for their thoughtful discussion, and Mamoru Yanaguichi from Shigematsu Works Co. for his continued interest in my research. I also gratefully acknowledge the Department of Mechanical Engineering Fellowship in 2008, the American Filtration and Separation Society Fellowship in 2012, and the Doctoral Dissertation Fellowship from the graduate school in 2013-2014.

Finally, I am indebted to my parents for their constant love, trust, and support.

Abstract

The potential involvement of virus aerosols (i.e., airborne virus-carrying particles) in the transmission of human respiratory diseases has led to increased public concern. This dissertation focuses on 1) measurement of laboratory generated virus aerosols as a function of particle size, virus type, and composition of nebulizer suspensions (Chapter 2 and 3) and 2) performance evaluation of filtering facepiece respirators against virus aerosols (Chapter 4 and 5) with the long term goal to better understand and better control the airborne transmission of viral diseases.

Although laboratory generated virus aerosols have been widely studied in terms of infectivity and survivability, how they are related to particle size, especially in the submicron size range, is little understood. In the first study (Chapter 2), four viruses (MS2 bacteriophage, transmissible gastroenteritis virus, swine influenza virus, and avian influenza virus) were aerosolized, size classified (100–450 nm) using a differential mobility analyzer (DMA), and collected onto gelatin filters. Uranine dye was also nebulized with the virus, serving as a particle tracer. Virus infectivity assay and quantitative reverse transcription-polymerase chain reaction (qRT-PCR) were then used to quantify the amount of infectious virus and total virus present in the samples, respectively. The virus distribution was found to be better represented by the particle volume distribution rather than the particle number distribution. The capacity for a particle to carry virus increased with the particle size and the relationship could be described by a power law. Virus survivability was dependent on virus type and particle

size. Survivability of the three animal viruses at large particle size (300–450 nm) was significantly higher than at particle size close to the size of the virion (100–200 nm), which could be due to the shielding effect. The data suggest that particle size plays an important role in infectivity and survivability of airborne viruses and may, therefore, have an impact on the airborne transmission of viral illness and disease. The data do not support the use of MS2 bacteriophage as a general surrogate for animal and human viruses.

Laboratory studies of virus aerosols have been criticized for generating airborne viruses from artificial nebulizer suspensions (e.g., cell culture media), which do not mimic the natural release of viruses (e.g., from human saliva). Therefore, the objectives of the second study (Chapter 3) were to determine the effect of human saliva on the survival of airborne virus and to compare it with those of artificial saliva and cell culture medium (i.e., 3% tryptic soy broth). A stock of MS2 bacteriophage was diluted in one of the three nebulizer suspensions, aerosolized, size selected (100 to 450 nm) using a differential mobility analyzer, and collected onto gelatin filters. Uranine was used as a particle tracer. The resulting particle size distribution was measured using a scanning mobility particle sizer. The amounts of infectious virus, total virus, and fluorescence in the collected samples were determined by infectivity assays, qRT-PCR, and spectrofluorometry, respectively. For all the nebulizer suspensions tested, the virus content generally followed a particle volume distribution rather than a number distribution. The survival of airborne MS2 was independent of particle size but was strongly affected by the type of nebulizer

suspension. Human saliva was found to be much less protective than cell culture medium and artificial saliva. These results indicate the need for caution when extrapolating laboratory results, which often use artificial nebulizer suspensions. To better assess the risk of airborne transmission of viral diseases in real-life situations, the use of natural suspensions such as saliva or respiratory mucus is recommended.

In the third study (Chapter 4), particle number penetration (one form of physical penetration) and infectivity penetration of human adenovirus and swine influenza virus aerosols through respirators were measured to better characterize the effectiveness of filtering facepiece respirators against airborne viruses. Particle number penetration was found to range from 2% to 5%. However, aerosol loading and large sample-to-sample variation made it difficult to quantify the difference in particle number penetration caused by the different virus aerosols. Infectivity penetration of human adenovirus was much lower than particle number penetration, indicating that the latter provides a conservative estimate for respirator performance against airborne viruses.

In the fourth study (Chapter 5), infectivity, viral RNA, photometric, fluorescence (particle volume), and particle number penetration of MS2 bacteriophage through three different models of respirators were compared to better understand the correlation between infectivity and physical penetration. Although infectivity and viral RNA penetration were better represented by particle volume penetration than particle number penetration, they were several-fold lower than photometric penetration, which was

partially due to the difference in virus survival between upstream and downstream aerosol samples. Results suggest that the current NIOSH (photometer-based) certification method may be used to prescreen respirators for infection control applications.

These four studies comprise the main body of this dissertation and have been published or currently under review.

Chapter 2: Zuo Z, Kuehn TH, Verma H, Kumar S, Goyal SM, Appert J, Raynor PC, Ge S, Pui DYH. Association of airborne virus infectivity and survivability with its carrier particle size. *Aerosol Science and Technology*. 47:373-382, 2013.

Chapter 3: Zuo Z, Kuehn TH, Bekele AZ, Mor SK, Verma, H, Goyal SM, Raynor PC, Pui DYH. Survival of airborne MS2 bacteriophage generated from human saliva, artificial saliva, and cell culture medium. *Applied and Environmental Microbiology*. 80:2796-2803, 2014.

Chapter 4: Zuo Z, Kuehn TH, Pui DYH. Performance evaluation of filtering facepiece respirators using virus aerosols. *American Journal of Infection Control*. 41:80-82, 2013.

Chapter 5: Zuo Z, Kuehn TH, Pui DYH. Respirator testing using virus aerosol: comparison between infectivity penetration and physical penetration. Submitted to *Annals of Occupational Hygiene*, currently under review.

Table of Contents

List of Tables

List of Figures

Chapter 1: Introduction

1.1 Background

1.1.1 Definition of virus aerosols

Bioaerosols are aerosols of variable biological origin, including viruses, bacteria, and fungi, or components, residues, or products of organisms such as fungal spores, pollen, and fractions of insects (Cox and Wathes 1995). Comprehensive reviews on various aspects of bioaerosols, particularly bacteria aerosols, are available in the literature (Griffiths and DeCosemo 1994; Reponen et al. 2005; Srikanth et al. 2008; Xu et al. 2011).

As one category of bioaerosols, virus aerosols are assemblies of solid particles or liquid droplets suspended in a gaseous medium (e.g. air), that each carries 1) a single virion, 2) aggregates of virions, or 3) fragments of virions. In virology, a virion is defined as a complete virus particle consisting of an inner core of viral genome made from nucleic acid (either RNA or DNA) and an outer protein shell called a capsid. For some viruses (e.g. influenza virus), the viral capsid is further enclosed by a lipid membrane and these viruses are known as enveloped viruses (Flint et al. 2004). In the literature, virus particles as well as other terms including airborne viruses, viral particles, viral aerosols, virus aerosol particles, virus-laden particles, and virus containing particles, usually have the same meaning as virus aerosols defined above and are often used interchangeably.

1.1.2 Sources of virus aerosols

Although viruses can only replicate inside living host cells, they can be made airborne naturally and transmit through air without the presence of host cells. In the natural environment, viruses can be spread by the infected host cells to fluids and become airborne due to air movement and wave action on the surface of contaminated liquids, such as spray irrigation (Moore et al. 1979), waste water treatment (Carducci et al. 1995), toilet flushing (Barker and Jones, 2005), bubble eruption at sea surface microlayers (Aller et al. 2004), rain splashing, wind blowing, etc. Animals can also be sources of virus aerosols. For example, one of the most widely studied animal virus, foot-and-mouth disease virus, has been detected in the air contaminated by infected pigs (Alexandersen et al. 2002; Gloster and Alexandersen 2004; Gloster et al. 2007). Airborne viruses have also been shown to shed from other animals, e.g. bats with rabies virus (Winkler 1968), rabbits with rabbit pox virus (Thomas 1970), mice with polyoma virus (McGarrity and Dion 1978), and poultry flocks with Newcastle disease (Hietala et al. 2005).

However, the virus aerosol sources representing the most risk for human health are almost always other infected humans (Reponen et al. 2005; Verreault et al. 2008). Human expiratory activities such as coughing, sneezing, talking, and even tidal breathing can all generate droplets/particles (Morawska 2006; Chao et al. 2009; Johnson and Morawska 2009; Morawska et al. 2009; Johnson et al. 2011). Given the fact above, it is not difficult to imagine that viruses can be carried by these droplets and thus become airborne. In fact, Coxsackievirus A-21, influenza virus, human rhinovirus, parainfluenza virus, and human metapneumovirus have all been detected in particles generated by coughing, talking, and

tidal breathing from infected human subjects (Huynh et al. 2008; Fabian et al. 2008; Stelzer-Braid et al. 2009; Lindsey et al. 2010a). Although viruses are small with sizes ranging from 25 to 300 nm, they are often carried by other materials such as respiratory secretions of larger sizes (Reponen et al. 2005). For this reason, virus aerosol particles may cover a wide size range from ultrafine (<100 nm) to sub-micrometer (<1 μm) and micrometer (>1 μm).

The amount of virus present in human respiratory droplets is generally believed to be very low. For example, for all ten human subjects infected by rhinovirus, only one breathing sample and one coughing sample were positive for cell culture analysis, with an infectious virus titer of 2.0×10^2-2.0×10^3 and 2.0×10^2 $TCID_{50}$/mL, respectively (Stelzer-Braid et al. 2009). In another study (Lindsey et al. 2010a), infectious influenza virus was found in cough aerosols from only two of 21 influenza-infected subjects. For this reason, samples of human expiratory aerosols are often analyzed by quantitative PCR (see Section 1.1.4) for the amount of viral nucleic acids present. Fabian et al. (2008) estimated that breathing generated <3.2 to 20 influenza virus RNA per minute. Lindsley et al. (2010a) reported that an average of 15.8±29.3 influenza virus RNA was produced per cough. In addition, not all infected subjects can shed detectable virus aerosols. For example, Stelzer-Braid et al. (2009) reported that among the 25 subjects with PCR-positive nasal mucus, 12 subjects had positive samples from breathing, nine subjects had positive samples from talking, and only two had positive samples from coughing. In another study, influenza viral RNA were detected in coughs from 38 of 47 (81%) human subjects who were positive for influenza (Lindsley et al. 2010b). In other cases, no virus

could be detected in exhaled breath samples from 16 people infected with human rhinovirus (Fabian et al. 2011). Moreover, similar to what was found for human expiratory droplets, there was a wide variation in the amount of virus detected among infected subjects. Lindsley et al. (2010a) found that 45% of the influenza viral RNA from coughed aerosols came from just four of the 38 subjects with influenza, suggesting that some patients may serve as "superspreaders" and have a higher chance to spread the disease via the airborne route.

1.1.3 Disease transmission by virus aerosols

Virus aerosols are raising more and more heath concerns due to their potential involvement in transmission of diseases, particularly respiratory viral diseases. Three possible modes of transmission for respiratory viral diseases have been proposed, including contact, large droplets, and aerosols (Brankston et al. 2007 and references therein). Transmission by contact occurs when the transfer of virus results from direct contact with infected individuals or indirect contact with contaminated intermediate objects (fomites). Transmission can also occur by large droplets ($\geq$ 5 μm) generated from infected human respiratory tract by sneezing, coughing, talking, etc. This mode of transmission is considered to be within a distance of <1 m since large droplets settle quickly. Transmission by aerosols, also known as airborne transmission, occurs due to the spread of virus aerosols. Viruses can be carried by droplet nuclei (< 5 μm), can be suspended in air for a long time, can be inhaled by susceptible hosts, and finally may cause infection.

Unfortunately, the relative contribution of different transmission modes remains unclear and is currently under hot debate. For example, for influenza virus, after reviewing the almost identical literature, Brankston et al. (2007) have supported large-droplets as the dominant mode of transmission while others (Tellier 2006; Weber and Stilianakis 2008; Tellier 2009) have argued in favor of transmission by aerosols. Nevertheless, epidemiologic studies, field measurements, and computer simulations all indicate that the aerosol route could be an important mode of transmission for viral diseases.

Epidemiologic evidence for disease transmission by virus aerosols has been reported over the years. As nicely reviewed by Sattar et al. (1987), a wide range of naturally occurring viral infections could be spread via the air, including small pox, measles, chicken pox, rabies, rotavirus, foot-and-mouth disease virus, Newcastle disease virus, etc. The same mode of transmission has also been proposed for porcine reproductive and respiratory syndrome virus (Otake et al. 2002) and Norwalk-like virus (Marks et al. 2003).

Recently, several field measurements have been performed to sample ambient air in hospitals, day-care centers, and on airplanes (Blachere et al. 2009; Lindsey et al. 2010b; Yang et al. 2011). Due to the low concentration of infectious virus in the ambient, the collected samples were all analyzed by quantitative PCR (see Section 1.1.4). Therefore, the results were expressed as the amount of viral nucleic acids rather than infectious virus. The reported fraction of virus content associated with particle size varied considerably. For example, Yang et al. (2011) found that 36% of the detected influenza A virus fell in the size range of < 1 μm while only 4% was found by Blachere et al. (2009) for the same

size range. It is possible that human generated virus aerosol particles coagulate with ambient particles over time and thus change their size distribution. In addition, even if quantitative PCR with high sensitivity was used, not all the collected samples yielded positive results. For instance, Lindsley et al. (2010a) found that less than 20% of 21 personal samplers and 46 stationary samplers were positive for influenza A virus. In another study, only half of the 16 samples were positive (Yang et al. 2011). These findings suggest that virus aerosols may not be uniformly distributed in the ambient. Interestingly, a larger fraction of respiratory syncytial virus was found in the first stage of the NIOSH sampler compared with influenza A virus, indicating that respiratory syncytial virus aerosol particles are generally larger than those containing influenza virus (Lindsley 2010b).

In addition to epidemiologic studies and field measurements, disease transmission by virus aerosols is also suggested by many computer-based simulation models. For example, by using a virus production model and airborne spread prediction models combined with the knowledge of aerobiology of foot-and-mouth disease (FMD) virus and meteorological data, in a worst case scenario, the plume generated by infected pigs could infect cattle as far away as 20-300 km and sheep up to 10-100 km (Donaldson and Alexandersen 2002). In another study, the findings of atmospheric dispersion models assisted by the original records strongly confirmed that airborne virus was the most likely cause of FMD development out to 60 km from the source (Gloster et al. 2005). Similarly, the accurate prediction of the spread of a virus-laden aerosol plume and air flow patterns by using computational fluid dynamics and multi-zone models revealed that the large community

outbreak of severe acute respiratory syndrome (SARS) in a hospital had a common source and was best explained by airborne transmission (Yu et al. 2004).

1.1.4 Sampling and analysis of virus aerosols

Measurement of virus aerosols generally requires two steps: 1) virus particles are first removed from the air and 2) the collected virus aerosol sample is then analyzed. Common sampling devices used for inert aerosols of non-biological origins including cyclones, impactors, liquid impingers, and filters have also been used for sampling virus aerosols based on the same sampling principles, which has been nicely reviewed by Verreault et al. (2008). However, due to the biological nature of virus aerosols, a good virus aerosol sampler should have not only high physical collection efficiency (i.e. to collect particles efficiently), but also high biological collection efficiency (i.e. to maintain the infectivity and the integrity of the collected virus aerosol particles). The high sampling flow rate of cyclones and impactors is beneficial in situations where virus aerosol concentration is low, but the strong mechanical stress during sampling may cause structural damage to the collected viruses and thus decrease their infectivity (Bourgueil et al. 1992; Tseng and Li 2005a). Liquid impingers, the most popular sampler for virus aerosol studies, are believed to have relatively high biological collection efficiency, but they have poor physical collection efficiency for particles smaller than 300 nm (Hogan et al. 2005). In addition, the performance of a liquid impinger is also a strong function of the type of collection liquid (Agranovski et al. 2004; Yu et al. 2009), sampling time (Grinshpun et al. 1997), and reaerosolization (Riemenschneider et al. 2010). Although filters have high physical collection efficiency, they are not recommended for collecting virus aerosols,

because 1) the desiccation during sampling significantly affects virus infectivity and 2) it is difficult to dislodge the collected virus aerosol particles from the filter media, making it difficult to quantify the amount of virus sampled (Zuo et al. 2013a). In short, traditional aerosol samplers have limited performance when sampling virus aerosols.

Collected virus aerosol samples are often eluted from samplers or transferred into a liquid for analysis. Although a variety of methods are available for virus detection and quantification, as described elsewhere (Flint et al. 2004), infectivity assay and polymerase chain reaction (PCR) are still the two methods most widely used in virus aerosol studies.

Infectivity assay is a standard microbiological method to determine the concentration of infectious virus in a sample. Typical examples include plaque assay and endpoint dilution assay, both requiring a serial dilution of the virus sample to be analyzed. In a plaque assay, freshly-grown host cells are mixed with virus at varying dilutions, covered with a semi-solid nutrient medium such as agar, and incubated for a certain period. After incubation, each infectious virus produces a circular zone of damaged cells (known as plaque forming unit, or PFU) and results are expressed as PFU per unit volume of the virus sample. In an endpoint dilution assay, virus at different dilutions is added to a confluent monolayer of cultured cells followed by incubation. After incubation, cells are checked under a microscope for cytopathic effect, a sign of viral infection, and results are mathematically calculated in the unit of median tissue culture infective dose ($TCID_{50}$) per unit volume of the virus sample, which means the highest number of times that the

original virus sample can be diluted to still have a 50% chance to infect the inoculated cells.

Polymerase chain reaction (PCR) amplifies short DNA sequences (known as templates) within a long double-stranded DNA (dsDNA). It can also amplify RNA, when preceded by a reverse transcription incubation at 42-55 ^{o}C (Mackay et al. 2002). A basic PCR set up requires several components, including 1) a DNA or RNA template, 2) a pair of forward and reverse primers (synthetic oligonucleotides) with the pair spanning a region to be amplified, 3) a DNA polymerase, 4) deoxynucleotides, and 5) a buffer solution providing a suitable environment for PCR. The PCR process can be summarized in three steps: denaturation, annealing, and elongation (Mackay et al. 2002). In step one (denaturation), the dsDNA containing the target template is heated at temperatures > 90 ^{o}C, where the dsDNA is separated into two single strands. In step two (annealing), temperature is reduced to 50-60 ^{o}C so that each primer hybridses to one strand. In step three (elongation), temperature is raised to 72-78 ^{o}C, where the hybridised primers are extended by the DNA polymerase to synthesize a new complementary DNA strand with continued supply of deoxynucleotides. Theoretically, the amount of DNA template in a sample doubles after each thermal cycle and the template can be exponentially amplified with repeated cycles. The amplified template (amplicon) can then be stained with ethidium bromide, analyzed using agarose gel electrophoresis, and visualized under ultraviolet light.

Traditional PCR analysis can only provide qualitative (yes/no) or at most semi-quantitative results while true quantification of target nucleic acids can be achieved using real-time quantitative PCR (Mackay 2004). By labeling primers, probes, or amplicon with fluorogenic molecules, the accumulation of amplicon as PCR progresses can be visualized as fluorescence signals and thus monitored in real time (Mackay et al. 2002). For quantification of a template in a sample, threshold cycle (Ct) values are usually collected from PCR cycles that occur within the log-linear amplification portion of the reaction (where the fluorescence accumulates proportional to the amount of amplicon) and are compared with a standard curve made from serial dilution of the template in a similar matrix of known concentration (Mackay et al. 2002; Mackay 2004).

In short, quantitative PCR can detect and quantify viruses at very low concentrations. Therefore, it is mostly used in studies where low concentration or poor survival of airborne viruses is expected, e.g., human subject studies (see Section 1.1.2) and field measurements (see Section 1.1.3). However, because PCR amplifies viral nucleic acids, results only represent the amount of total virus (i.e. both infectious and non-infectious virus) present in a sample. In other words, the lack of information regarding virus infectivity is a big disadvantage of PCR. This piece of information can only be obtained by performing the abovementioned infectivity assays, though they could be time-consuming with limited detection sensitivity.

1.1.5 Laboratory studies of virus aerosols

Airborne viruses have been artificially generated and widely studied in laboratories (Sattar et al. 1987). Because the probability of airborne transmission of viral diseases highly depends on how well virus survive (i.e. maintain infectivity) in air, infectivity and survivability of virus aerosols are often the main focus of such studies. A common approach involves generating virus aerosols from a liquid virus suspension (usually by a spray gun or a Collison type nebulizer), keeping the generated virus in a container (e.g. a rotating drum or chamber), taking virus aerosol samples periodically (usually by a liquid impinger), and analyzing the samples (almost always by infectivity assay).

For most laboratory generated airborne viruses, a rapid decrease in infectivity was noticed immediately after it is aerosolized followed by a slower logarithmic decay with time (Songer 1967; Warren and Hatch 1969; Ijaz et al. 1987). In aerobiology, such a reduction of infectivity at the beginning is generally referred to as "initial loss", which can be considerable, often ranging from 10 to 100 fold (Ijaz et al. 1987; Sattar et al. 1987).

Several major factors affecting survivability of airborne viruses have been identified (Sattar et al. 1987; Sobsey and Meschke 2003), including 1) the type of virus, 2) relative humidity (RH), 3) air temperature, 4) composition of the nebulizer suspension from which the virus is aerosolized, 5) air pollutants, and 6) irradiation. Table 1.1 summarizes the findings reported in the literature for the survival of four airborne viruses (adenovirus, coronavirus, influenza virus, and MS2 bacteriophage) that were used in this research. Other factors such as the host cells used for virus propagation (Schaffer et al. 1976) and

the fluids in liquid impingers used for virus aerosol collection (Warren and Hatch 1969) may also play a role. The effects of air pollutants (e.g. ozone) and irradiation (e.g. ultraviolet germicidal irradiation) are topics of airborne virus decontamination and will not be discussed here.

Table 1.1 Survival of airborne adenovirus, coronavirus, influenza virus, and MS2 bacteriophage reported in the literature.

Virus (strain/serotype)	Virus suspension media	RH (%)	T (^{o}C)	Effect on survival and remarks	Reference
Adenovirus (1, 3, and SV17)	Applied as 1 μL droplets (modified Hank's saline) followed by air drying	20, 84	~20	Better survival at higher RH	Buckland and Tyrrell (1962)
Adenovirus (4 and 7)	Undiluted virus with cell culture fluids	20, 50, 80	~23.9	Survival at 80% RH was significantly lower than 20 and 50% RH.	Miller and Artenstein (1967)
Adenovirus (12)	Undiluted virus + 1% antifoam	32, 51, 89	28-29.5	Survival increased with RH. The effect of RH on survival seemed to be rapid.	Davis et al. (1971)
Bovine adenovirus (3)	Eagle's medium or bovine nasal secretion	30, 90	6, 32	Survival increased with RH; low temperature and Eagle's medium enhanced survivability.	Elazhary and Derbyshire (1979a)
Adenovirus (encoded with green fluorescent protein)	Minimum essential medium (MEM)	32-99	21-34	Temperature > 29 ^{o}C completely blocked virus infectivity.	Li et al. (2008)
Human coronavirus (229E)	?	30, 50, 80	6, 20	Survival at 20 C: 50% > 30% > 80% RH. Survival at 6 C, 50% > 80% > 20% RH. Low T enhanced survival.	Ijaz et al. (1985)
TGEV (Purdue strain)	MEM	30, 50, 70, 90	~23	Survival decreased with increased RH	Kim et al. (2007)
Coronavirus (SARS)	Applied as 10 μL droplets (MEM + 1% FCS) followed by air drying	40-50, 80-85, >95	22-25, 33, 38	Survival decreased with increased RH and T; at 40-50% RH and 22-25 ^{o}C, dried virus showed similar inactivation rate to virus suspension without drying	Chan et al. (2011)
TGEV (?)	Applied as 10 μL droplets (cell culture medium) followed by air drying	20, 50, 80	4, 20, 40	At 4 ^{o}C, survival decreased with increased RH; survival at 20 and 40 ^{o}C, 20% > 80% > 50% RH. Low T enhanced survival.	Casanova et al. (2010)

Influenza A virus (PR8)	10% horse serum and broth	23, 48, 89	27-29	Survival decreased with increased RH.	Loosli (1943)
Influenza A virus (PR8)	Horse serum and heart infusion broth	23-80	22-24	High survival at 23-40% and 70-80% RH, low survival at 45-65% RH. Sharp transition at 40-45% RH; Increased NaCl concentration may be harmful.	Lester (1948)
Influenza A virus (WS)	Allantoic fluid and 0.1 M Sorensen's phosphate buffer	30-70	?	High survival at 32 and 68% RH and lowest survival at 60% RH.	Shechmeister (1950)
Influenza A virus (PR8)	One part allantoic fluid and one part 2% Difco peptone	15-90	Indoor T	Survival was high at 15-40% and low at 50-90% RH. The transition was rather sharp.	Hemmes et al. (1960)
Influenza A virus (PR8)	Allantoic fluid and casein McIlvaine's buffer	20, 35, 50-80	7-8, 20.5-24, and 32	Better survival at lowest RH and T; infectivity decay rate suddenly decreased when RH above 35%; similar decay rate at RH 50-80%	Harper (1961); Harper (1963)
Influenza A virus (WS and swine)	Applied as 1 µL droplets (modified Hank's saline) followed by air drying	20, 84	~20	Higher survivability at lower RH	Buckland and Tyrrell (1962)
Influenza A virus (PR8)	Allantoic fluid and 0.2% gelatin	20, 50, 80	~23	High survival at low RH; Egg inoculation and test mice exposure showed similar results.	Hood (1963)
Influenza A virus (WSN)	Cell culture fluid or clarified allantoic fluid	20-80	21	Survival highest at low RH, lowest at mid-range RH, and moderate at high RH; polyhydroxl compounds generally enhanced survivability.	Shaffer et al. (1976)
MS2 bacteriophage	Salt solution or trypton broth	20, 50, 80	21	Salt solution: highest survival at 20% RH, followed by 80% and 50% RH; trypton broth: equal survival at all RH; trypton greatly enhanced survival.	Dubovi and Akers (1970)
MS2 bacteriophage	0.1 M NaCl or NaCl with 0.01-0.1% peptone	20-90	20	0.1 M NaCl: highest survival at low RH, followed by high and mid RH; Peptone greatly enhanced survival	Trouwborst and De Jong (1973)

MS2 bacteriophage	DI water, 0.25% trypton, or artificial saliva	25, 45, 85	?	For all three suspension media, survival highest at 25% RH, no difference between 45% and 85% RH	Lee (2009)
MS2 bacteriophage	DI water, 3% TSB, or 3% TSB with 7.6% glycerol	35, 50	19-26	Better survival at 50% RH for water and TSB with 7.6% glycerol; the opposite for TSB	Appert et al. (2011)
MS2 bacteriophage	DI water, 0.3% beef extract (BE), or artificial saliva (AS)	30, 60, 90	?	For DI water, survival 30% > 90% > 60% RH; for BE, lowest survival at 30% RH, no difference between 60% and 90% RH; for AS, no difference between the three RH	Woo (2012)

A unique airborne survival pattern exists for each virus species or even the same virus but different stains (Donaldson 1972), though generally enveloped viruses are more sensitive to physical and chemical changes than non-enveloped viruses (Tseng and Li 2005b).

As a general rule, enveloped viruses survive better at low RH while non-enveloped viruses prefer high RH (Sattar et al. 1987). Typical examples include influenza virus, parainfluenza virus, coronavirus, vaccinia virus for enveloped viruses and adenovirus, foot-and-mouth disease virus, rhinovirus, poliovirus, and T3 bacteriophage for non-enveloped viruses (Harper 1961; Miller and Artenstein 1967; Warren and Hatch 1969; Davis et al. 1971; Donaldson 1972; Schaffer et al. 1976; Ijaz et al. 1985; Karim et al. 1985; Kim et al. 2007). However, many viruses have been reported not to follow this general rule. Mayhew et al. (1968) found that the biological decay rates of yellow fever virus were not significantly affected by the three RH tested. Sometimes the dependence of virus survival on RH is more complex. For example, Newcastle disease virus, Langat virus, influenza A virus, reovirus were found to be relatively stable at low/high RH and minimally stable at mid-range RH (Songer 1967; Benbough 1971; Schaffer et al. 1976; Adams et al. 1982) while mid-range RH was reported to be more favorable to rotavirus compared to the other two RH levels (Sattar et al. 1984).

Generally, airborne virus survival is inversely proportional to air temperature (Sattar et al. 1987; Tang 2009). For instance, Harper (1961) found virus survival was better at low temperature (7-11 ^{o}C) than high temperature (21-23 ^{o}C and ~30 ^{o}C) for all four viruses tested. However, exceptions were also reported. For example, temperature was found to

have no significant effect on the survival of airborne yellow fever virus and Venezuelan equine encephalitis virus (Mayhew et al. 1968; Ehrlich and Miller 1971).

The effect of composition of nebulizer suspension on the survival of airborne viruses is well recognized. Certain additives to the nebulizer suspension have been shown to provide protection to airborne viruses, overcome the harmful effect of RH and/or the toxic effect of solutes in the nebulizer suspension, and thus significantly improve their survival. These protective agents are generally believed to be proteinaceous in nature (Sattar et al. 1987). Bovine serum albumin, proteins containing cell culture fluid, tryptic soy broth, phenylalanine, and peptone have all been shown to increase the airborne survival of Langat virus, influenza virus, foot-and-mouth disease virus, and MS2 bacteriophage, respectively (Benbough 1971; Barlow and Donaldson 1973; Trouwborst and De Jong 1973; Trouwborst et al. 1974; Schaffer et al. 1976; Appert et al. 2012). Additional protection was also offered by non-protein chemicals including 1) polyhydroxy compounds such as glycerol, inositol, sucrose, and glucose, 2) surface active agents, and 3) salts (Benbough 1971; Trouwborst and De Jong 1973; Trouwborst et al. 1974; Schaffer et al. 1976). However, there are no universal protective agents that work for all airborne viruses. Instead, certain solutes may have totally different effects on survival, depending on the type of virus. For example, monovalent chlorides lead to inactivation of arbovirus but the opposite for poliovirus, T1 and MS2 bacteriophages (Benbough 1971; Trouwborst and De Jong 1973). Amino acid and glucose in minimum essential medium was considered to increase the stability of bovine adenovirus type 3 (Elazhary and Derbyshire 1979a) but showed minimal protection for human adenovirus

type 1 (Appert et al. 2012). In addition, inositol was found to stabilize influenza virus at 50% RH and enhanced virus inactivation at high RH, but had little effect at low RH (Schaffer et al 1976), suggesting that RH may also affect the performance of protective agents.

Any loss of infectivity of an airborne virus must eventually result from the damage of its protein coat, nucleic acid, or both (Sattar et al. 1987). Phosphor-lipid-protein complexes usually denature most readily at mid to high RH while proteins denature most readily at low RH (Cox and Wathes 1995). However, the exact inactivation mechanisms remain unclear. It seems that the surface characteristic of virus (either envelope or capsid), the environmental conditions (RH and temperature), and the chemical compositions of virus aerosol particles have a complex and combined effect on the survival of airborne viruses. Dehydration may be the most fundamental stress to airborne viruses (Cox 1989), especially considering the water retention capability of polyhydroxyl compounds. It is hypothesized that the presence of organic matter in the virus growth medium decreases the vapor pressure of droplets, and thus reduces evaporation and provides better protection (Marthi et al. 1990). Cox (1989) also proposed that the cross-linking reactions happening on the surface proteins of viruses may partially explain the effect of RH. Work by Trouwborst et al. (1974) suggested a surface inactivation mechanism since virus at air-water interfaces (AWI) is subjected to unbalanced forces and therefore virus inaction can be reduced by having a dense monolayer of surface active agent at the AWI. Inactivation of virus by crystallization of solutes may be another mechanism. As water evaporates, the

dissolved chemicals in a droplet become supersaturated and start to crystallize under certain RH, which may be toxic to virus (Trouwborst and De Jong 1973).

1.1.6 Filtration of virus aerosols by respirators

One of the most straightforward ways to help reduce airborne transmission of viral diseases is filtration (e.g. by wearing respirators). In fact, the Centers for Disease Control and Prevention (CDC) have recommended the use of National Institute of Occupational Safety and Health (NIOSH)-approved N95 filtering facepiece respirators in healthcare occupational settings to reduce exposure to airborne influenza virus (CDC, 2009). Filtering facepiece respirators are commonly made of electret filter media. Due to the embedded electrostatic charges, the electret filter media can provide similar filtration efficiency to purely mechanical filters, but with a lower pressure drop and therefore less breathing resistance (Barrett and Rousseau 1998). Filtering facepiece respirators are currently certified according to a NIOSH standard under title 42 of Code of Federal Regulations (CFR) part 84 (DHHS, 1995), which uses NaCl (solid particles) or dioctylphthalate (DOP, oil droplets) aerosol to challenge a respirator and determine its filtration efficiency by measuring upstream and downstream aerosol concentration using a laser photometer. Respirators are certified for 95, 99, or 99.97% efficiency for removing the challenge aerosol and labeled as 95, 99, or 100 class efficiency. Certified respirators are further categorized as N (not resistant to oil), R (somewhat resistant to oil), or P (permanently, or strongly resistant to oil). For example, an N95 respirator means that it can remove at least 95% of the challenge NaCl aerosol.

However, since the current NIOSH standard for respirator certification uses inert particles (e.g. NaCl) as a challenge aerosol, this certification method does not tell how well a NIOSH-certified respirator may perform against airborne viruses. Therefore, it is of particular interest to evaluate respirator performance using virus aerosols.

Several studies have investigated the efficiency of respirators against virus aerosols (Table 1.2). A general approach for respirator testing using virus aerosols described in the literature includes the following steps: 1) generating virus aerosols (almost always by Collison nebulizers), 2) challenging a respirator using the generated virus aerosols at certain face velocity, and 3) sampling and analyzing virus aerosols upstream and downstream of the respirator.

Respirator filtration performance against airborne viruses is commonly quantified by two parameters (Eninger et al. 2008a). One is physical penetration, which is defined as the percentage of challenge particles that penetrates through the respirator, without considering infectivity. Examples of physical penetration include particle number penetration, particle surface area penetration, particle volume penetration, etc., which are relatively easy to measure using real-time aerosol instruments (Li et al. 2012). Previous studies have found that particle number penetration (one form of physical penetration) of virus aerosols is similar or slightly lower than that of NaCl aerosol (Balazy et al. 2005; Eninger et al. 2008b; Lore et al. 2012). This slight difference in penetration was believed to be caused by the higher dielectric constant of virus than NaCl, which increases particle collection efficiency by electrostatic deposition in electret filter media (Eninger et al.

2008a). This finding suggests that inert aerosols such as NaCl may be generally appropriate to conservatively predict penetration of virus aerosol particles of similar sizes (Eninger et al. 2008a). The other parameter is infectivity penetration, which is defined as the percentage of infectious virus that penetrates through the respirator. Although infectivity penetration is time-consuming to measure, it certainly better represents respirator performance against infectious virus aerosols than physical penetration. Physical penetration (particle number penetration), defined differently in different studies, is found to be generally higher than infectivity penetration, suggesting the former can be used as a conservative estimate for respirator performance against airborne viruses (Zuo et al. 2013b).

Table 1.2 Infectivity and physical penetration of different challenge virus aerosols through respirators.

Virus aerosol	Method to determine infectivity penetration, P_{inf}	Method to determine physical penetration, P_{phy}	Comparison	Reference
MS2	Gelatin filter, 25 mm diameter	SMPS*, 22-29 nm virus aerosol particles	$P_{inf} \approx P_{phy}$	Eninger et al. 2008a
MS2	Liquid impinger, AGI-30	SMPS, 25-407 nm virus aerosol particles	$P_{inf} < P_{phy}$	Lore et al. 2012
Human adenovirus	Liquid impinger, AGI-30	SMPS, 70-90 nm virus aerosol particles	$P_{inf} < P_{phy}$	Zuo et al. 2013b
Influenza A virus	Liquid impinger, AGI-30	APS**, 0.8 μm PSL particles	$P_{inf} < P_{phy}$	Harnish et al. 2013
Influenza A virus	Liquid impinger, midget	PortaCount, 0.02-1 μm virus aerosol particles	$P_{inf} < P_{phy}$	Booth et al. 2013
MS2	Gelatin filter, 47 mm diameter	CPC***, monodisperse 50 nm NaCl particles	$P_{inf} < P_{phy}$	Gardner et al. 2013

*SMPS: scanning mobility particle sizer
**APS: aerodynamic particle sizer
***CPC: condensation particle counter

1.2 Motivation and objectives

The outbreak of coronavirus-caused severe acute respiratory syndromes (SARS) in 2004, highly pathogenic avian influenza A (H5N1) in 2004-2006, and pandemic H1N1 novel flu in 2009 have all raised public concerns for the health effects of virus aerosols. Ideally, human subject studies (see Section 1.1.2) and field measurements (see Section 1.1.3) are preferred for investigating disease transmission by virus aerosols. However, as discussed earlier, due to extremely low concentration of infectious virus aerosol particles in the natural environment, large intersubject variation, non-uniform dispersion of virus aerosols, uncontrolled ambient conditions, and potential interference of PCR with ambient contaminants (Alcarez et al. 1995), a large number of human subjects or air samples must be tested and analyzed before statistically significant results can be obtained. From this viewpoint, laboratory studies of virus aerosols under well controlled test conditions are a good alternative.

Survival of viruses in aerosol form, one of the key factors affecting airborne transmission of viral diseases, has been widely studied in the laboratory (see Section 1.1.5). However, previous laboratory studies have often overlooked the following: 1) particle size and how it is associated with the survival of airborne viruses, 2) surrogate or model viruses and how they represent the survival of airborne viruses of interest (e.g., human and animal viruses), and 3) the composition of the nebulizer suspension from which virus is aerosolized and how it represents the survival of airborne viruses in real-life situations.

Particle size plays an important role in airborne transmission of viral diseases (Morawska 2006; Gralton et al. 2011), governing virus aerosol transport in air, its deposition in human respiratory tract, and its control by filtration. However, previous studies provided limited size information. For example, most studies relied on liquid impingers for sampling virus aerosols, which does not provide size fractionation. The physical collection efficiency of liquid impingers decreases as particle size decreases (e.g. ~85% at 1 μm, ~70% at 0.5 μm, and ~50% at 0.3 μm) (Lin et al. 1997; Hogan et al. 2005), which means those reported results for virus survival better represent that of larger size virus aerosols. Although size-segregated sampling instruments such as cascade impactors and cyclones are available, due to their limitations such as large cut-off size and low size resolution, insufficient attention has been given to virus aerosols in the submicron size range, the size of most human respiratory particles (Haslbeck et al. 2010; Holmgren et al. 2010). More importantly, what is unknown is how virus survival is associated with it carrier particle size. For example, Yang et al. (2011) raised the question "Are the viruses found across different sizes of particles equally viable, or are those in one size fraction more so?" What does infectious or total virus size distribution look like and how is it compared with particle size distribution? Does the chance of a particle to carry virus depend on particle size, surface area, or volume?

Nowadays many laboratory studies use MS2 bacteriophage as a model virus, since it is non-pathogenic (bio-safety level one) and easy to work with (e.g. fast growth to high titers). However, the suitability of MS2 bacteriophage as a general model virus has been

questioned (Appert et al. 2012). Is MS2 bacteriophage an appropriate surrogate for animal and human viruses such as influenza virus or SARS virus?

The composition of the nebulizer suspension from which virus is aerosolized greatly affects survival of virus aerosols (see Section 1.1.5). Given the fact that 1) virus aerosol particles of human origin often contain compounds from respiratory secretion and 2) many laboratory studies produced virus aerosols from nebulizer suspensions that were quite different from human saliva and mucus, it is likely that previously reported survival results may not represent that of naturally generated virus aerosols. Human saliva has been found to increase survival of aerosolized bacteria on respirators (Wang et al. 1999). Can human saliva also preserve virus survival in aerosols?

Due to their important role in infection control in hospitals and healthcare facilities, filtration efficiency of filtering facepiece respirators has been evaluated using laboratory generated virus aerosols (see Section 1.1.6). However, early studies (before the year 2013) often used MS2 bacteriophage as a challenge aerosol, whose characteristics (e.g. virion size and airborne survival) may be quite different from those of human and animal viruses. Therefore, the exact performance of filtering facepiece respirators against human and animal viruses is little understood. In addition, it remains unclear whether there would be any difference in filtration between different airborne viruses.

Correlation between infectivity and physical penetration through respirators is always a research problem of interest, because a better understanding of the correlation is helpful

to eventually predict infectivity penetration (which is time-consuming and sometimes difficult to measure) based on physical penetration measurements (which are fast and relatively easy). Although researchers have compared infectivity and physical penetration through respirators (see Section 1.1.6), all selected physical penetration is limited to particle number penetration and the selection of the method used to determine particle number penetration seems arbitrary (Table 1.2). No previous studies have compared infectivity penetration with other forms of physical penetration, e.g., particle volume penetration. Is it possible that physical penetration other than particle number penetration can better represent infectivity penetration? In addition, since respirators are currently certified using the NIOSH (photometer-based) standard, what does the current NIOSH certification tell us about respirator performance against virus aerosols?

The long-term goal of this research was to better understand and to better control airborne transmission of viral diseases. The objectives of this study were to 1) measure laboratory generated virus aerosols as a function of particle size, virus type, and composition of nebulizer suspensions and 2) evaluate performance of filtering facepiece respirators against virus aerosols. To achieve the objectives, the specific aims of this study were:

1. to develop a size-segregated sampling method for virus aerosol particles in the sub-micrometer size range with high size resolution, high collection efficiency, and easy virus recovery,

2. to determine the survival of airborne MS2 bacteriophage with animal viruses including transmissible gastroenteritis virus (coronavirus), avian influenza virus, and swine influenza virus as a function of particle size,
3. to compare the survival of airborne MS2 bacteriophage generated from human saliva, artificial saliva, and cell culture medium as a function of particle size,
4. to determine the filtration performance of filtering facepiece respirators against human adenovirus and swine influenza virus aerosols, and
5. to correlate infectivity penetration through respirators with various physical penetration, particularly particle volume penetration and photometric penetration.

1.3 Dissertation outline

A brief literature review, motivation, and research objectives are presented in this Chapter. The next four chapters consist of the main body of the dissertation, each based on a separate manuscript that has been published or currently under review. Specific aims 1 and 2 have been addressed in Chapter 2, where the newly developed virus aerosol sampling method and the survival of four airborne viruses as a function of particle size are described. Specific aim 3 has been addressed in Chapter 3, where the effect of four nebulizer suspensions on the survival of airborne MS2 bacteriophage is presented. Chapter 4 addresses specific aim 4 and reports filtration performance of respirators against two different types of virus aerosols. Chapter 5 (specific aim 5) compares infectivity penetration through respirators with a variety of physical penetration measurements. Finally, conclusions and future work are given in Chapter 6.

Chapter 2: Effect of Particle Size on the Airborne Survival of MS2 Bacteriophage vs. Three Animal Viruses

2.1 Introduction

The world-wide outbreaks of coronavirus-caused severe acute respiratory syndrome (SARS), H5N1 bird flu, and H1N1 novel influenza have caused substantial health impacts and have increased public concern for the spread of viral diseases. Respiratory viruses such as influenza are traditionally believed to be transmitted by direct contact, indirect contact with fomites, and large-sized droplets. However, recent human subject studies and field measurements have suggested that the aerosol route could also be an important mode of virus transmission (Satter et al. 1987; Fabian et al. 2008; Tellier 2009).

For aerosol transmission to occur, a particle must carry infectious virus and the virus in the carrier particle must survive (i.e., remain infectious) in air before it reaches a susceptible host to initiate infection. In general, infectious airborne virus in the natural environment is difficult to recover due to 1) the extremely low concentration of virus in ambient air and 2) the unsatisfying performance of traditional aerosol samplers. As a result, virus-carrying particles are often artificially generated and their survivability has been studied under laboratory conditions since the 1930s. It has been found that airborne influenza virus and coronavirus survive best at low relative humidity and low ambient temperature (Hemmes et al. 1960; Harper 1961; Schaffer et al. 1976; Ijaz et al. 1985; Ijaz et al. 1987; Kim et al. 2007).

However, most of the laboratory studies mentioned above used aerosol sampling instruments such as liquid impingers that provide little information on particle size of the collected virus aerosol, which has been identified to be one of the most important factors affecting airborne virus transmission (Morawska 2006; Gralton et al. 2011). Particle size governs virus aerosol transport, its deposition in the human respiratory tract, as well as its control by filtration (Eninger et al. 2008; Zuo et al. 2013b). Particle size may also play a role in the minimum infectious dose of a given virus. For instance, small-sized aerosol inhalation of human influenza virus and adenovirus yielded a much lower median infectious dose than intranasal inoculation with droplets of much larger size (Alford et al. 1966; Hamory et al. 1972; Douglas 1975). In an exposure study using a murine model (Scott and Sydiskis 1976), airborne influenza virus of small particle size (2 μm) resulted in a lower infectious dose than the larger-sized particles (10 μm). Therefore, it is not sufficient to measure only particle size-integrated survival of airborne viruses.

In order to better understand virus transmission by aerosols, it is important to determine the relationship between airborne virus survival and particle size (Gralton et al. 2011). Only a few studies are available on this issue in the scientific literature. To determine the distribution of infectious virus among polydisperse particles, an Andersen cascade impactor was used to sample aerosols of coxsackie virus A-21 (Gerone et al. 1966) and simian rotavirus (Ijaz et al. 1987). The concentration of infectious virus appeared to be related to particle volume distribution for particle size >0.5 μm. Using the same instrument, Appert et al. (2012) confirmed the above findings for MS-2 bacteriophage, but not for adenovirus. Tyrrell (1967) found that rhinovirus survived better in coarse

particles (>4 μm) than in smaller particles (0-4 μm) while adenovirus infectivity was best preserved in the size range of 0.56-1.9 μm compared with 1.9-10 μm (Appert et al. 2012), indicating that particle size does affect the survival of certain airborne viruses.

Although the use of size-segregated samplers such as impactors provides size fractionation for virus infectivity, not much is known about virus aerosol particles of size less than 0.5 μm, the size of most human respiratory particles (Haslbeck et al. 2010; Holmgren et al. 2010), probably because of the large cutoff size and low size resolution of impactors. To extend the understanding to submicron particles, Hogan et al. (2005) used a differential mobility analyzer (DMA) in combination with a liquid impinger to collect size-classified MS2 and T3 bacteriophage aerosol particles. The virus distribution was found to be different from particle number distribution. Lee (2009) later applied the same sampling approach for MS2 and showed that both virus infectivity and survivability increased with particle size. Nevertheless, both studies used bacteriophages and how well the results of bacteriophages represent those of human and animal viruses remains an issue (Appert et al. 2012).

The objective of this study was to examine the infectivity and survivability of three airborne animal viruses as a function of their carrier particle size in the submicron size range using a newly developed sampling method. In addition, the behavior of widely used MS2 bacteriophage was studied for comparative purposes.

2.2 Materials and methods

2.2.1 Propagation and titration of MS2 bacteriophage

MS2 bacteriophage (ATCC 15597-B1) is a small (27-34 nm), icosahedral, non-enveloped, single stranded, positive sense RNA virus, infecting only the male *Escherichia coli* (those bearing an F pilus) (Valegard et al. 1990). For the purposes of this study, we considered MS2 as a model virus because it has been widely used in many virus aerosol studies (Eninger et al. 2008; Lee 2009; Appert et al. 2012). The virus was propagated in *E. coli* famp (ATCC 700891), as described elsewhere (Appert et al. 2012). Briefly, 0.1 mL of MS2 and 1 mL of a log phase culture of *E. coli* were added to top agar tubes held at 48°C. After mixing, the contents of the tubes were poured on trypticase soy agar (TSA) plates. The top agar was allowed to solidify followed by inversion and incubation of the plates at 37°C for 24 hours. After plaques were confluent (within 24 hrs of incubation), 5 mL of 3% (wt/vol) tryptic soy broth (TSB) was added to each plate. After 2 hours at room temperature, the solution was aspirated, centrifuged at 2,500 $\times g$ for 15 min, and sterile-filtered. The resulting bacteriophage stock was aliquoted into 50 mL tubes, followed by storage at -80°C until use. The titer of MS2 bacteriophage in the virus stock and other samples was determined by using a double agar layer procedure as described elsewhere (Appert et al. 2012). The amount of virus was expressed as plaque forming units per unit volume of the sample (PFU/mL).

2.2.2 Propagation and titration of animal viruses

Three animal viruses were used, e.g., transmissible gastroenteritis virus (TGEV; Purdue strain) of pigs, avian influenza virus (AIV; A/chicken/Maryland/2007[H9N9]), and swine

influenza virus (SIV; A/swine/Minnesota/2010 [H3N2]). TGEV, a member of *Coronaviridae*, is spherical (100-150 nm), enveloped, single stranded, positive sense RNA virus, causing gastrointestinal infections in pigs (Tajima 1970). AIV and SIV are also spherical (80-120 nm) and contain eight segments of single-stranded RNA, causing respiratory disease in pigs, poultry, and other animal species (Lamb and Choppin 1983). The three animal viruses share physical and genetic similarity to human viruses (Lamb and Choppin 1983; Jackwood 2006) and were, therefore, used as surrogates for human SARS virus and influenza virus, respectively.

TGEV was propagated in swine testicular (ST) cells while SIV and AIV were propagated in Madin-Darby canine kidney (MDCK; ATCC CCL-34) cells. The cells were grown in Minimum Essential Medium (MEM) with Earle's salts supplemented with L-glutamine, (Mediatech, Herndon, VA), 8% fetal bovine serum (FBS; Gibco, Life Technologies, New York), 50 µg/mL gentamicin (Mediatech), 150 µg/mL neomycin sulfate (Sigma, St. Louis, MO), 1.5 µg/mL fungizone (Sigma), and 455 µg/mL streptomycin. Before virus inoculation, the cells were washed three times with Hanks' balanced salt solution (pH 7.3). After virus inoculation, the cells were kept at 37°C for 1 hr for virus adsorption. Maintenance medium without FBS was used for propagation of TGEV. For SIV and AIV, the maintenance medium contained trypsin (1.5 µg/mL, Sigma) and 4% bovine serum albumin (BSA; Gibco, Life Technologies). Inoculated cells were incubated at 37°C under 5% CO_2. After the appearance of virus-induced cytopathic effects (CPE), usually at 4-5 days post-infection, the cells were subjected to three freeze-thaw cycles (-80°C/25°C) followed by centrifugation at 2,500 $\times g$ for 15 min at 4°C. The supernatant was collected

and aliquoted into 50 mL tubes followed by storage at -80°C until use. For titration of TGEV, serial 10-fold dilutions of virus samples were prepared in MEM. For titration of SIV and AIV, 4% BSA and trypsin were added to MEM. Sample dilutions were inoculated in appropriate cell monolayers in 96-well cell culture plates (Nunc, New York) using 100 μL/well. Four wells were used per dilution. Inoculated cells were incubated at 37°C under 5% CO_2 for 4-5 days until CPE appeared. Virus titers were then calculated as 50% tissue culture infectious dose per mL ($TCID_{50}$/mL) using the Karber method (Karber, 1931).

2.2.3 Quantification of total virus by qRT-PCR

Viral RNA was extracted from 140 μL of sample using the QIAamp viral RNA kit (Qiagen, Valencia, CA). The extracted RNA was eluted in 40 μL of elution buffer and stored at -20°C until used for qRT-PCR (quantitative reverse transcription-polymerase chain reaction). The amount of viral RNA present in each sample was quantified by qRT-PCR performed in a Mastercycler Realplex thermocycler (Eppendorf, Hamburg, Germany) using QIAGEN One Step RT-PCR kit (Qiagen, Valencia, CA). Forward primers, reverse primers, and probes have been described by O'Connell et al. (2006) and Spackman et al. (2002). Samples were loaded in a 96-well plate and analyzed in duplicate, each containing 3 μL of viral RNA template in a final volume of 20 μL. Standard curves were constructed using serial 10-fold dilution of viral RNA extracted from the virus stock of known titer. In each run of qRT-PCR, standard curve samples and no template control were used as positive and negative controls. The thermal cycling conditions for reverse transcription (RT), RT inactivation, and PCR of the four viruses were the same: 50°C for

30 min and 95^{o}C for 15 min. The thermal cycling parameters were as follows: 40 cycles of 95^{o}C for 15 sec and 55^{o}C for 45 sec for MS2; 40 cycles of 95^{o}C for 15 sec and 60^{o}C for 45 sec for TGEV; and 45 cycles of 94^{o}C for 1 sec and 60^{o}C for 20 sec for SIV and AIV. Final results were expressed as cycle threshold (Ct) values. After qRT-PCR was performed, the amplification efficiency was determined for each sample using the DART-PCR method to correct the raw Ct values (Peirson et al 2003). The average amplification efficiency was 0.87, 0.85, 0.84, and 0.90 for MS2, TGEV, SIV, and AIV, respectively. The corrected Ct values were then used, along with the standard curve, to calculate the concentration of total (infectious and non-infectious) virus, which was expressed as projected $TCID_{50}$/mL.

2.2.4 Aerosol test tunnel and experiment procedure

Experiments were performed in a one-pass aerosol test tunnel located in a biosafety level 2 laboratory (Figure 2.1). The vertical tunnel was 1.7 m long and 14 cm in diameter, enclosed by a negative pressure containment to minimize release of virus aerosol into the surrounding environment. This facility has been used in a variety of virus aerosol studies (Kim et al. 2007; Appert et al. 2012; Zuo et al. 2013b). Virus aerosol was generated using a 6-jet Collison nebulizer (BGI, Waltham, MA) at a compressed air pressure of 10 psi. The nebulizer suspension consisted of 45 mL thawed virus stock, 0.1 mL antifoam Y-204 (Sigma), and 5 mL uranine dye (0.25 g/mL, Fluka, Buchs, Switzerland), which served as a fluorescent particle tracer (Appert et al. 2012). The use of uranine allowed particle losses in the test system to be quantified. Virus titer in the freshly prepared nebulizer suspension was 3.1×10^{9}-5.8×10^{9} PFU/mL, 1.45×10^{6}-3.16×10^{6} $TCID_{50}$/mL, 3.16×10^{6}-

6.76×10^6 $TCID_{50}$/mL, and 3.16×10^5-1.48×10^6 $TCID_{50}$/mL for MS2, TGEV, SIV, and AIV, respectively.

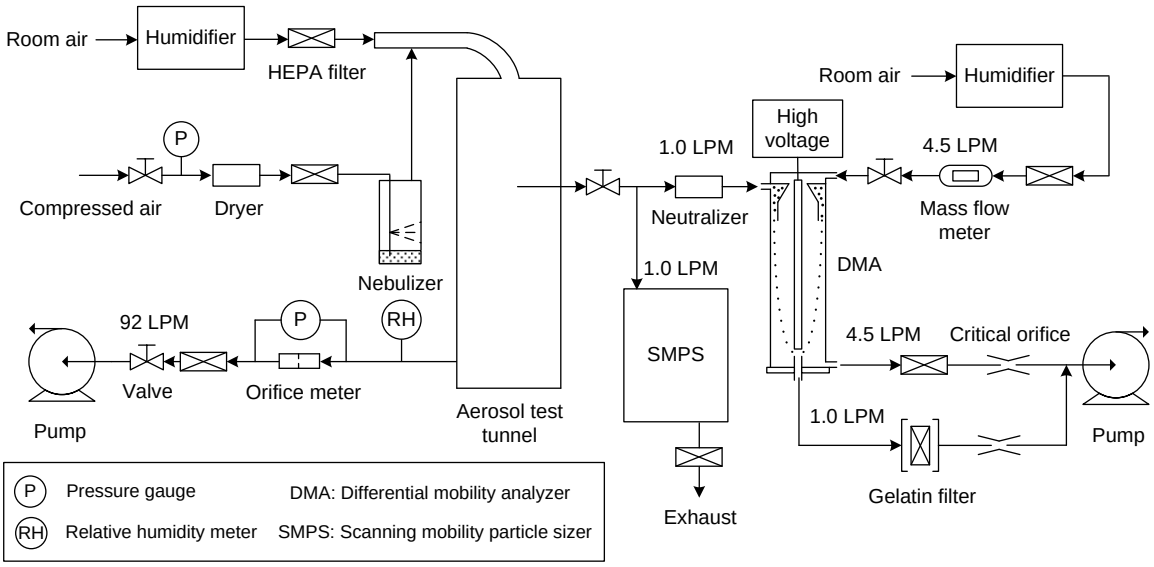

Figure 2.1 Schematic diagram of the experimental setup for the measurement of virus aerosols.

The generated virus aerosol was mixed with HEPA-filtered and relative humidity (RH)-controlled room air, and then directed to the test tunnel at a flow rate of 92 L/min. Two minutes were allowed for the produced virus aerosol to become well mixed and stabilized before samples were taken. Virus aerosol particles were passed through a polonium-210 neutralizer before being selected by a DMA (Model 3071; TSI, Shoreview, MN) at 100, 200, 300, 400, and 450 nm. The sheath flow rate was 4.5 L/min, control by a critical orifice, and its RH was also controlled. The size-classified virus aerosol particles were collected onto 25 mm diameter gelatin filters with a pore size of 3 μm (SKC Inc., Eight-Four, PA) held in a stainless steel holder (Millipore Corp., Bedford, MA) at a sampling

flow rate of 1 L/min for 15 min. Compared with the liquid impingers used previously (Hogan et al. 2005; Lee 2009), gelatin filters have excellent physical collection efficiency for virus aerosol particles (Burton et al. 2006) and do not significantly affect virus infectivity (Verreault et al. 2008) and were therefore used in this study.

The sampling time was limited to 15 min in order to minimize variation in the nebulizer output (Eninger et al. 2009) and desiccation of the collected virus. During the gelatin filter sampling, a scanning mobility particle sizer (SMPS) (Model 3034, TSI) was used to simultaneously measure the particle size distribution of the generated virus aerosol from 10 to 470 nm at a flow rate of 1 L/min. Immediately after sampling, the gelatin filter was removed from the filter holder, broken apart using sterile forceps, and dissolved in 1 mL of elution buffer (1.5% beef extract with 0.05 M glycine at pH of 7.2), followed by vortexing (American Scientific Products, McGaw Park, IL) at maximal speed for 9-10 sec, six times at 1 min intervals. The unsampled virus aerosol passed through the test tunnel and was finally filtered at the outlet. After each test, the nebulizer was turned off and the tunnel was purged for 15 min at 92 LPM using HEPA filtered clean air to remove any residual airborne particles.

In each test, 1 mL samples of nebulizer suspension taken before and after the test and 1 mL virus samples collected from the gelatin filter were split into three portions. The first portion was stored at 4^{o}C until analyzed by a spectrofluorometer (Model RF-5201PC; Shimadzu Scientific Instruments, Columbia, MD) to quantify the concentration of uranine in the sample (Appert et al. 2012). The results were expressed as fluorescence

unit per mL. The other two portions were stored at -80^{o}C until virological analysis. Virus infectivity assay and qRT-PCR were used to quantify the amount of infectious and total (both infectious and non-infectious) virus present in the samples.

The tests were repeated in triplicate for MS2, TGEV, and SIV and twice for AIV. During the experiments, the RH and temperature in the test tunnel were maintained at 40-50 % and 22-25^{o}C, respectively.

2.2.5 Data analysis

To determine the distribution of virus in polydisperse particles and compare it with particle size distribution, the infectious virus size distribution, $IV(D_p)$ was defined particularly for particles carrying infectious virus (Hogan et al. 2005) and calculated as:

$$IV(D_P) \equiv \frac{dC_{IV}(D_P)}{d\log_{10} D_P} \approx \frac{C_{IV,gel}(D_P)V_{gel}}{Q_{gel}t[\Delta \log_{10} D_P]} \frac{1}{f_{+1}(D_P)P(D_P)}, \quad [1]$$

where C_{IV} is the concentration of airborne infectious virus, $C_{IV,gel}$ is the concentration of infectious virus recovered in the effluent from the gelatin filter, V_{gel} is the volume of eluent used to dissolve the gelatin filter, Q_{gel} is the air sampling flow rate through the gelatin filter, t is the sampling time, $\Delta log_{10}D_p$ is the logarithm of the width of the size interval of the DMA, f_{+1} is the fraction of singly positively charged particles (Wiedensohler 1988), and P is penetration of particles through the DMA (Reineking and Porstendorfer 1986). Similarly, by replacing the concentration of infectious virus with that of total virus, the total virus size distribution, $TV(D_p)$ can be calculated as:

$$TV(D_P) \equiv \frac{dC_{TV}(D_P)}{d\log_{10} D_P} \approx \frac{C_{TV,gel}(D_P)V_{gel}}{Q_{gel}t[\Delta \log_{10} D_P]} \frac{1}{f_{+1}(D_P)P(D_P)}. \quad [2]$$

The amount of infectious virus carried per particle, *iv*, was calculated as the ratio of infectious virus concentration to particle number concentration, assuming the $\Delta log_{10}D_p$ interval is the same for the DMA and the SMPS:

$$iv(D_P) \equiv \frac{dC_{IV}(D_P)}{dC_{n,SMPS}(D_P)} \approx \frac{C_{IV,gel}(D_P)V_{gel}}{Q_{gel}t\Delta C_{n,SMPS}(D_P)} \frac{1}{f_{+1}(D_P)P(D_P)}, \text{[3]}$$

where $\Delta C_{n,SMPS}$ is the number concentration of particles within a size interval with geometric diameter D_p measured by the SMPS. Similarly, the amount of total virus carried per particle, *tv*, was calculated as:

$$tv(D_P) \equiv \frac{dC_{TV}(D_P)}{dC_{n,SMPS}(D_P)} \approx \frac{C_{TV,gel}(D_P)V_{gel}}{Q_{gel}t\Delta C_{n,SMPS}(D_P)} \frac{1}{f_{+1}(D_P)P(D_P)}. \text{[4]}$$

Power-law curve fitting with least squares was conducted for $iv(D_p)$ and $tv(D_p)$ using Microsoft Excel.

The effect of nebulization stress on virus infectivity and viral RNA integrity was also examined by calculating two terms, γ_{IV} and γ_{TV} (Appert et al. 2012):

$$\gamma_{IV} = \frac{(C_{IV,neb}/C_{F,neb})_a}{(C_{IV,neb}/C_{F,neb})_b} \qquad \gamma_{TV} = \frac{(C_{TV,neb}/C_{F,neb})_a}{(C_{TV,neb}/C_{F,neb})_b}, \text{[5]}$$

which compare the ratio of infectious virus ($C_{IV,\,neb}$) or total virus concentration ($C_{TV,\,neb}$) to fluorescence intensity ($C_{F,\,neb}$) in the nebulizer suspension before (*b*) and after (*a*) the nebulization. If there is inactivation of virus infectivity or viral RNA due to nebulization, γ would be less than unity. The fluorescence intensity was included in the calculation to take into account the increase of virus concentration due to the evaporation of liquid from the nebulizer suspension.

To quantify how efficiently infectious virus could be recovered by the DMA and gelatin filter based sampling system, relative recovery of infectious virus, RR_{IV}, was calculated as a function of particle size (Ijaz et al. 1987; Agranovski et al. 2005; Appert et al. 2012):

$$RR_{IV}(D_P) = \frac{C_{IV,gel}(D_P)/C_{F,gel}(D_P)}{C_{IV,neb}/C_{F,neb}}, \quad [6]$$

where $C_{IV,neb}$ and $C_{F,neb}$ are the average of readings before and after tests.

Similarly, relative recovery of total virus, RR_{TV}, was also calculated, to evaluate how efficiently viral RNA was recovered:

$$RR_{TV}(D_P) = \frac{C_{TV,gel}(D_P)/C_{F,gel}(D_P)}{C_{TV,neb}/C_{F,neb}}. \quad [7]$$

Finally, the particle size dependent virus survivability, S, was determined by calculating the ratio of infectious virus to total (both infectious and non-infectious) virus carried by the particles normalized by the same ratio in the nebulizer suspension:

$$S(D_P) = \frac{C_{IV,gel}(D_P)/C_{TV,gel}(D_P)}{C_{IV,neb}/C_{TV,neb}}. \quad [8]$$

Data were statistically analyzed using one-way or multiple-way analysis of variance (ANOVA) in Matlab (MathWorks, Natick, MA). The limit of detection (LOD) of the Kaber method is 10 $TCID_{50}$/mL. For samples where no infectious virus was detected (two out of the three replicates of SIV at 100 nm), a value equal to LOD divided by square root of 2 was used in the calculation (Hornung and Reed 1990).

2.3 Results

2.3.1 Size distribution of virus aerosol particles

As a first step to characterize the virus aerosols, the size distributions of the four virus aerosols were determined using the SMPS (see Figure 2.2). The size distributions were generally lognormal with the statistics provided in Table 2.1. There was no clear correlation between the size of virion and the size of generated virus aerosol. Small virion size did not necessarily give a small count median diameter.

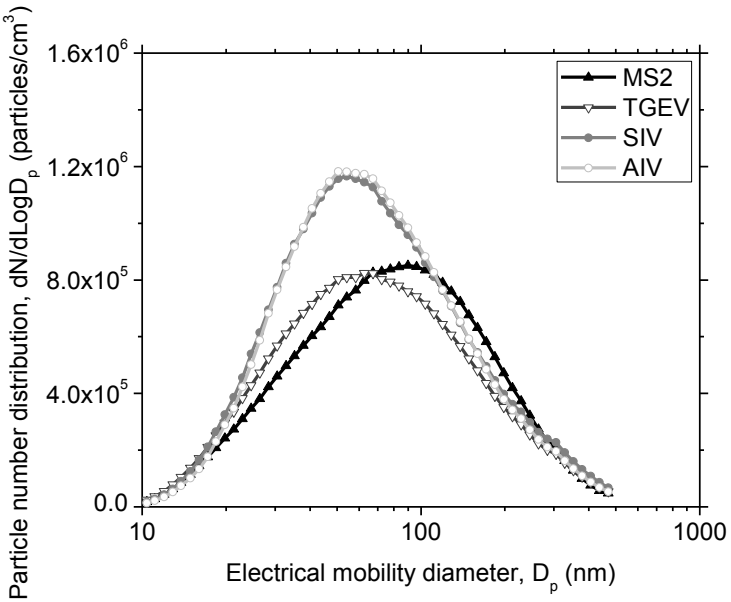

Figure 2.2 Representative size distributions of virus aerosol particles generated from the four virus suspensions, MS2 bacteriohpage (MS2), transmissible gastroenteritis virus (TGEV), swine influenza virus (SIV), and avian influenza virus (AIV).

Table 2.1 Particle size distribution statistics of the four virus aerosols as measured using an SMPS.

	MS2	TGEV	SIV	AIV
Virion size (nm)	27-34[a]	100-150[b]	80-120[c]	80-120[c]
Count median diameter (nm)	79.1	66.3	62.5	62.6
Geometric standard deviation	2.28	2.31	2.16	2.10
Total number concentration (particles/cm^3)	7.53×10^5	7.42×10^5	9.46×10^5	9.35×10^5

[a]Reference: Valegard et al. (1990)
[b]Reference: Tajima (1970)
[c]Reference: Lamb and Choppin (1983)

2.3.2 Infectious/Total virus size distribution

Figure 2.3 represents the infectious virus and total virus size distribution from 100 to 450 nm normalized by the maximum values. In general, both the infectious and total virus concentration increased with particle size and the maximum values at 400-450 nm were around 5000 PFU/cm^3, 35 $TCID_{50}$/cm^3, 180 $TCID_{50}$/cm^3, and 60 $TCID_{50}$/ cm^3 for MS2, TGEV, SIV, and AIV, respectively, which were several orders of magnitude lower than the particle number concentration at the same particle size (Figure 2.2). The virus size distributions were normalized to more easily compare them with particle size distributions. As seen in Figure 2.3 the infectious and total virus distributions had a similar trend, both appearing to follow particle volume distribution rather than particle number distribution.

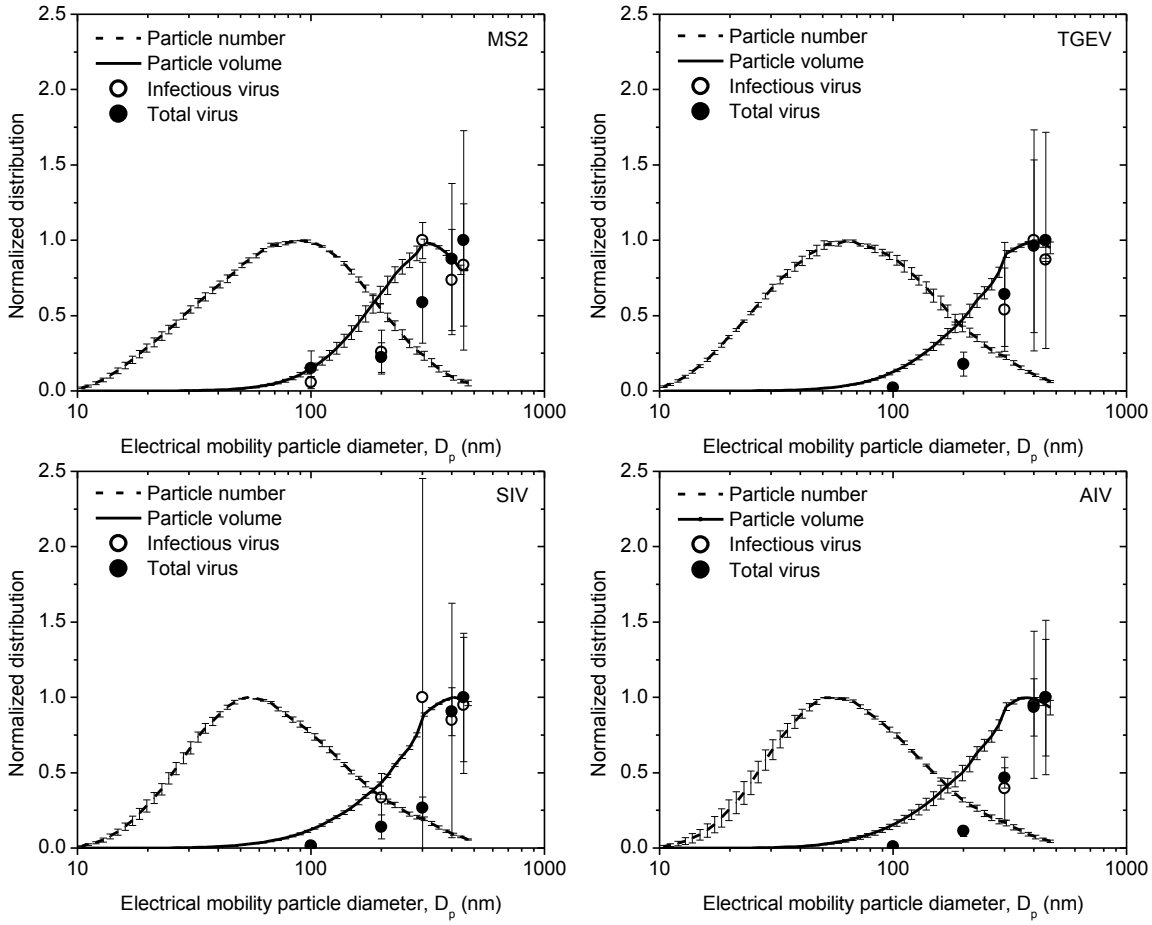

Figure 2.3 Normalized infectious virus size distribution, total virus size distribution, SMPS particle number distribution, and SMPS particle volume distribution for airborne MS2, TGEV, SIV, and AIV. Values are means ± one standard deviation (n = 3 for MS2, TGEV, and SIV; n = 2 for AIV).

2.3.3 Infectious/Total virus carried per particle

The average amount of infectious virus and total virus carried by each particle (*iv* and *tv*) were plotted as a function of particle size (Figure 2.4). For all four viruses, *iv* and *tv* increased with particle size. The values were much lower than unity, even at 450 nm.

Power-law curve fitting gave R^2-values ranging from 0.75 to 0.99, suggesting that there was a power-law correlation between *iv*/*tv* and particle size. Note that the slopes obtained from the curve fits were significantly greater than three in some cases.

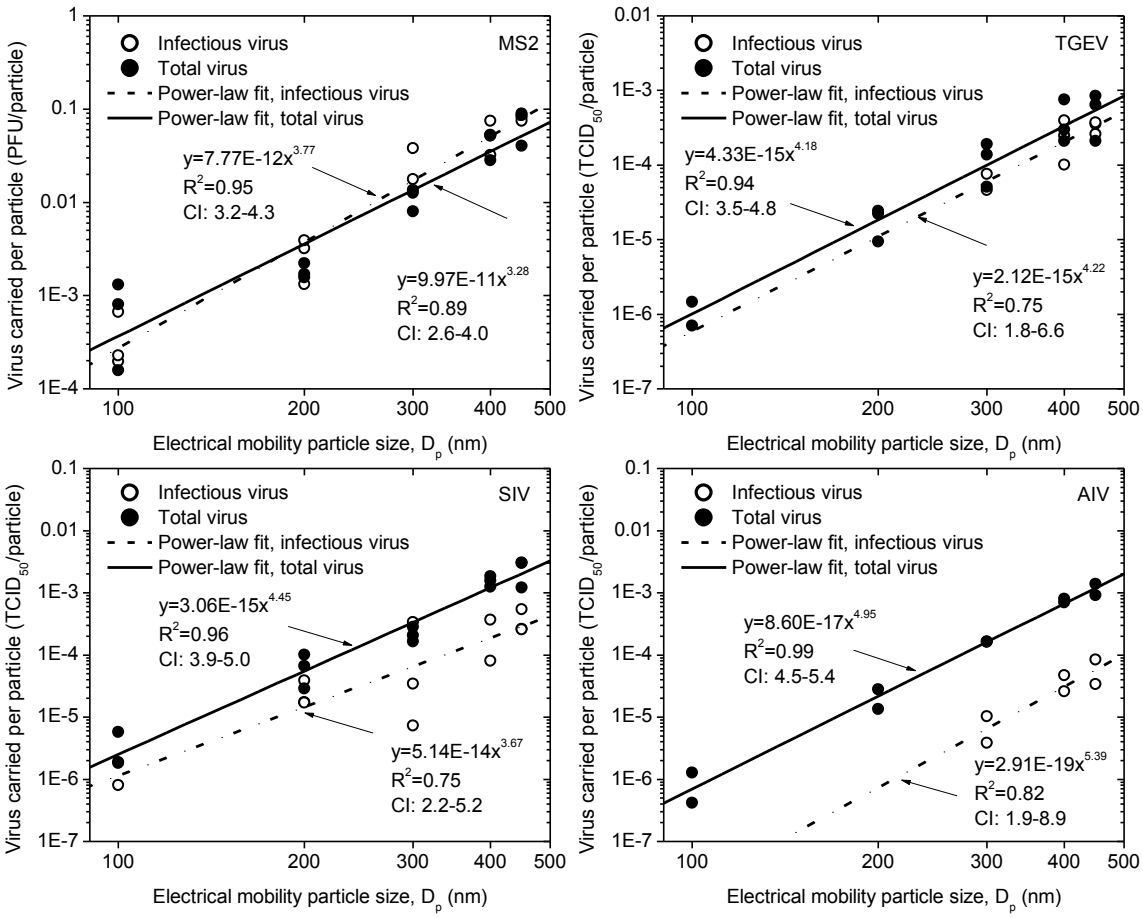

Figure 2.4 Infectious virus and total virus carried per particle as a function of particle size for airborne MS2, TGEV, SIV, and AIV. Also shown are the equations and R^2-values of the curve fitting and the 95% confidence intervals (CI) of the slopes, where x represents the particle size and y represents the amount of either infectious virus or total virus carried per particle. Note that the slopes of the lines are the exponents of the equations.

2.3.4 Nebulization stress on virus

As shown in Figure 2.5, terms γ_{IV} and γ_{TV} were not significantly different from unity for the four viruses. In addition, one-way ANOVA showed that neither γ_{IV} (P = 0.276) nor γ_{TV} (P = 0.536) were significantly dependent on the type of virus.

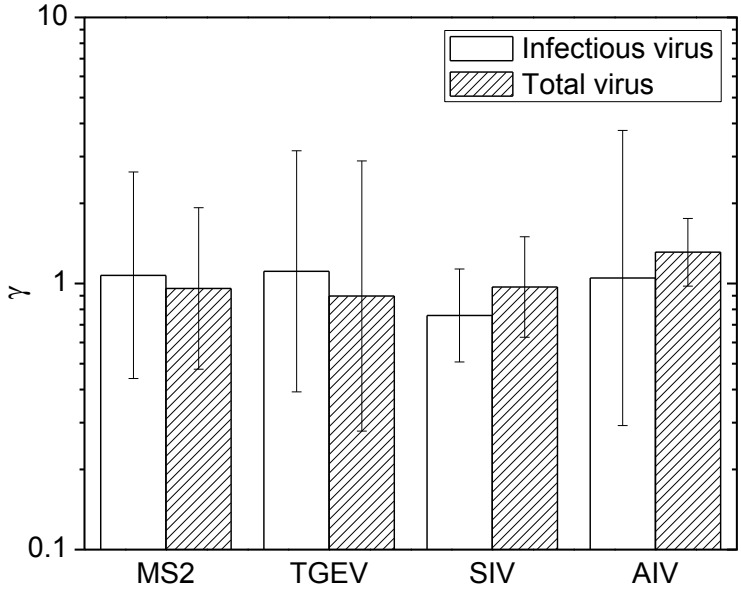

Figure 2.5 Effect of nebulization on the concentration of infectious and total viruses in the nebulizer suspension. The term γ, which compares the ratio of virus concentration to fluorescence intensity before and after nebulization, is calculated using Equation [5]. Each bar represents geometric mean with 95% confidence interval.

2.3.5 Relative recovery of infectious virus and total virus

Figure 2.6 shows RR_{IV} as a function of particle size for the four viruses. For MS2, RR_{IV} was around 0.3, independent of particle size (P = 0.245, one-way ANOVA). However, for the three animal viruses, RR_{IV} showed strong particle size dependence with values at

100-200 nm much lower than those at 300-450 nm. At particle sizes of 300 nm and above, RR_{IV} became independent of particle size (P = 0.948, two-way ANOVA) but was significantly affected by the type of virus (P = 0.001, two-way ANOVA). RR_{IV} of TGEV and SIV were generally higher than MS2 and AIV at particle sizes 300 nm and above.

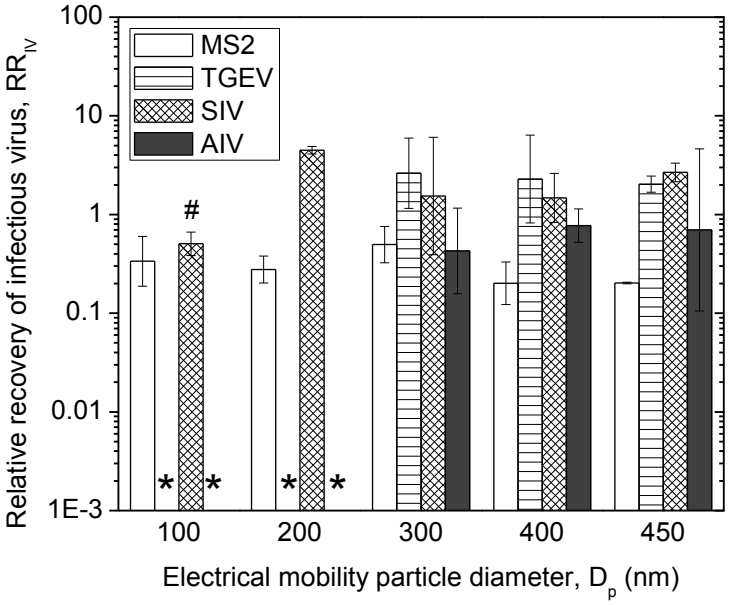

Figure 2.6 Relative recovery of infectious virus for MS2, TGEV, SIV, and AIV. Each bar represents geometric mean ± one standard deviation of the mean. In cases where no infectious virus was recovered (denoted by asterisks [*]), an infectious virus concentration of 10 $TCID_{50}$/mL was used to estimate RR_{IV}, which was lower than 0.47, 0.07, 0.86, and 0.10 for TGEV at 100 and 200 nm and AIV at 100 and 200 nm, respectively. The pound sign (#) denotes that infectious virus was recovered in only one of the three samples.

Contrary to RR_{IV}, RR_{TV} did not depend on particle size (P = 0.954, two-way ANOVA) for any of the four viruses (Figure 2.7). However, it was significantly affected by the type of virus (P <0.001, two-way ANOVA). The particle size-averaged RR_{TV} was 1.05, 2.22, 1.36 for TGEV, SIV, and AIV, respectively, much higher than MS2 (0.26).

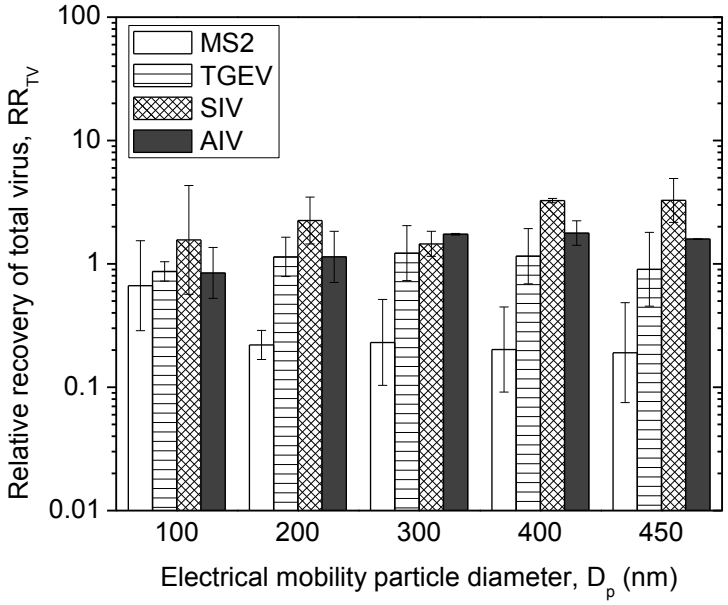

Figure 2.7 Relative recovery of total virus for MS2, TGEV, SIV, and AIV. Each bar represents geometric mean ± one standard deviation of the mean.

2.3.6 Survivability of airborne viruses

Virus survivability was plotted as a function of particle size for the four viruses (Figure 2.8). Similar to RR_{IV}, the survivability of MS2 was roughly a constant, independent of particle size (P = 0.397, one-way ANOVA). However, the three animal viruses demonstrated enhanced survivability at 300-450 nm, compared with 200 nm. At large particle size (300-450 nm), virus survivability was found to be independent of particle

size (P = 0.912, two-way ANOVA) and the particle size averaged survivability was 1.00, 1.86, 0.75, and 0.41 for MS2, TGEV, SIV, and AIV, respectively, though the difference was not statistically significant (P = 0.080, two-way ANOVA).

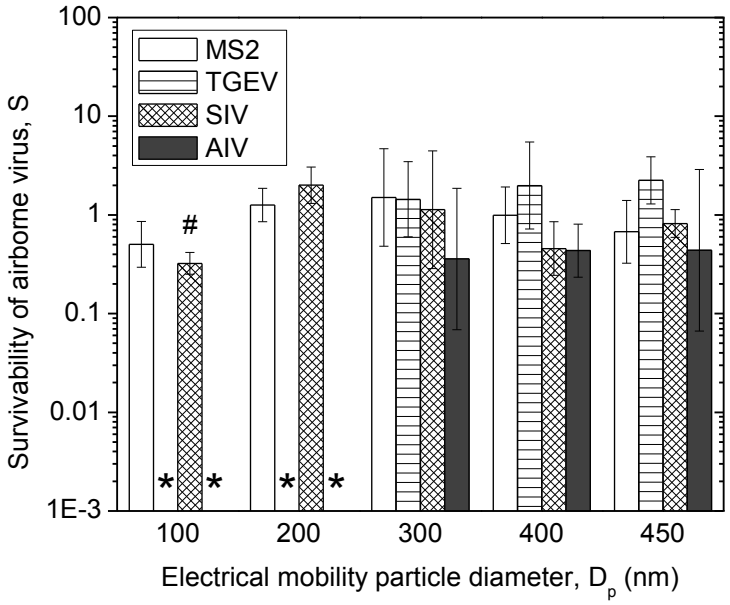

Figure 2.8 Survivability of airborne MS2, TGEV, SIV, and AIV. Each bar represents geometric mean ± one standard deviation of the mean. In cases where no infectious virus was recovered (denoted by asterisks [*]), an infectious virus concentration of 10 $TCID_{50}$/mL was used to estimate survivability, which was lower than 0.42, 0.06, 1.02, and 0.10 for TGEV at 100 and 200 nm and AIV at 100 and 200 nm, respectively. The pound sign (#) denotes that infectious virus was recovered in only one of the three samples.

2.4 Discussion

2.4.1 Comparison between particle size distribution and virus size distribution

Pneumatic nebulizers such as the Collison are commonly used in laboratory studies to produce virus aerosol from liquid suspensions (Reponen et al. 1997). However, the measured particle size distributions (Figure 2.2) showed that the traditional Collison nebulizer inevitably generated residue particles carrying no virus. For example, many particles were found at sizes smaller than the virion size. The mean particle size of MS2 virus aerosol was larger than other studies that also used Collison nebulizers (Hogan et al. 2005; Eninger et al. 2009), which could result from the much higher solute concentration (e.g. the addition of uranine) in the nebulizer suspension used in this study. Unlike the narrow size range of virions, the generated aerosol covered a much wider range (Table 2.1), suggesting that the nebulizer could generate high concentrations of residue particles, due to the chemicals dissolved in the virus/cell growth media, which is consistent with the observations by Hogan et al. (2005).

Therefore, the particle number distribution, though easily measured by an SMPS, does not necessarily indicate how virus is distributed among particles of different sizes. In fact, the virus size distribution was indeed masked by the particle number distribution (Figure 2.3). Lee (2009) found that infectious virus size distribution for MS2 at 30-230 nm followed particle volume distribution. This study confirmed Lee's observation for MS2 and showed for the first time that both infectious virus and total virus distributions of TGEV, SIV, and AIV were also much better represented by particle volume distribution than number distribution in the size range of 100-450 nm (Figure 2.3). Recently, there is

interest in evaluating filter performance using different particle size-integrated filter efficiency measurements (Li et al. 2012). Based on the understanding of virus size distributions presented here, perhaps particle mass-based filter efficiency may better represent the performance of a filter against airborne virus, compared with particle number- or surface area-based efficiency.

2.4.2 Probability for a particle to carry virus

As a further step to understand how virus infectivity depends on particle size, the amount of infectious virus (*iv*) and total virus (*tv*) carried per particle was determined as a function of particle size (Figure 2.4). Assuming one PFU represents one virion, the probability for a 450 nm particle to carry one MS2 virion was <10%. The reported ratio of infectious virus per $TCID_{50}$ in particles ranged between 30 and 300 for influenza virus (Wei et al. 2007; Fabian et al. 2008). Using a similar infectious virus to $TCID_{50}$ ratio, the probability for a 450 nm nebulizer-generated particle to carry one animal virus was estimated to be <100%. Therefore, the results suggest that only a small fraction of laboratory generated particles actually carry virus, even if a nebulization suspension of high virus titer is used and the particle size is larger than the virion. However, the capacity for a particle to carry virus increased with particle size, following a power law relationship. Interestingly, a slope of >3 was found in all the cases and some were even significantly greater than three, which indicate that the amount of virus carried by a particle is proportional to more than the particle volume. This finding also agreed with the virus size distributions, which seemed to shift to larger sizes compared with the particle volume distributions (Figure 2.3). Multiple-charged particles of larger size

(presumably carrying more virus) with the same electrical mobility could be collected by the gelatin filter, which may increase the slope. Nebulization suspension may also affect the slope. For example, Lee (2009) found the slope changed from ~3 for DI water to ~2.5 for tryptone solution. In general, *iv* and *tv* depend on particle size, the type of virus, and the nebulizer suspension.

2.4.3 Effect of aerosolization on virus infectivity and viral RNA

Although high shear stress during aerosolization can reduce viability of bacteria (Griffiths and DeCosemo 1994), aerosolization for a short time period (2-30 min) has been shown to have a negligible effect on virus infectivity (Harper 1961; Ijaz et al. 1985; Appert et al. 2012). This study evaluated the effect of a longer aerosolization time (~90 min) on both virus infectivity and total virus (viral RNA). As shown in Figure 2.5, the values of γ_{IV} and γ_{TV} suggest that neither infectious virus nor viral RNA was significantly affected by aerosolization. Fabian et al. (2009) also found that the ratio of total virus to infectious virus in the nebulizer suspension only slightly increased over an aerosolization time of 70 min. The four viruses had similar γ, indicating that aerosolization had a similar effect on each virus, independent of virion size and surface structure (e.g., naked or enveloped). The smaller size of viruses compared with bacteria might explain their resistance to aerosolization stress (Kim et al. 2007). Viruses tend to form aggregates in liquid suspensions (Hogan et al. 2004; Wei et al. 2007). The continuous recirculation of virus suspensions through the nebulizer nozzle may reduce the level of aggregation and thus increase virus titer (Teunis et al. 2005), which may also explain why γ_{IV} was close to unity.

2.4.4 Relative recovery of infectious virus and total virus

For TGEV and AIV, RR_{IV} at 200 nm was much lower compared with 300-450 nm (Figure 2.6). Because no infectious virus was detected at 100-200 nm, an infectious virus concentration of 10 $TCID_{50}$/mL was used to estimate RR_{IV}. Since 200 nm particles carried much more fluorescence than those at 100 nm, the estimated RR_{IV} at 100 nm was much higher than 200 nm for TGEV and AIV. RR_{IV} is often used to evaluate how efficiently certain sampling systems can recover infectious virus aerosol shortly after its generation and theoretically $RR_{IV} \leq 1$ (Ijaz et al. 1987; Agranovski et al. 2005; Appert et al. 2012). However, $RR_{IV} > 1$ was sometimes found for TGEV and SIV, which could be due to the large uncertainty of the endpoint dilution assay used for animal viruses. For example, change in only one well with CPE can almost double or halve the final titration result.

If there is no loss of total virus (viral RNA), then $RR_{TV} = 1$, assuming the amount of virus carried by a particle is proportional to the particle volume and measurement errors are negligible. As demonstrated in Figure 2.7, the animal virus nucleic acids were generally recovered without loss, suggesting they were as stable as the fluorescence tracer. Therefore, for the three animal viruses tested, their viral RNAs could potentially be used as an alternative to traditional chemical tracers such as uranine, though their lower detection limit (Verreault et al. 2008) and longtime stability should be further tested.

2.4.5 Survivability of airborne viruses

Similar to RR_{IV}, survivability of TGEV and AIV was much lower at 200 nm than at larger size (Figure 2.8). One could argue that the discretization phenomenon is responsible for this finding, i.e., as the carrier particle size gets smaller and approaches the size of virion, it becomes more difficult for the particle to carry virus. However, the particle size-independent RR_{TV} shown in Figure 2.7 suggests the presence of virus in particles even at 100 nm. Therefore, the discretization phenomenon was probably not the reason. The main reason for the particle size associated survivability could be the shielding effect. More specifically, compared with viruses existing as singlets or in association with fewer organics (e.g. solutes in the nebulizer suspension), viruses in larger particles may be surrounded by more organic material, which may form a shield. The shielding effect has been demonstrated to protect virus from environmental stress such as ultraviolet irradiation (Woo et al. 2012). It may also reduce sampling stress such as desiccation and sampler dependent-mechanical forces, thus better maintaining the infectivity of airborne viruses. However, as particle size increased to 300 nm and above, virus survivability seemed to reach a plateau, suggesting the shielding effect was maintained once a specific particle size was reached. The same explanation applies to MS2. Because all collected particle sizes were more than four times the virion size of MS2 (25-30 nm), survivability of MS2 reached the plateau regime and therefore no longer depended on particle size (Figure 2.8). This explanation is supported by Lee (2009), who showed that survivability of MS2 at 120-200 nm was higher than at 30 nm, despite the large experimental variation.

Any loss of airborne virus survivability must eventually result from the inactivation of outer virus protein coat and/or inner nucleic acid core (Sattar et al. 1987). Figures 2.6-2.8 suggest that MS2 was inactivated mainly by damage to its viral RNA. For MS2 with intact viral RNA, its infectivity was well maintained with survivability of close to unity. Because 1) aerosolization had little effect on virus infectivity or viral RNA (Figure 2.5) and 2) exposing MS2 collected on gelatin filters to an air stream for 10 min did not affect virus infectivity (Grinshpun et al. 2007), we believe that the loss of MS2 virus infectivity and its viral RNA mostly occurred in the aerosol phase. Since the three animal viruses generally had intact viral RNAs ($RR_{TV} \approx 1$), their inactivation was probably due to the damage of the virus envelope and/or capsid. By comparing the decay rate of whole virus and its infectious viral RNA, inactivation of picornavirus and poliovirus, both non-enveloped viruses, has been shown to result from denaturation of the virus protein coat and viral nucleic acid, respectively (Aker and Hatch 1968; De Jong and Winkler 1968). In general, MS2 and TGEV survived best, followed by SIV and AIV. Unfortunately, without additional tests (e.g. exposing viruses collected on gelatin filters to air streams and determining infectivity loss), we could not determine if the inactivation of animal viruses happened during the aerosol phase, sampling phase, or both. Note that SIV showed much higher survivability at 200 nm than AIV (Figure 2.8), suggesting that influenza virus of different subtypes may have different survivability, which confirms the findings in other studies (Schaffer et al. 1976; Pyankov et al. 2012).

2.4.6 Use of MS2 bacteriophage as a surrogate virus

Several advantages such as non-pathogenicity, high virus titer, and simple infectivity assay make MS2 bacteriophage widely used in virus aerosol studies. However, similar to a previous study (Appert et al. 2012), its different recovery and survival compared with coronavirus and influenza virus suggests that it may not be an appropriate surrogate for animal or human viruses. Using surrogates that over-/underestimate the inactivation of the target microorganisms may negatively impact risk assessment (Sinclair et al. 2012).

2.4.7 Limitations

One of the limitations of this study was that virus was aerosolized from its stock suspension which is unlikely to represent the liquid surrounding airborne viruses when they are generated from infected animals or humans. In addition, it is not clear if the generation mechanism of human expiratory particles is the same as the Collison nebulizer. Therefore, one should be cautious in generalizing these experimental results to real life situations since infectivity and survivability of airborne virus may heavily depend on the composition of the nebulizer suspension (Satter et al. 1987) and the way it is generated.

Chapter 3: Effect of Nebulizer Suspensions on the Survival of Airborne MS2 Bacteriophage

3.1 Introduction

The potential involvement of virus aerosols in the transmission of human respiratory diseases, although still under considerable debate (Brankston et al. 2007; Weber and Stilianakis 2008; Tellier 2009), has led to increased public concern. Several studies have found that a variety of respiratory viruses including influenza virus and severe acute respiratory syndrome (SARS) coronavirus could be present at high concentrations in human saliva and respiratory mucus (Wang et al. 2004; Robinson et al. 2008; Slots and Slots 2011). When infected individuals cough, sneeze, speak, or simply breathe, particles of saliva and/or respiratory mucus that carry viruses can be easily generated (Fabian et al. 2008; Stelzer-Braid et al. 2009), resulting in an increased risk of viral infection by aerosols.

In an effort to understand and control transmission of viral diseases via aerosols, researchers have generated airborne viruses in laboratories to study their infectivity and survival (i.e., the ability to remain infectious) since the 1930s. Laboratory-generated virus aerosols are commonly produced from liquid suspensions using pneumatic nebulizers such as Collison nebulizers, as the wet dispersion technique simulates many dispersion processes of viruses in the natural environment (Reponen et al. 1997). However, the composition of liquid suspensions from which virus aerosols are generated (also known

as nebulizer suspensions) is known to affect the survival of airborne viruses (Sattar et al. 1987; Sobsey and Meschke 2003). Given that many laboratory studies use artificial nebulizer suspensions (e.g., cell culture media) that do not mimic the natural release of virus aerosols from body secretions (e.g., human saliva), it has been suggested that survival of airborne viruses determined in laboratories may not represent real life situations (Snider et al. 2010).

To better simulate the generation of virus aerosols from human saliva, several researchers have developed a recipe for making artificial saliva and have used it as a nebulizer suspension (Lee 2009; Woo et al. 2010; Woo et al. 2012; Woo 2012). The same artificial saliva was later adopted by the American Society for Testing and Materials (ASTM) to evaluate decontamination efficacy of air-permeable materials and surfaces challenged with bioaerosols (ASTM 2011a; ASTM 2011b). MS2 bacteriophage aerosolized from artificial saliva has been found to survive better than that from deionized (DI) water, but no better than that from 0.25% tryptone solution or 0.3% beef extract (Lee 2009; Woo 2012), suggesting that indeed artificial saliva may affect the survival of airborne viruses differently from other commonly used artificial nebulizer suspensions. However, it remains unclear how closely artificial saliva could represent human saliva in terms of preserving airborne virus infectivity.

The literature on the effect of human saliva on airborne viruses and comparison with other nebulizer suspensions is limited. In one study (Trouwborst and Kuyper 1974), survival of airborne bacteriophage T3 from saliva and 0.1% peptone was found to be

similar at relative humidity (RH) ranging from 20% to 80%, but lower than that from 0.1 M NaCl at low to mid RH. At high RH, highest survival was observed using saliva, followed by peptone and salt. In another study (De Jong et al. 1975), saliva was found to offer less protection to airborne encephalomyocarditis virus than Hanks balanced salt solution over a wide range of RH and the virus decay in saliva was even larger than in water below 40% RH. These results indicate that saliva may not necessarily be more effective in maintaining airborne virus infectivity than artificial nebulizer suspensions, depending on RH. However, in both studies, spray guns were used to produce micrometer-sized particles and the virus aerosols were collected by liquid impingers. One limitation of liquid impingers is that they provide only particle size-integrated results. As demonstrated previously, particle size can significantly affect survival of airborne viruses (Zuo et al. 2013c) as well as their removal by filtration (Zuo et al. 2013b). Therefore, it would be interesting to explore how human saliva affects virus in aerosols as a function of particle size. In addition, liquid impingers are inefficient in collecting submicrometer-sized particles (Hogan et al. 2005). Consequently, the reported infectivity and survival results mainly represent those of micrometer-sized particles. What happens to virus aerosol particles of <0.5 μm, the size of most respiratory particles (Haslbeck et al. 2010; Holmgren et al. 2010), remains unclear.

The objective of this study was to determine how human saliva could affect the infectivity and survival of airborne MS2 bacteriophage in the submicrometer size range and to compare the use of human saliva with artificial saliva and cell culture medium. Due to its non-pathogenicity and ease of propagation, MS2 is one of the most popular

surrogates for human-pathogenic viruses and has been extensively used in various virus aerosol studies including investigation of aerosol generation techniques (Eninger et al. 2009), sampler evaluation (Hogan et al. 2005; Appert et al. 2012), virus survival (Lee 2009; Zuo et al. 2013c), virus inactivation (Woo et al. 2012; Grinshpun et al. 2007), and virus filtration (Eninger et al. 2008a). For these reasons, MS2 was selected in this study.

3.2 Materials and methods

3.2.1 Virus stock

MS2 bacteriophage is a small (27 nm), tailless, non-enveloped, single-stranded RNA coliphage. MS2 bacteriophage (ATCC 15597-B1) was propagated and titrated using *E. coli* famp (ATCC 700891) as host cells. Briefly, 1 mL of virus stock was mixed with 100 mL of log-phase *E. coli* grown in 3% (wt/vol) tryptic soy broth (TSB). After incubation at 37^{o}C for 20 hours with shaking at 60 RPM, the culture was centrifuged at 6000 $\times g$ for 15 minutes and the supernatant was filtered through a 0.45 μm cellulose acetate filter (Vanguard International, Neptune, NJ). The resulting virus stock was aliquoted in 2 mL vials and stored at -80^{o}C until used.

3.2.2 Nebulizer suspensions

Three types of nebulizer suspensions were evaluated, including human saliva (HS), artificial saliva (AS), and artificial saliva with no mucin (ASNM). ASNM was tested to further evaluate the effect of mucin on the survival of airborne MS2.

(i) Whole human saliva was collected from a subject under unstimulated conditions, at least two hours after eating and drinking, using the spitting method (Navazesh 1993). The subject first rinsed the mouth thoroughly using DI water and sat upright with the head slightly tilted forward and the eyes open. Saliva was then allowed to accumulate in the mouth and the subject spitted it out every 1 min into a 50 mL tube until ~45 mL of saliva was collected. The collected saliva was treated with 455 μg/mL streptomycin and 1.5μg/mL fungizone to inhibit microbial growth. Since the composition of saliva varies on a daily basis (Humphrey and Williamson 2001) and is also affected by freezing and thawing (e.g., formation of white precipitates) (Schipper et al. 2007), saliva collected on different days was pooled together, well mixed, aliquoted into 50 mL tubes, and stored at 4^{o}C until used (within seven days of collection). (ii) Artificial saliva was prepared using the same recipe as described elsewhere (Woo et al. 2010). It consisted of ~0.3% various salts and 0.3% mucin from porcine stomach (M1778, Sigma Chemical Co., St. Louis, MO) to simulate the electrolytes and mucus in human saliva (HS), respectively. (iii) Mucin-free artificial saliva was prepared using the salts only. On each day of testing, 4.5 mL of thawed MS2 stock was diluted in 40.5 mL of one the three nebulizer suspensions supplemented with 2 mL of uranine (0.625 g/mL, Fluka, Buchs, Swizerland) and 0.1 mL of antifoam Y-204 (Sigma). Uranine was used as a fluorescent particle tracer (Ijaz et al. 1987; Appert et al. 2012; Zuo et al. 2013c), which allowed the quantitation of particle transport loss in the test system. The titer of freshly prepared nebulizer suspensions ranged from 2×10^{8} to 6×10^{8} PFU/mL.

3.2.3 Experimental setup and test procedure

The experimental setup schematically shown in Figure 3.1 has been described elsewhere (Zuo et al. 2013c). The main element is a one-pass vertical aerosol test tunnel, which has been used in different virus aerosol studies (Appert et al. 2012; Kim et al. 2007; Zuo et al. 2013a; Zuo et al. 2013b; Zuo et al. 2013c). Before each experiment, the tunnel was first purged using HEPA-filtered air at 92 L/min for 15 min to remove any residual particles. MS2 bacteriophage was then aerosolized from one of the nebulizer suspensions using a six-jet Collison nebulizer (Model CN25, BGI Inc., Waltham, MA) operated at 10 psig. The generated MS2 aerosol was mixed and diluted with humidity-controlled and HEPA-filtered room air, entering the tunnel at a flow rate of 92 L/min. The virus aerosol was sampled by a scanning mobility particle sizer (SMPS, Model 3034, TSI, Inc., Shoreview, MN) at 1 L/min to measure the particle number distribution from 10 nm to 470 nm. Simultaneously, some of the aerosol was charge-equilibrated to the Boltzmann distribution using a polonium-210 neutralizer and particles with size of 100, 200, 300, 400, and 450 nm were selected by a differential mobility analyzer (DMA, Model 3071, TSI), one size at a time. The size-classified virus aerosol particles were then collected over a 15 minute duration at a flow rate of 1.0 L/min using a 25 mm diameter gelatin filter (SKC, Inc., Eighty Four, PA) held in a stainless steel holder (Millipore Corp., Bedford, MA). Gelatin filters have very high collection efficiency for MS2 aerosol (Burton et al. 2007). The sampling time was limited to 15 min in order to minimize desiccation, which adversely affects the infectivity of the collected virus (Verreault et al. 2008). Immediately after sampling, the gelatin filter was broken apart using a sterile forceps and dissolved in 1 mL of 1.5% beef extract-0.05 M glycine solution (pH 7.2),

followed by vortexing (American Scientific Products, McGaw Park, IL) at maximum speed for ~10 sec, six times at 1 min intervals. Any unsampled virus aerosol was removed by a HEPA filter located at the outlet of the tunnel.

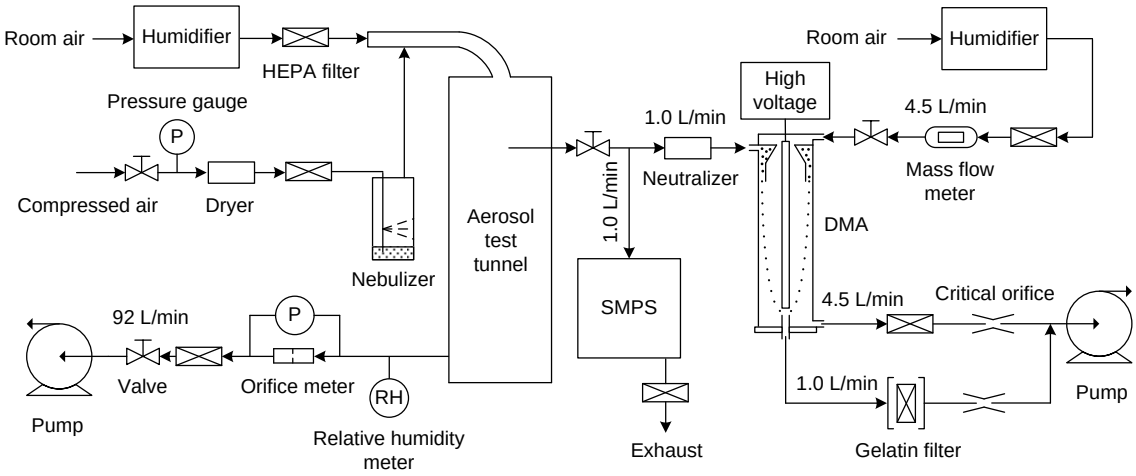

Figure 3.1 Schematic diagram of the experimental setup for the measurement of virus aerosols.

The experiments were performed at a RH of 45±5% and a temperature of 22-24^{o}C with three replicates for each nebulizer suspension. All equipment including the nebulizer, filter holders, and forceps were sterilized prior to testing. The entire setup was enclosed by secondary containment with exhaust ventilation to prevent the release of aerosols into the surrounding laboratory environment.

3.2.4 Sample analysis

Before and after each experiment, a 1 mL sample of nebulizer suspension was collected. Each nebulizer suspension sample and gelatin filter sample was split into three portions. The first portion was diluted in 0.01 mol/L NaOH and the concentration of fluorescence

was measured by a spectrofluorometer (Model RF-5201PC, Shimadzu Scientific Instruments, Columbia, MD) at excitation and emission wavelengths of 485 nm and 515 nm, respectively. The remaining two portions were stored at –80^{o}C until used in analysis of infectious and total virus.

Infectious virus was enumerated using a double agar layer plaque assay (USEPA 2001). Briefly, serially diluted samples in phosphate buffered saline were added to 4 mL of 0.75% tryptic soy agar (TSA) maintained at 48^{o}C along with 0.1 mL of log-phase *E. coli*. This "top agar" was poured onto pre-prepared 1.5% TSA "bottom agar" plates and allowed to solidify. The plates were then inverted, incubated at 37^{o}C for 18 hours, and examined for the production of viral plaques. The plaques were counted and viral titers were expressed as PFU/mL.

Total virus was quantified by qRT-PCR, as described elsewhere (Zuo et al. 2013c). Since qRT-PCR measures both infectious and non-infectious virus, the results are referred to as total virus. Briefly, viral RNA was extracted from 140 µL of each sample and eluted in 40 µL of elution buffer using the QIAamp viral RNA kit (Qiagen, Valencia, CA). The extracted viral RNA (3 µL) was mixed with specific primers and probe (O'Connell et al. 2006) and One Step RT-PCR kit (Qiagen) to a final volume of 20 µL. qRT-PCR was then performed in duplicate in a Mastercycler ep Realplex2 thermocycler (Epperdorf, Hamburg, Germany). Viral RNA extracted from the virus stock of a known titer was serially diluted in RNAse-free water and used to construct standard curves, which translated Ct-values into projected titers in PFU/mL.

3.2.5 Data analysis

To evaluate the effect of nebulization on the stability of virus infectivity and viral RNA in the nebulizer suspensions, two parameters, γ_{IV} and γ_{TV}, were calculated:

$$\gamma_{IV} = \frac{(C_{IV,neb}/C_{F,neb})_a}{(C_{IV,neb}/C_{F,neb})_b} \qquad \gamma_{TV} = \frac{(C_{TV,neb}/C_{F,neb})_a}{(C_{TV,neb}/C_{F,neb})_b}, \qquad [1]$$

which compare the concentration ratio of infectious ($C_{IV,neb}$) or total virus ($C_{TV,neb}$) to fluorescence intensity ($C_{F,neb}$) in the nebulizer suspension before (*b*) and after (*a*) nebulization. The inclusion of $C_{F,neb}$ in the equations takes into account the possible artificial increase of virus concentration due to water evaporation from the suspensions during nebulization (Appert et al. 2012; Zuo et al. 2013c).

To understand how viral content (either infectious or total virus) was distributed among various particle sizes, we defined the virus size distribution, $dC_V(D_p)/d\log_{10}D_p$, a size distribution function particularly for particles carrying virus (Hogan et al. 2005; Zuo et al. 2013c):

$$\frac{dC_V(D_P)}{d\log_{10}D_P} \approx \frac{C_{V,gel}(D_P)V_{gel}}{Q_{gel}t[\Delta\log_{10}D_P]}\frac{1}{f_{+1}(D_P)P(D_P)}, \qquad [2]$$

where $C_{V,gel}$ is the concentration of infectious virus or total virus recovered from the gelatin filter at certain particle size D_p, V_{gel} is the volume of gelatin filter sample, Q_{gel} and *t* are the gelatin filter sampling flow rate and sampling time, $\Delta\log_{10}D_p$ is the logarithm of the width of the size interval of the DMA, f_{+1} is the fraction of singly positively charged particles (Wiedensohler 1988), and *P* is the penetration of particles through the DMA (Reineking and Porstendorfer 1986).

The amount of infectious or total virus carried per particle, $v(D_p)$, was calculated as the ratio of the total amount of virus collected by the gelatin filter to the total number of particles measured by the SMPS at a given particle size:

$$v(D_P) \approx \frac{C_{V,gel}(D_P)V_{gel}}{Q_{gel}t\Delta C_{n,SMPS}(D_P)} \frac{1}{f_{+1}(D_P)P(D_P)}, \quad [3]$$

where $\Delta C_{n,SMPS}$ is particle number concentration measured by the SMPS within a size interval with geometric mean diameter D_p.

To quantify how efficiently infectious virus was recovered, relative recovery of infectious virus (RR_{IV}) was calculated:

$$RR_{IV}(D_P) = \frac{C_{IV,gel}(D_P)/C_{F,gel}(D_P)}{C_{IV,neb}/C_{F,neb}}, \quad [4]$$

where $C_{IV,neb}$ and $C_{F,neb}$ were the averaged values before and after nebulization. The infectious virus concentrations are normalized by fluorescence concentrations to take into account any artificial loss of virus infectivity due to the transport loss of particles (e.g., sedimentation and deposition) in the test system. If there is no inactivation of virus (i.e., 100% survival), then $RR_{IV} = 1$, assuming no measurement error. Therefore, RR_{IV} represents the fraction of infectious virus recovered relative to the fluorescence recovered and it serves as an indication of the survival of airborne virus (Appert et al. 2012; Zuo et al. 2013c). Similarly, we also calculated relative recovery of total virus, RR_{TV}:

$$RR_{TV}(D_P) = \frac{C_{TV,gel}(D_P)/C_{F,gel}(D_P)}{C_{TV,neb}/C_{F,neb}}. \quad [5]$$

One method to quantify the survival of airborne viruses is to compare the ratio of infectious virus to total (both infectious and non-infectious) virus (Fabian et al. 2009; Lee 2009; Woo 2012; McDevitt et al. 2013; Zuo et al. 2013c). The lower the ratio, the poorer the survival. Here, the infectious to total virus ratio (*ITR*) in the aerosol sample was normalized by the same ratio in the nebulizer suspensions:

$$ITR(D_P) = \frac{C_{IV,gel}(D_P)/C_{TV,gel}(D_P)}{C_{IV,neb}/C_{TV,neb}}, \qquad [6]$$

where $C_{IV,neb}$ and $C_{TV,neb}$ were the averaged values before and after nebulization.

Data obtained for different nebulizer suspensions at different particle sizes were statistically analyzed using one-way or multi-way analysis of variance (ANOVA) in MATLAB R2010b. A p-value of ≤0.05 was considered statistically significant.

3.3 Results

In a previous study (Zuo et al. 2013c), we measured MS2 bacteriophage aerosolized from a cell culture medium (i.e., 3% TSB), supplemented with the same amount of uranine and antifoam as in this study. Therefore, those results are also presented here for comparison purposes.

3.3.1 Stability of virus in nebulizer suspensions

Table 3.1 shows the geometric mean and 95% confidence interval of γ_{IV} and γ_{TV} for the four nebulizer suspensions. Neither γ_{IV} nor γ_{TV} was significantly different from unity, suggesting that the composition of nebulizer suspension, along with uranine and antifoam, did not inactivate the virus. In addition, one-way ANOVA showed that there was no

statistically significantly difference in γ_{IV} ($p = 0.429$) or γ_{TV} ($p = 0.142$) among the four nebulizer suspensions.

Table 3.1 Geometric mean (with 95% lower and upper confidence interval) of γ_{IV} and γ_{TV} for the four nebulizer suspensions.

Nebulizer suspension	γ_{IV}	γ_{TV}
Cell culture medium (i.e., 3% TSB)[a]	1.07 (0.44, 2.62)	0.96 (0.48, 1.93)
Human saliva	0.86 (0.63, 1.18)	0.87 (0.41, 1.87)
Artificial saliva	1.08 (0.95, 1.21)	0.66 (0.36, 1.19)
Artificial saliva no mucin	1.13 (0.79, 1.61)	1.12 (0.90, 1.41)

[a] Data from Zuo et al. (2013c)

3.3.2 Particle size distributions

Typical SMPS-measured particle number distributions of virus aerosols generated from the four nebulizer suspensions and their particle statistics are shown in Figure 3.2. The size distributions of TSB and ASNM were generally lognormal with a count median diameter of 76.5 and 64.3 nm, respectively. However, the size of particles generated from HS was bimodally distributed. The primary mode at ~50 nm had a magnitude almost twice that of the secondary mode at ~80 nm. Unlike the abovementioned three nebulizer suspensions, the particle size distribution of AS measured before, during, and after the experiment were multimodal and all different (Figure 3.2.b). During a nebulization period of ~90 min, the two peaks at 15 and 33 nm continued to diminish (with a decrease in number concentration by 62% and 25%, respectively) while a third peak at ~110 nm gradually appeared (with an increase in number concentration by 53%). This large variation with time indicates an unstable output of the Collison nebulizer when AS was nebulized.

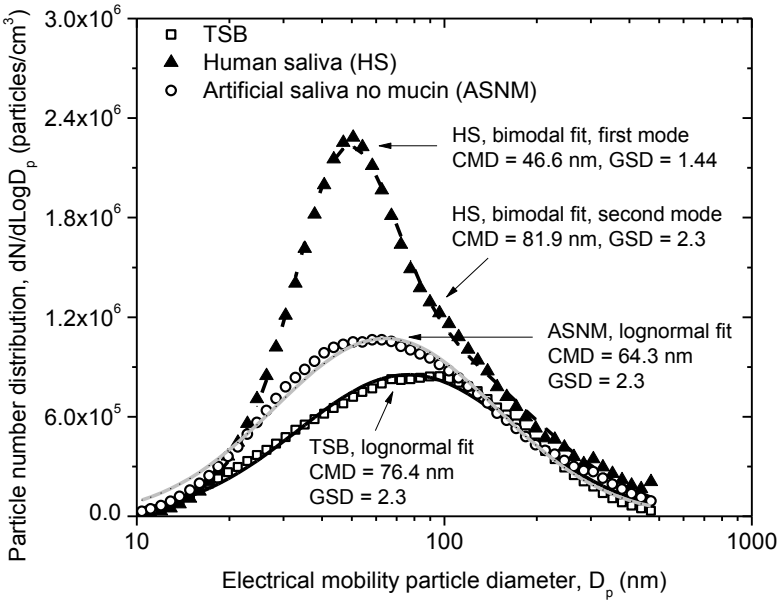

(a)

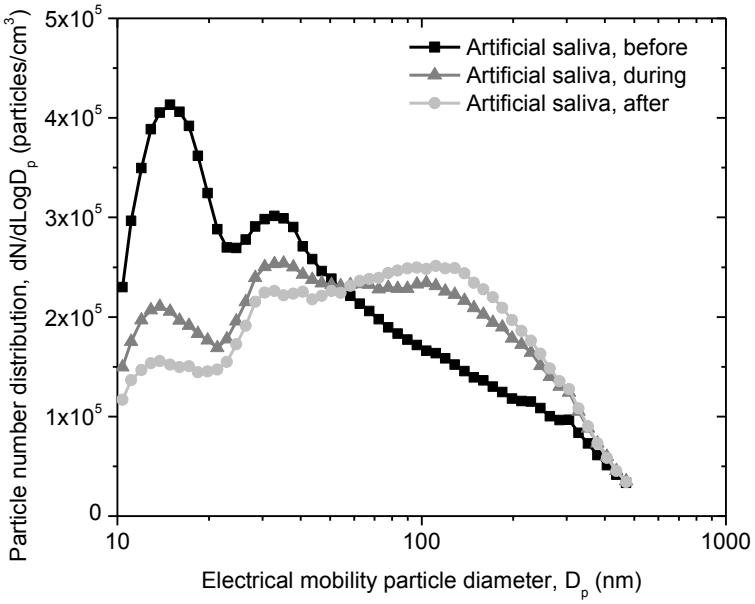

(b)

Figure 3.2 Representative number distributions of virus aerosol particles generated from cell culture medium (TSB), human saliva, artificial saliva without mucin (a), and artificial saliva (b). Also shown are the lognormal and bimodal curve fittings with count median diameter (CMD) and geometric standard deviation (GSD).

3.3.3 Virus size distributions

Figure 3.3 presents the infectious virus and total virus size distributions for the four nebulizer suspensions. The concentration of airborne virus generally increased with particle size and the maximum mean concentration of infectious virus (at 400 or 450 nm) was 3600, 25, 220, and 33 PFU/cm^3 for TSB, HS, AS, and ASNM, respectively, which was several orders of magnitude lower than particle number concentration (Figure 3.2). For all four nebulizer suspensions, the infectious virus and total virus size distributions followed the particle volume distribution better than the particle number distribution, despite the large error bars.

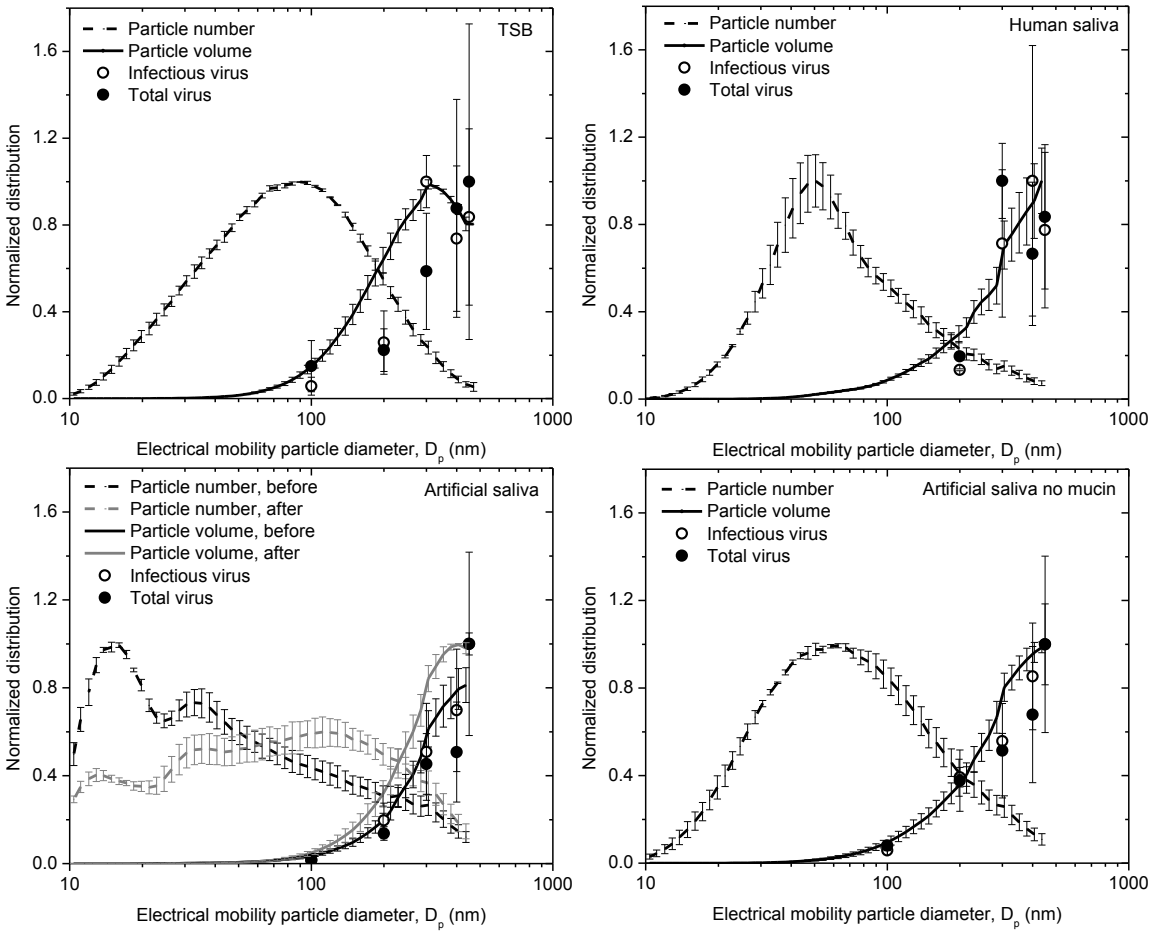

Figure 3.3 Normalized particle number, particle volume, infectious virus, and total virus size distributions for cell culture medium (i.e., 3% TSB), human saliva, artificial saliva, and artificial saliva without mucin. Virus size distributions and particle size distributions were normalized by their highest values and superimposed for easy comparison. Values are means ± one standard deviation (n = 3). Data points of infectious virus and total virus size distributions at 100 nm were not plotted for human saliva since no virus was recovered. Results of TSB are from Zuo et al. (2013c).

3.3.4 Virus carried per particle

As shown in Figure 3.4, the amount of infectious virus (*iv*) and total virus (*tv*) carried per particle increased with particle size for each of the four nebulizer suspensions. Results of curve fitting suggest that the association of *iv* and *tv* with particle size reasonably followed a power law, where the power was not significantly different from 3. However, even for the largest particles (450 nm), *iv* and *tv* were much lower than 1 PFU/particle.

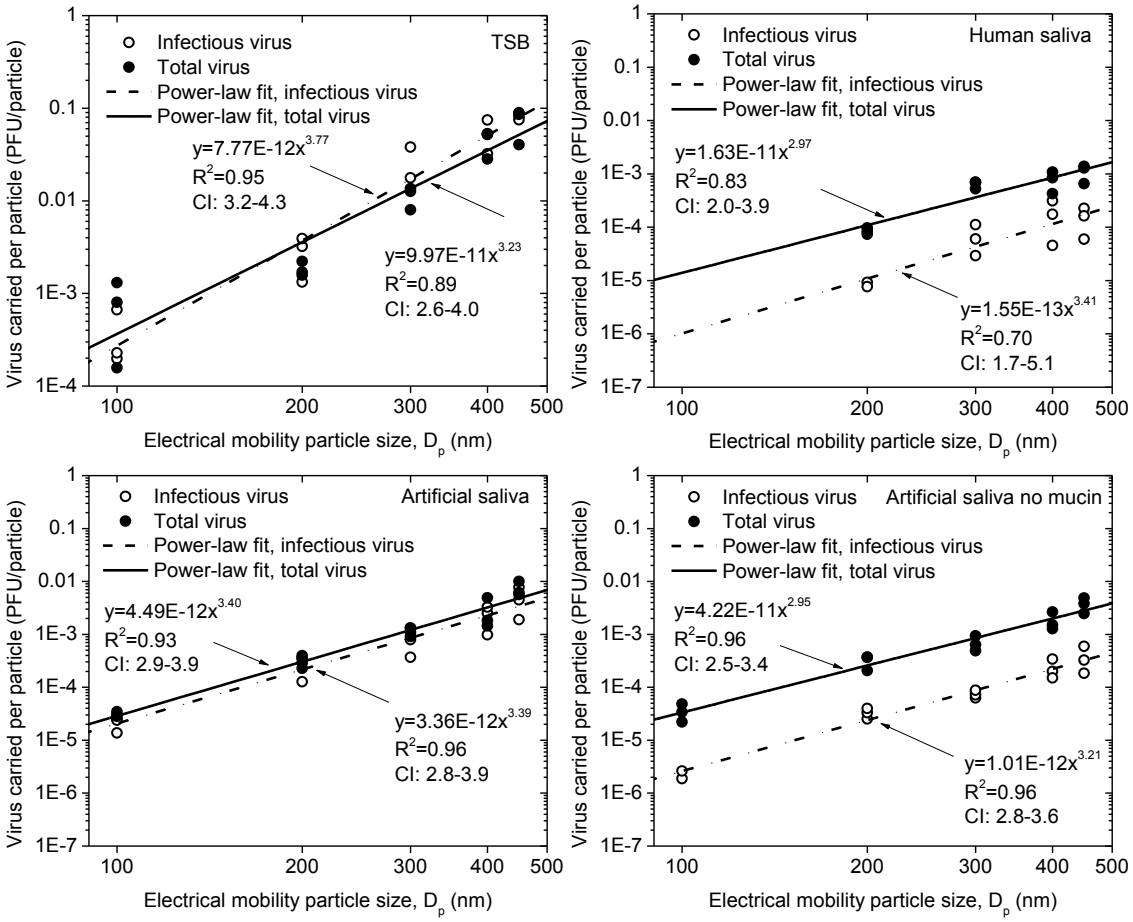

Figure 3.4 Amount of infectious and total virus carried per particle as a function of particle size for cell culture medium (i.e., 3% TSB), human saliva, artificial saliva, and artificial saliva without mucin. Also shown are the curve-fitting results with R-square values and 95% confident interval (CI) of the slopes, where x represents particle size in

nm and y represents virus carried per particle in PFU/particle. Results of TSB are from Zuo et al. (2013c).

3.3.5 Relative recovery of infectious virus

RR_{IV} was plotted in Figure 3.5 as a function of particle size for the four nebulizer suspensions. Two-way ANOVA showed that RR_{IV} was independent of particle size ($p = 0.168$), but significantly depended on the type of nebulizer suspension ($p < 0.001$). RR_{IV} of TSB and AS were similar and much higher than that of HS and ASNM. Particle size-averaged RR_{IV} was 0.285, 0.032, 0.218, and 0.024 for TSB, HS, AS and ASNM, respectively.

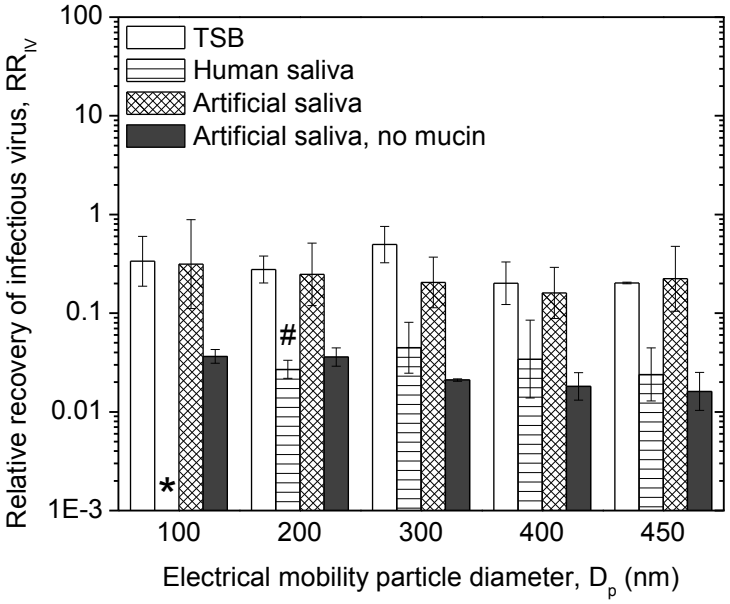

Figure 3.5 Relative recovery of infectious virus for the four nebulizer suspensions. Each bar represents geometric mean ± one standard deviation of the mean (n = 3). The asterisk sign (*) denotes that infectious virus was below the limit of detection in all the three

samples. The pound sign (#) denotes that infectious virus was recovered in only two of the three samples. Results of TSB are from Zuo et al. (2013c).

3.3.6 Relative recovery of total virus

Similar to RR_{IV}, RR_{TV} (Figure 3.6) was also independent of particle size (two-way ANOVA, p = 0.853). Particle size-averaged RR_{TV} was 0.265, 0.130, 0.414, and 0.215 for TSB, HS, AS and ASNM, respectively. Therefore, RR_{TV} was generally comparable between the four nebulizer suspensions, as confirmed by statistical analysis (two-way ANOVA, p = 0.053).

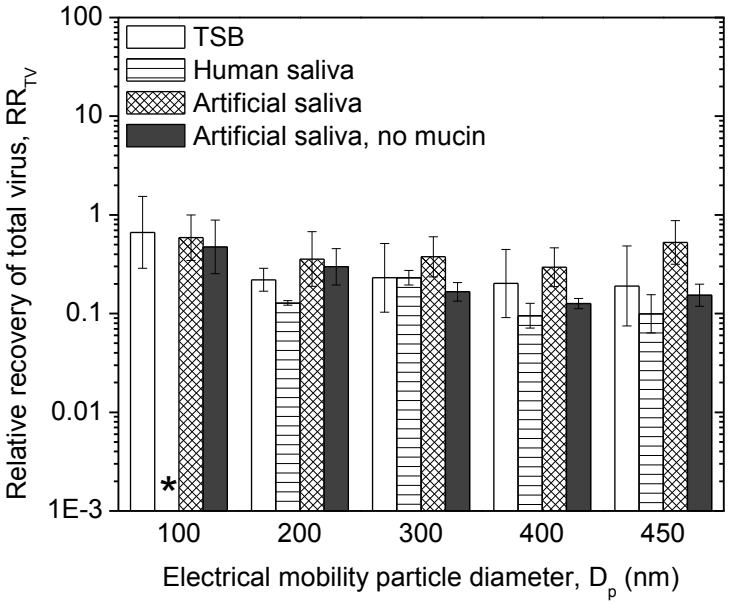

Figure 3.6 Relative recovery of total virus for the four nebulizer suspensions. Each bar represents geometric mean ± one standard deviation of the mean (n = 3). The asterisk sign (*) denotes that the viral RNA was below the limit of detection in all three samples. Results of TSB are from Zuo et al. (2013c).

3.3.7 Infectious-to-total virus ratio

Figure 3.7 shows *ITR* for the four nebulizer suspensions at different particle sizes. Similar to RR_{IV} and RR_{TV}, particle size had little effect on *ITR* (two-way ANOVA, p = 0.399). However, *ITR* was strongly affected by the type of nebulizer suspension (two-way ANOVA, p < 0.001). TSB gave the highest particle size-averaged *ITR* (0.915), followed by AS (0.527), HS (0.242), and ASNM (0.114).

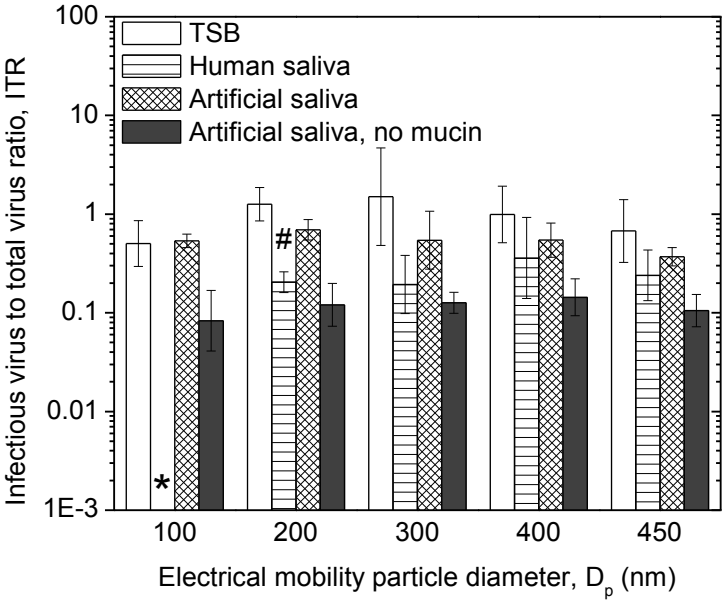

Figure 3.7 Infectious-to-total ratio. Each bar represents geometric mean ± one standard deviation of the mean (n = 3). The asterisk sign (*) denotes that infectious virus and viral RNA were below the limit of detection in all three samples. The pound sign (#) denotes that infectious virus was recovered in only two of the three samples. Results of TSB are from (Zuo et al. 2013c).

3.4 Discussion

3.4.1 Effect of nebulization on virus survival

The high shear stress during nebulization often substantially reduces the viability of bacteria (Griffiths and DeCosemo 1994). However, values of γ_{IV} and γ_{TV} (Table 3.1) indicate that neither infectivity nor viral RNA of MS2 bacteriophage was affected by the nebulization stress. This finding is consistent with the literature, where both enveloped and non-enveloped viruses were aerosolized from cell culture media (Ijaz et al. 1987; Kim et al. 2007; Appert et al. 2012; Zuo et al. 2013c). The four nebulizer suspensions gave similar γ, suggesting that the insensitivity of virus to nebulization stress is not unique for cell culture media but occurs for other suspensions also. One possible reason for the insensitivity could be the small physical size and inertia of the virus, which makes it experience lower nebulization stress than bacteria (Kim et al. 2007).

3.4.2 Particle size distribution

The particle size distributions generated from the four nebulizer suspensions did not reflect the physical size of the virus itself (Figure 3.2). Instead, they were primarily determined by the composition of the nebulizer suspensions. Due to the higher volume fraction of solid material (solute) in the nebulizer suspension, the size distribution of TSB gave a mean diameter larger than that of ASNM. Interestingly, the size distribution of HS was bimodal, indicating two different sources of particles. One source was certainly the various chemicals (e.g., salts and uranine) dissolved in the suspension, similar to TSB and ASNM. The other source might come from salivary micelles. As revealed by electron microscopy, salivary micelles are multi-component protein complexes in HS with

globular structures (Rykke et al. 1995). They are often in the form of individual particles or aggregates, ranging from 50-400 nm (Rykke et al. 1995; Soares et al. 2004), with mean size close to the second mode of the bimodal distribution. The addition of mucin to ASNM changed the size distribution from lognormal to multimodal (Figure 3.2). Mucins are large glycoproteins with long-chain structures that tend to be entangled with each other (Bansil and Turner 2006). Due to the high recirculation rate of the suspension during nebulization (e.g., once every 6 sec) (May 1973), shear stress might gradually break up these entanglements, thus causing unstable output from the nebulizer.

3.4.3 Virus size distribution and virus carried per particle

Similar to TSB (Zuo et al. 2013c), HS, AS, and ASNM produced infectious and total virus size distributions that were generally represented by the particle volume distribution (Figure 3.3), suggesting that the amount of virus carried per particle was proportional to particle volume. This finding is further supported by the curve fitting results for *iv* and *tv* (Figure 3.4), which showed a power of ~3. A similar trend was also observed for various animal viruses aerosolized from cell culture media in the submicrometer (Zuo et al. 2013c) and cicrometer size range (Ijaz et al. 1987; Appert et al. 2012). Assuming that one PFU represents one infectious virus, values much lower than 1 PFU/particle for *iv* and *tv* (Figure 3.4) indicate that only a small fraction of the generated particles actually carried virus. This is because conventional Collison nebulizers inevitably generate many virus-free residual particles, even if suspensions with high virus titers are used, as explained earlier (Zuo et al. 2013c).Therefore, compared with cell culture medium, the use of non-

cell culture medium did not change how virus was distributed among or carried by particles of different sizes.

3.4.4 Effect of nebulizer suspensions on virus survival

Virus survival was a strong function of the type of nebulizer suspension. Survival of airborne MS2 was highest for TSB and AS, moderate for HS, and lowest for ASNM, as indicated by the values of RR_{IV} (Figure 3.5) and *ITR* (Figure 3.7). Although it is well known that the composition of nebulizer suspensions plays a significant role in survival of airborne viruses (Sattar et al. 1987; Sobsey and Meschke 2003), how it preserves or reduces virus infectivity is less understood.

Multiple inactivation mechanisms have been proposed and reviewed regarding the effect of nebulizer suspension composition (De Jong and Winkler 1968; Yang and Marr 2012). However, for MS2 bacteriophage, the loss of its survival (RR_{IV}< 1 and *ITR* <1) could be most plausibly explained by the exposure to an air-water interface (AWI), where the virus experiences “deforming forces”, which causes irreversible folding and rearrangement of virus protein molecules and thus inactivates the virus (Trouwborst and De Jong, 1973; Trouwborst et al. 1974). Considering the moderate RH used during the experiments and the highly hygroscopic nature of uranine (Chan et al. 1997) and other salts (e.g., NaCl) used in the nebulizer suspensions, the generated particles might carry substantial water content rather than being completely dried, thus creating AWI. MS2 bacteriophage, though non-enveloped, is very hydrophobic (Thompson and Yates 1999) and thus tends to accumulate at the AWI. The increased concentration of salts in the generated droplets

due to water evaporation decreases the size of the virus double layer, further promoting virus adsorption at the AWI (Trouwborst et al. 1974; Thompson and Yates 1999). All these observations suggest that inactivation of MS2 in the aerosol phase could be a combined result of exposure to AWI and the hygroscopic nature of the particles.

The addition of proteins to liquid suspensions may reduce the solution surface tension, which makes it more difficult for the virus to reach the AWI, thereby reducing virus inactivation (Trouwborst et al. 1974; Thompson and Yates 1999). This may be the reason why MS2 nebulized from protein-rich TSB survived much better than that from salt-dominant ASNM. Other proteinacious solutions such as peptone were also reported to increase the survival of airborne MS2 (Trouwborst and De Jong 1973; Dubovi and Akers 1970).

The use of mucin significantly enhanced virus survival (Figure 3.5 and 3.7). Woo et al. (2012) showed that the cross-linking network of mucin forms a thin layer to encapsulate virus in aerosol particles. This layer may reduce virus exposure to AWI and thus boost survival. However, the protection level offered by mucin may not monotonically increase with its concentration. For example, Schoenbaum et al. (1990) recovered much less infectious pseudorabies virus when mucin concentration increased from 1% to 2%. HS, although also containing mucin, gave a much lower survival than AS, suggesting that exposure to AWI was probably not the only inactivation mechanism. Airborne foot-and-mouth disease virus has been found particularly sensitive to an undefined organic molecule present in bovine salivary fluid (Barlow and Donaldson 1973). A similar

situation may also exist for MS2 in HS, especially considering the numerous trace components in HS (Humphrey and Williamson 2001) and many of them possess antiviral activities (Malamud et al. 2011).

3.4.5 Instability of viral RNA in aerosol

RR_{TV}<1 (Figure 3.6) suggests that viral RNA was not fully preserved in aerosol form. The average (1-RR_{TV})/(1-RR_{IV}) (i.e., the fraction of virus inactivation due to viral RNA damage) was 0.97, 0.89, 0.72, and 0.76 for TSB, HS, AS, and ASNM, respectively, suggesting that inactivation of airborne MS2 was largely due to its damaged viral RNA. Inactivation of several enveloped viruses, however, has been shown to result mainly from their damaged envelope proteins and/or viral capsids (Zuo et al. 2013c). Perhaps a virus envelope could protect viral RNA more effectively than viral capsid in aerosol form. The exact inactivation mechanisms could be potentially determined using the promising methods described by Wigginton et al. (2012).

The instability of viral RNA also raises the question of using viral nucleic acids as a particle tracer for virus aerosol studies. If viral nucleic acids degrade in aerosol, then infectious to total virus ratio (*ITR*), which is often used in the literature (Fabian et al. 2009; Lee 2009; Woo 2012; McDevitt et al. 2013; Zuo et al. 2013c) as an indicator for airborne virus survival, may underestimate it. An ideal particle tracer must be highly stable in aerosol form and be easily quantifiable so that the tracer concentration is directly proportional to virus concentration. From this viewpoint, uranine is still the most reliable particle tracer (Ijaz et al. 1987; Verreault et al. 2008).

3.4.6 Effect of particle size on survival

The survival of airborne MS2 was found to be a weak function of particle size (Figures 3.5 and 3.7). However, large particle size has been found to increase virus survival due to the shielding effect (Woo et al. 2012; Zuo et al. 2013c) of other material. It is possible that the size of particles sampled (100-450 nm) was already much larger than the physical size of the MS2 virus (27 nm), so further increase in particle size did not enhance survival. Woo (2012) extended the measurement of MS2 down to 30-230 nm and did observe an increase of survival with increased particle size.

3.4.7 Use of natural nebulizer suspensions for risk assessment

To assess the risk of airborne transmission of viral diseases, information on survival of viruses in aerosol is of critical importance. However, as clearly demonstrated in this study, artificial nebulizer suspensions, even artificial saliva, did not produce the same effect as human saliva on the infectivity and survival of airborne MS2 bacteriophage. Significant differences in the survival of several veterinary viruses between cell culture media and animal salivary fluid were also reported (Barlow and Donaldson 1973; Elazhary and Derbyshire 1979a, 1979b, 1979c). These findings strongly suggest that the use of artificial nebulizer suspensions may over- or underestimate the survival of airborne viruses in real life situations, and therefore negatively impact risk assessment. To increase the clinical or epidemiological values of a study, the use of natural nebulizer suspensions is recommended. However, we should be cautious about 1) the potential unstable aerosol output from nebulizers (e.g., AS in our study), particularly when aerosol

has to be sampled for a prolonged time period and 2) the possible PCR inhibition by natural suspensions, as shown elsewhere (Detmer et al. 2011).

3.4.8 Limitations

One of the main limitations in this study is that the saliva used came from only one subject. Given that there exists large inter-subject variation in terms of salivary components and antiviral properties of saliva (Humphrey and Williamson 2001; White et al. 2009; Malamud 2011), saliva from multiple donors should be tested in the future to determine variation in the population and to allow intra-study comparison. In addition, only one value of RH was tested in these experiments. Several studies (Barlow and Donaldson 1973; Elazhary and Derbyshire 1979a, 1979b, 1979c) have found that RH affects how well cell culture media and natural fluids protect airborne viruses. Moreover, although uranine was used as a particle tracer, it changed the composition of the nebulizer suspensions and could have potentially affected virus survival. For example, uranine has been shown to be toxic to airborne virus (Berendt and Dorsey 1971). The effect of RH and uranine on survival of airborne viruses warrants further investigation.

3.5 Supplemental information

3.5.1 Use of gelatin filters for sampling infectious virus aerosols

Filters are usually not recommended for collecting infectious virus aerosols, because of the detrimental effect of desiccation during sampling (Verreault et al. 2008). To evaluate whether gelatin filters would impose sampling stress on the collected virus, an additional experiment was designed and repeated in triplicate by running two gelatin filters in

parallel. After sampling airborne MS2 at 1 LPM for 3 min, one filter was immediately analyzed by plaque assay, while the other was exposed to HEPA-filtered air for an additional 15 min (to simulate the level of desiccation experienced by the collected virus during sampling) and then analyzed. One-way ANOVA suggested that there was no significant difference ($p = 0.737$) between the exposed ($7.4 \times 10^5 \pm 1.1 \times 10^5$ PFU/mL) and unexposed samples ($7.7 \times 10^5 \pm 0.9 \times 10^5$ PFU/mL). These results are similar to what has been reported elsewhere (Jaschhof 1992; Grinshpun et al. 2007) and further confirm that gelatin filters caused minimum sampling stress for airborne bacteriophages, which may be attributed to the high moisture content of the gelatin.

As there was little nebulization and sampling stress, the loss of virus infectivity in the present experiments seems to occur primarily in the aerosol phase.

3.5.2 Use of qRT-PCR technique for quantifying total virus

One concern for the use of qRT-PCR technique for quantifying total virus is that different nebulizer suspensions (especially HS) might have various contaminants (e.g., RNase), which can degrade viral RNA to different levels. If this is true, then qRT-PCR may be an inaccurate method and it would be invalid to compare the recovery of total virus from different nebulizer suspensions.

To test this possibility, MS2 stock of known titer was ten-fold serially diluted in 3% TSB, HS, and AS supplemented with uranine and antifoam (i.e., the same three suspensions as used in the aerosol experiments). Viral RNA was extracted from the samples and

analyzed by qRT-PCR. Meanwhile, viral RNA was extracted from the same MS2 stock, ten-fold serially diluted in RNAse free water, and analyzed by qRT-PCR (i.e., the same method as used in the aerosol study). As shown in Figure 3.8, the standard curve prepared using viral RNA diluted in RNase-free water was similar to those prepared using TSB, HS, or AS as a diluent, suggesting that there was little RNA degradation due to the presence of different nebulizer suspensions. Therefore, it is concluded that qRT-PCR used in this study is a valid technique for the quantification of total virus.

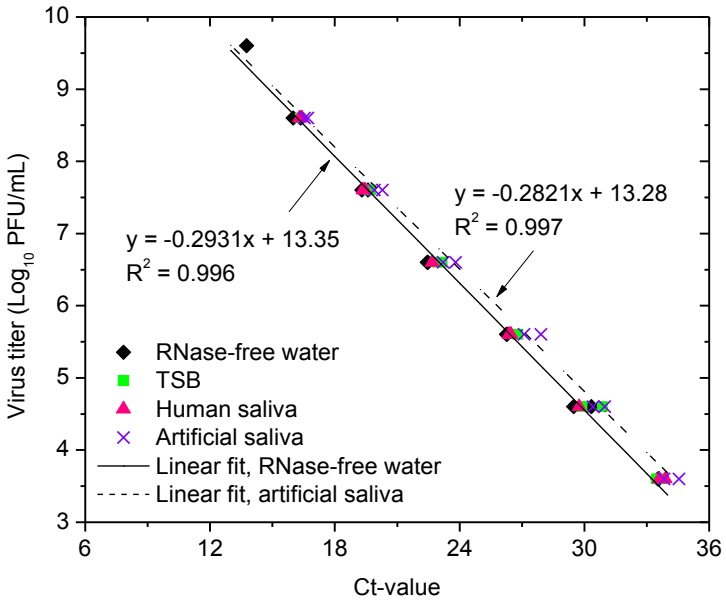

Figure 3.8 Standard curves made from MS2 viral RNA serially diluted in RNase-free water, 3% TSB, human saliva, and artificial saliva. Also shown are the linear regression curves and results for RNase-free water and artificial saliva, where x represents Ct-value and y represents virus titer in Log_{10} PFU/mL.

3.5.3 Effect of human saliva on animal viruses

Although MS2 is one of the most popular model viruses used in the field of virus aerosols, unfortunately it has been found to be a poor surrogate for certain human and animal viruses in the aerosol phase (Appert et al. 2012; Zuo et al. 2013c). Given the fact that the effect of nebulizer suspensions generally varies for different viruses (Satter et al. 1987), it is therefore difficult to predict the effect of human saliva and artificial suspensions on airborne human viruses simply based on the results of MS2 reported in this study. In order to answer the ultimate question (i.e., the role of human saliva in airborne transmission of viral diseases), it would be best to use surrogates with closer characteristics to human viruses than MS2.

An attempt was made to recover swine influenza virus (SIV; A/swine/Minnesota/2010 [H3N2]), a surrogate for human influenza virus, aerosolized from human saliva using the same test protocol and apparatus as described in Section 3.2. No infectious virus was recovered in any of the aerosol samples, in contrast to the high recovery when SIV was aerosolized from cell culture medium (see Section 2.3). The virus titer in the nebulizer suspension was found to be from 3.2×10^{3} to 6.8×10^{3} $TCID_{50}$/mL, more than ten times lower than expected (The titer of the SIV stock was around 3.2×10^{5} $TCID_{50}$/mL and after dilution in human saliva by approximately ten times, the titer of the nebulizer suspension should be around 3×10^{4} $TCID_{50}$/mL). Such low virus titer in the nebulizer suspension was probably one of the reasons why no infectious virus was detected in the aerosol samples. This phenomenon also motivated us to perform the following incubation experiments.

SIV was first mixed with human saliva, uranine, and antifoam (with the same mixing ratios as used in the nebulizer suspension for the aerosol experiments) and then incubated at room temperature for up to three hours (a time period twice as long as one aerosol experiment). The mixture was analyzed in duplicate by infectivity assay and qRT-PCR at incubation times of 0, 90, and 180 min. The same experiment was later repeated using avian influenza virus (AIV; A/chicken/Maryland/2007 [H9N9]) and transmissible gastroenteritis virus (TGEV; Purdue strain), which were used as surrogates for human influenza virus and Severe Acute Respiratory Syndrome (SARS) coronavirus, respectively. For all three viruses, the concentration of infectious virus decreased by approximately one log while the concentration of total virus generally remained constant during incubation (Figure 3.9), suggesting that human saliva had antiviral properties against these three animal viruses, probably by neutralizing virus envelope proteins, not viral nucleic acids. Similar virucidal effect of human saliva against influenza virus was also reported by White et al. (2009). The same incubation experiment, however, showed no significant decrease in virus titer for MS2 bacteriophage, suggesting that MS2 was resistant to human saliva. Although the low virus titer in the nebulizer suspensions prevented us from making any solid conclusions regarding the relative protection effect of human saliva and artificial nebulizer suspensions on airborne animal viruses, the antiviral properties of human saliva revealed by the incubation experiments are expected to contribute to the inactivation of animal or similar human viruses in the aerosol phase.

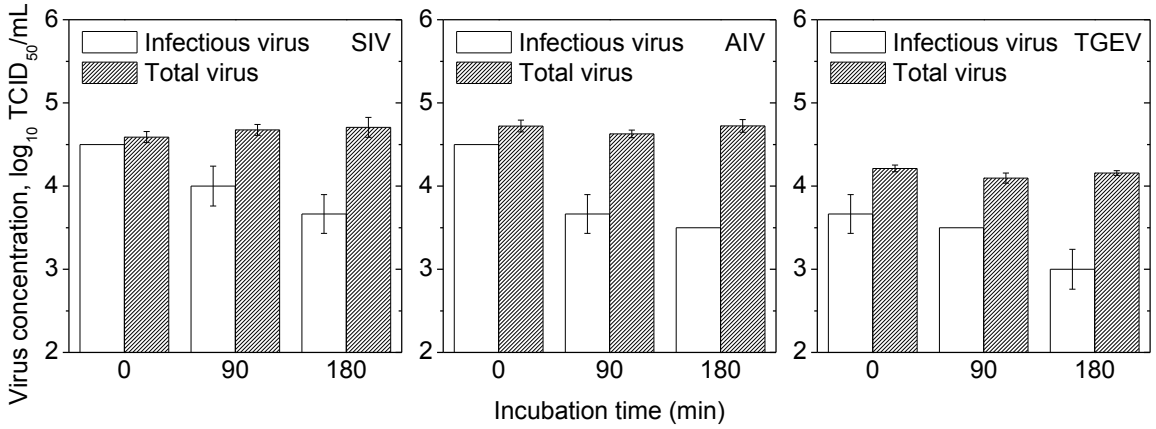

Figure 3.9 Concentration of infectious virus and total virus (viral RNA) for swine influenza virus (SIV), avian influenza virus (AIV), and transmissible gastroenteritis virus (TGEV) mixed with human saliva after different incubation periods at room temperature. Each bar represents mean ± one standard deviation (n = 2).

Chapter 4: Performance Evaluation of Filtering Facepiece Respirators Using Human Adenovirus and Influenza Virus Aerosols

4.1 Introduction

Respiratory protection devices, such as N95 respirators, have been widely used as an infection control measure in recent outbreaks of H5N1 and H1N1 influenza pandemics. However, assessing the efficacy of respirators and other personal protective equipment in reducing the airborne transmission of influenza is a research gap that remains to be filled (Aiello et al. 2010).

Performance of respirators against virus aerosols has been widely investigated, but most studies have used MS2 bacteriophage as the challenge aerosol (Balazy et al. 2006; Einger et al. 2008a; Einger et al. 2008b), whose physical characteristics do not well represent those of human pathogenic viruses. Two recent studies used influenza virus aerosol and measured its penetration through N95 respirators (Borkow et al. 2010; Richardson and Hofacre 2010). However, the size information of the generated virus aerosol and the physical penetration (i.e., particle number penetration) were not reported. In the present study, we compared the physical penetration and virus infectivity penetration through respirators. In addition, we examined whether the physical penetration depended on the type of challenge virus aerosol used.

4.2 Methods

Three models of commercially available filtering facepiece respirators were used for this study. Models A and C were National Institute of Occupational Safety and Health (NIOSH) -certified N95 respirators while model B was not. Before the test, the periphery of each respirator was sealed onto a plexiglas plate with a circular hole in the center. The plexiglas plate was then sandwiched between gaskets and held in place by a pneumatic chuck in an aerosol test tunnel (Figure 4.1).

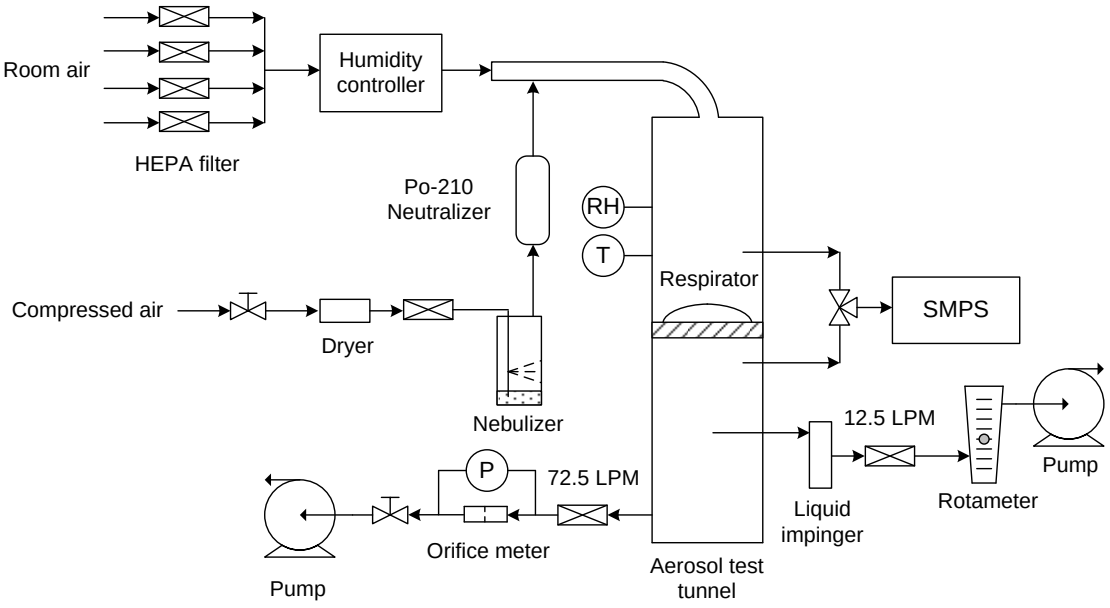

Figure 4.1 Schematic diagram of the experimental setup for respirator testing using virus aerosols.

Human adenovirus (serotype-1) and H3N2 swine influenza virus (SIV; A/swine/Minnesota/2010) were obtained from the Veterinary Diagnostic Laboratory at the University of Minnesota. Virus aerosol was generated using a six-jet Collison

nebulizer operated at 10 psi, loaded with 5 mL thawed virus stock diluted in 45 mL minimum essential medium (MEM) with 0.1 mL antifoam A. The generated virus aerosol passed through a Po-210 charge neutralizer, mixed with relative humidity-controlled (40-50%) and HEPA-filtered room air, and challenged the respirator at a flow rate of 85 LPM. Virus aerosol was sampled upstream and downstream of the respirator using a scanning mobility particle sizer (SMPS) (Model 3034, TSI, Shoreview, MN). The physical penetration (i.e., particle number distribution) was then determined as a ratio of downstream to upstream particle number concentration as a function of particle size and adjusted by a correction factor to address particle losses in the sampling system (Lee et al. 2008).

Since human adenovirus survives much better in aerosol form than SIV (data not shown), human adenovirus was selected for measuring its infectivity penetration through the respirators. An AGI-30 liquid impinger filled with 20 mL MEM was used to collect virus aerosols for 15 min at 12.5 LPM through the downstream sampling port both with and without a respirator in the tunnel. The sampling with a respirator measured virus concentration penetrating through the respirator, whereas the sampling without a respirator quantified concentration of the challenge virus. The infectivity penetration was then calculated as the ratio of the two values. The collection liquid was then analyzed using an endpoint dilution assay (Appert et al. 2012), with results expressed as median tissue culture infectious dose per unit volume of the collection liquid in the impinger ($TCID_{50}$/mL).

All tests were repeated in triplicate using three samples of each respirator model at a temperature at 23-25 ^{o}C. Data were analyzed by analysis of variance (ANOVA).

4.3 Results

The size distribution of the challenge adenovirus and SIV aerosols was similar, generally following a log-normal distribution with count median diameter of 48-52 nm and a geometric standard deviation of 2.0-2.1. The non-N95 respirator (model B) gave higher penetration than the other two models when challenged by different virus aerosols (Figure 4.2). The penetration curve exhibited an inverted bell shape, with the highest penetration of 3-6.5% and the most penetrating particle size at 40-60 nm, which agrees well with results obtained using MS2 bacteriophage and inert NaCl aerosols for respirators with electret filter media (Balazy et al. 2006; Einger et al. 2008a; Einger et al. 2008b). As indicated by the error bars in Figure 4.2, large sample-to-sample variation was observed.

Integrated physical penetration at particle sizes representing the nominal virus size (70-90 nm for adenovirus and 80-120 nm for SIV) and larger size was determined (Table 4.1). In all cases, SIV demonstrated greater penetration than human adenovirus. The penetration difference between human adenovirus and SIV was statistically significant ($P < 0.05$) for respirator model C, but not for model A, however. For model B, the difference was significant only in the larger particle size range.

The challenge human adenovirus titer (measured without a respirator in the tunnel) ranged from $10^{4.25}$ to $10^{4.75}$ $TCID_{50}$/mL. However, no infectious virus was recovered once the respirators were inserted in the tunnel. Using the lower detection limit of the endpoint dilution assay (10 $TCID_{50}$/mL), the infectivity penetration was measured at <0.0398 ± 0.014% for model A, <0.0480 ± 0.014% for model B, and <0.0224 ± 0.008% for model C, close to values reported elsewhere (Borkow et al. 2010).

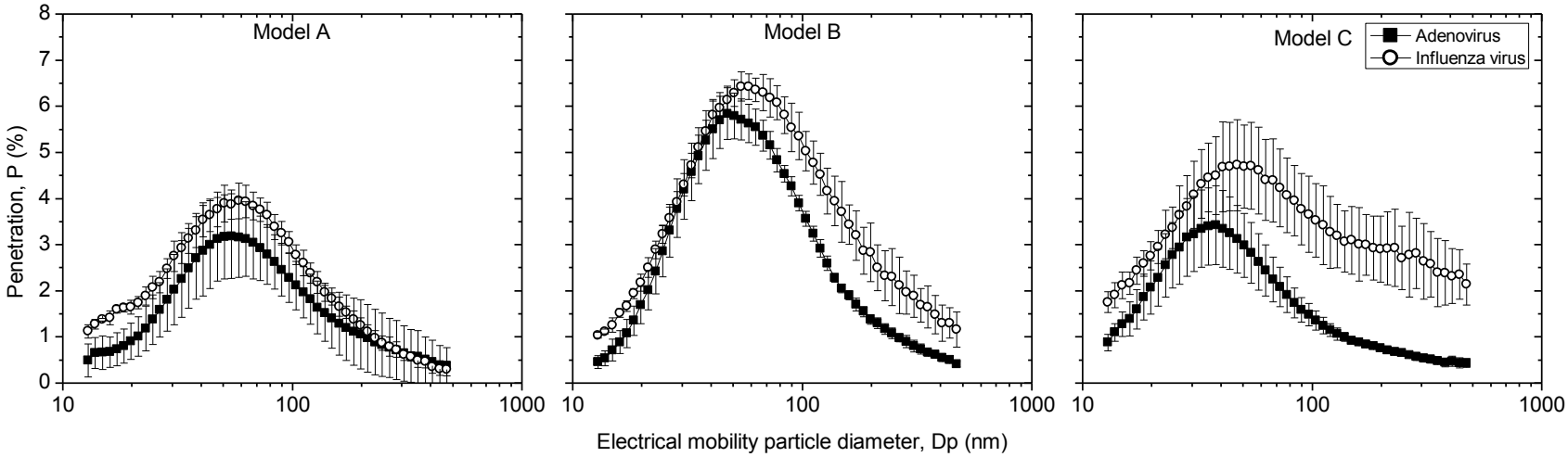

Figure 4.2 Physical (particle number) penetration of human adenovirus virus and swine influenza virus aerosols through three models of filtering facepiece respirators as a function of particle size. Values are means with error bars representing ± one standard deviation based on the measurement of three samples of each model.

Table 4.1 Penetration (mean ± one standard deviation) of adenovirus and swine influenza virus aerosols.

Respirator	Penetration at nominal virion size (%)			Integrated penetration over the size range tested (%)		
	Adenovirus, $P_{70\text{-}90\ nm}$	Influenza virus, $P_{80\text{-}120\ nm}$	P-value	Adenovirus, $P_{70\text{-}470\ nm}$	Influenza virus, $P_{80\text{-}470\ nm}$	P-value
Model A	2.71 ± 0.62	2.96 ± 0.24	0.564	1.91 ± 0.50	2.22 ± 0.20	0.381
Model B	4.73 ± 0.24	5.24 ± 0.46	0.166	3.12 ± 0.16	4.19 ± 0.49	0.022*
Model C	1.85 ± 0.36	3.63 ± 0.80	0.024*	1.32 ± 0.19	3.30 ± 0.76	0.012*

*P-value less than 0.05

4.4 Discussion

Particle size dependent penetration curves were determined for the three models of respirators and compared using two virus aerosols as surrogates for human pathogenic viruses. As expected, respirator performance varied among different models. SIV gave significantly higher physical penetration than adenovirus in some cases, possibly due in part to the different dielectric constant of viruses (Eninger et al. 2008b). However, the large sample-to-sample variation may overshadow the potential penetration difference related to the different type of challenge virus aerosol used. Tests using filter media with better uniformity may help address this issue.

Human adenovirus aerosol gave an infectivity penetration approximately two orders of magnitude lower than the physical penetration, suggesting the latter is a conservative estimate for evaluating respirator performance against virus aerosols. The large difference between physical and infectivity penetration might be related to the fact that the SMPS can easily detect particles at the nominal virion size while the liquid impinger has a physical collection efficiency of only ~10% at 100 nm (Hogan et al. 2005). Other factors possibly contributing to the low infectivity penetration could be the low virus titer in the nebulizer, the relatively low sensitivity of the endpoint dilution assay, and the rapid decay of airborne adenovirus infectivity (Miller and Artenstein 1967), e.g., a mean decay rate of 2.9-3.6%/min. With increased concentration of challenge virus aerosol, improved sampling and infectivity assay methods, and better airborne virus stability, much higher infectivity penetration was found for MS2 aerosol (Eninger et al. 2008a). The above findings may also indicate that not all the generated particles contain infectious virus.

Work is currently underway in our laboratory to investigate the association between virus content and its carrier particle size.

4.5 Additional information

This study on the respirator performance against human adenovirus and swine influenza virus aerosols (Chapter 4) was finished in 2012. Since then, we have worked on the measurement of laboratory-generated animal virus and MS2 bacteriophage aerosols as a function of particle size (Chapter 2) and type of nebulizer suspensions (Chapter 3) and later performed another virus aerosol filtration study (Chapter 5). The results found in these follow-up studies provide a better explanation for the different physical (particle number) penetration between human adenovirus and SIV aerosols through respirators (Figure 4.2 and Table 4.1) observed in this study, which is presented as follows.

The much higher dielectric constant of viruses than inert particles (e.g., NaCl) has been used to explain the lower particle number penetration of virus aerosols than inert aerosols through electret filter media at similar particle sizes (Eninger et al. 2008b). Therefore, in this study (Chapter 4; Zuo et al. 2013b), it was also speculated that the difference in particle number penetration between human adenovirus and SIV aerosol might be caused by the different dielectric constant of the two viruses. However, our later studies found that in fact only a small fraction of particles generated by Collison nebulizer carry virus (e.g., on average less than 1% of 100 nm particles carry virus), even if a nebulizer suspension with high virus titer is used (Zuo et al. 2013c; Zuo et al. 2014). Instead, the majority of the nebulizer output is residue particles coming from the solute dissolved in

nebulizer suspensions (Zuo et al. 2013c; Zuo et al. 2014). Given that human adenovirus and SIV were aerosolized from the same nebulizer suspension (i.e., MEM), it is expected that most human adenovirus and SIV aerosol particles would have similar dielectric constant (to that of MEM) and consequently give similar particle number penetration.

One more likely reason for the difference in the particle number penetration between human adenovirus and SIV is probably the decrease in respirator penetration due to virus aerosol particle loading. In a later virus aerosol filtration study (Chapter 5), a new sample of respirator model A was continuously loaded with MS2 bacteriophage aerosol for up to 40 min. During the respirator loading, the upstream and downstream particle number distributions were measured alternately using an SMPS to determine particle size dependent penetration as a function of loading time. As shown in Figure 4.3, there was a clear decrease in the penetration with increased loading time, especially at particle sizes close to the most penetrating particle size. Considering the fact that the respirators were first tested using SIV aerosol in this study (Chapter 4; Zuo et al. 2013b), it is possible that when the same respirators were further challenged with human adenovirus aerosol, they had been partially loaded and therefore gave a lower particle number penetration than that of SIV aerosol.

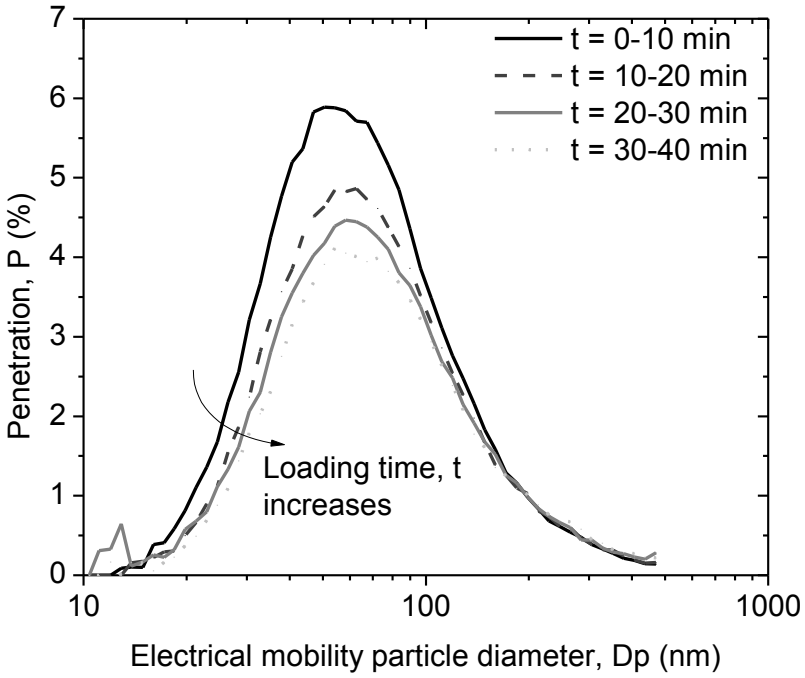

Figure 4.3 Effect of virus aerosol loading on respirator penetration.

Chapter 5: Respirator Testing Using Virus Aerosol: Comparison between Infectivity Penetration and Physical Penetration

5.1 Introduction

Performance of filtering facepiece respirators against airborne viruses is often quantified in two ways. One is infectivity penetration (i.e., the percentage of infectious virus that penetrates through the respirator) and the other is physical penetration (i.e., the percentage of challenge particles/viruses that penetrates through the respirator, regardless of virus infectivity) (Eninger et al. 2008a). From an infection control perspective, measurement of the former, though labor-intensive, provides more valuable information than the latter.

Particle number penetration is the only physical measurement that has been compared with infectivity penetration (Eninger et al. 2008a; Lore et al. 2012; Booth et al. 2013; Gardner et al. 2013; Harnish et al. 2013; Zuo et al. 2013b). As shown in Table 1.2 (Chapter 1), infectivity penetration is consistently determined using particle size-integrated samplers, while the selection of the method used to determine particle number penetration seems to be arbitrary. For example, some researchers chose particle number penetration at sizes representing the nominal virus size (Eninger et al. 2008a; Zuo et al. 2013b) while others used particle number penetration at the most penetrating particle size (Gardner et al. 2013). However, without knowing the size distribution of infectious virus among polydisperse aerosol particles, such comparisons between infectivity and particle

number penetration may be inappropriate (Gardner et al. 2013). Recent studies (Zuo et al. 2013c; Zuo et al. 2014) have shown that for a variety of viruses and nebulizer suspensions, infectious virus distribution generally follows particle volume distribution in the size range of 100-450 nm, which suggests that infectivity penetration may be particle volume-based. In addition, the photometric penetration measured by the current NIOSH standard for respirator certification using photometers is also particle volume-based (Biermann and Bergman 1988; Eninger et al. 2008c; Rengasamy et al. 2011). Therefore, it is of interest to compare infectivity penetration with various physical measurements, particularly particle volume and photometric penetration.

5.2 Methods

Circular flat sheet filter media samples (16 cm diameter) for three models of commercially available respirators were clamped in a pneumatic chuck and evaluated using MS2 bacteriophage in an aerosol tunnel, following a previous protocol (Zuo et al. 2013b). As shown in Figure 5.1, virus was aerosolized by a 6-jet Collison nebulizer at 10 psi from a suspension consisting of virus stock (4.5 mL), 3% (wt/vol) tryptic soy broth (40.5 mL), and antifoam (0.1 mL). Uranine (2 mL, 0.625 g/mL) was also added to the suspension as a fluorescent particle tracer (Zuo et al. 2013c; Zuo et al. 2014). After passing through a diffusion dryer and a Kr-85 charge neutralizer, the generated virus aerosol was mixed with HEPA-filtered room air and used to challenge the respirator filter media sample at 85 LPM. Upstream and downstream aerosol concentrations were measured by a laser photometer (DustTrak II, Model 8530, TSI, Shoreview, MN) for particle light scattering and a scanning mobility particle sizer (SMPS, Model 3034, TSI,

Shoreview, MN) for particle number distribution. In addition, samples were collected through upstream and downstream ports by two 25 mm diameter gelatin filters (SKC, Eighty Four, PA) at 2 LPM for 15 min. These filters were then analyzed by infectivity assay, quantitative RT-PCR, and spectrofluorometry for the amount of infectious virus, viral RNA, and fluorescence collected, respectively, as described earlier (Zuo et al. 2013c; Zuo et al. 2014). After the virus aerosol challenge, the same respirator filter sample was also tested using 1% (wt/vol) NaCl aerosol. Each test was repeated in triplicate using new samples of each model filter media at 10-20% relative humidity and 22-24 ^{o}C.

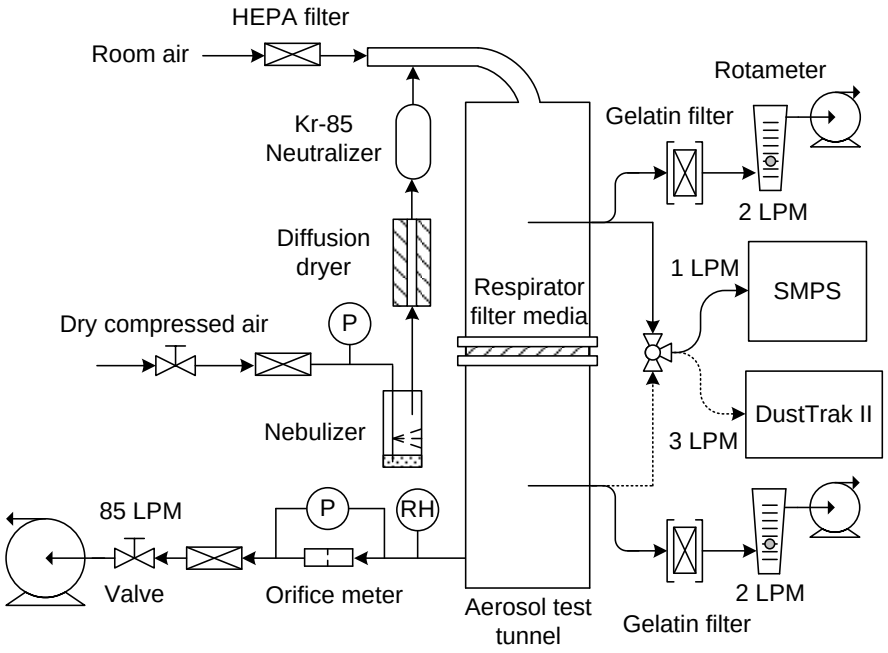

Figure 5.1 Schematic diagram of the experimental setup for respirator testing using virus aerosols.

Penetration was calculated as the concentration ratio downstream to upstream of the respirator filter sample for light scattering, infectious virus, viral RNA, fluorescence, and

particle number. Assuming the amount of fluorescence carried per particle is proportional to the particle volume, the fluorescence penetration represents particle volume penetration. Relative recovery of infectious virus, RR_{IV}, was calculated by comparing the concentration ratio of infectious virus (C_{IV}) to fluorescence (C_F) in the gelatin filter (*gel*) and in the nebulizer suspension (*neb*): $RR_{IV} = (C_{IV,gel}/C_{F,gel})/(C_{IV,neb}/C_{F,neb})$. Relative recovery of total virus, RR_{TV}, was calculated similarly by replacing infectious virus concentration with total virus concentration (C_{TV}) in the above equation: $RR_{TV} = (C_{TV,gel}/C_{F,gel})/(C_{TV,neb}/C_{F,neb})$. Both terms are indicators for the survival of airborne viruses (Zuo et al. 2013c; Zuo et al. 2014).

5.3 Results

Both upstream and downstream particle size distributions of MS2 aerosol were generally lognormal, with a count median diameter (CMD) of 86 nm and a geometric standard deviation (GSD) of 2.0 upstream and a GSD of 1.6 and a CMD of 70, 55, and 59 nm downstream for filter samples used for respirator models A, B, and C, respectively. The highest penetration was found to be between 3 and 6% within a particle size range of 40-60 nm (Figure 5.2), similar to what reported in the literature (Balazy et al. 2006; Eninger et al. 2008a; Eninger et al. 2009b; Zuo et al. 2013b). For all three models, infectivity and viral RNA penetration were closer to fluorescence (particle volume) and photometric penetration than particle number penetration (Table 5.1). However, infectivity penetration was lower than physical penetration and was approximately 1/2 of viral RNA penetration, 1/5 to 1/3 of fluorescence (particle volume) penetration, and 1/10 to 1/5 of photometric penetration. Note that MS2 and NaCl aerosol gave almost identical photometric

penetration (Table 5.1). RR_{IV} was found to be 1.04 ± 0.12 and 0.27 ± 0.06 (n = 9) for upstream and downstream aerosol samples, respectively. RR_{TV} was found to be 0.86 ± 0.19 and 0.43 ± 0.10 (n = 9) for upstream and downstream aerosol samples, respectively.

To better compare the results, fluorescence (particle volume), infectivity, and viral RNA penetration were plotted vs. MS2 photometric penetration for the three models of respirators (Figure 5.3). As expected, there was a good linear correlation (R^2 = 0.95) between fluorescence (particle volume) penetration and photometric penetration. Infectivity and viral RNA penetration were also reasonably correlated with photometric penetration and follow a power-law relationship.

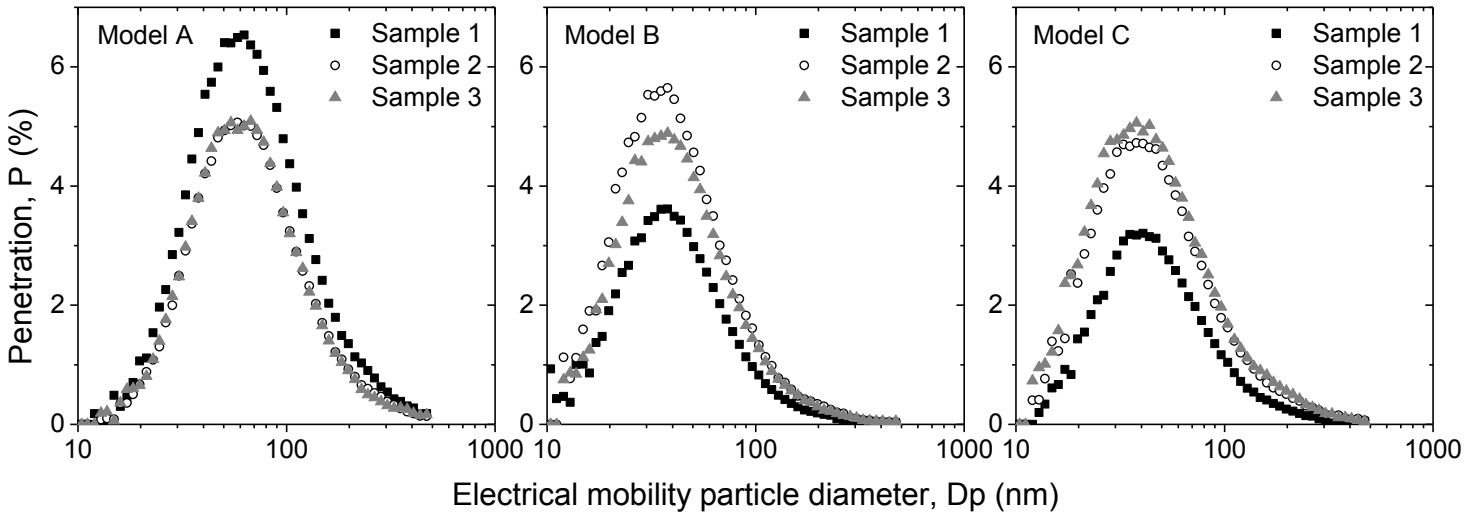

Figure 5.2 Penetration of MS2 bacteriophage aerosol through filter samples used in three models of respirators as a function of particle size.

Table 5.1 Photometric, infectivity, viral RNA, fluorescence, and particle number penetration through different models of respirators.

Respirator Model	Penetration (%)						
	Photometric MS2	Photometric NaCl	Infectivity	Viral RNA	Fluorescence* (Particle volume)	Particle number 10-470 nm	Particle number All sizes**
A	0.23 ± 0.01	0.24 ± 0.08	0.024 ± 0.004	0.051 ± 0.006	0.12 ± 0.01	3.44 ± 0.57	3.40 ± 0.57
B	0.040 ± 0.007	0.040 ± 0.003	0.008 ± 0.003	0.016 ± 0.004	0.029 ± 0.004	2.00 ± 0.42	1.97 ± 0.41
C	0.070 ± 0.015	0.070 ± 0.006	0.014 ± 0.004	0.024 ± 0.008	0.042 ± 0.007	2.09 ± 0.47	2.06 ± 0.47

Note: Data are reported as mean ± one standard deviation (n = 3).
*Fluorescence penetration represents particle volume penetration, assuming that the amount of fluorescence carried by a particle is proportional to the particle volume.
**Assumes lognormal particle size distributions for aerosol samples upstream and downstream of the respirators.

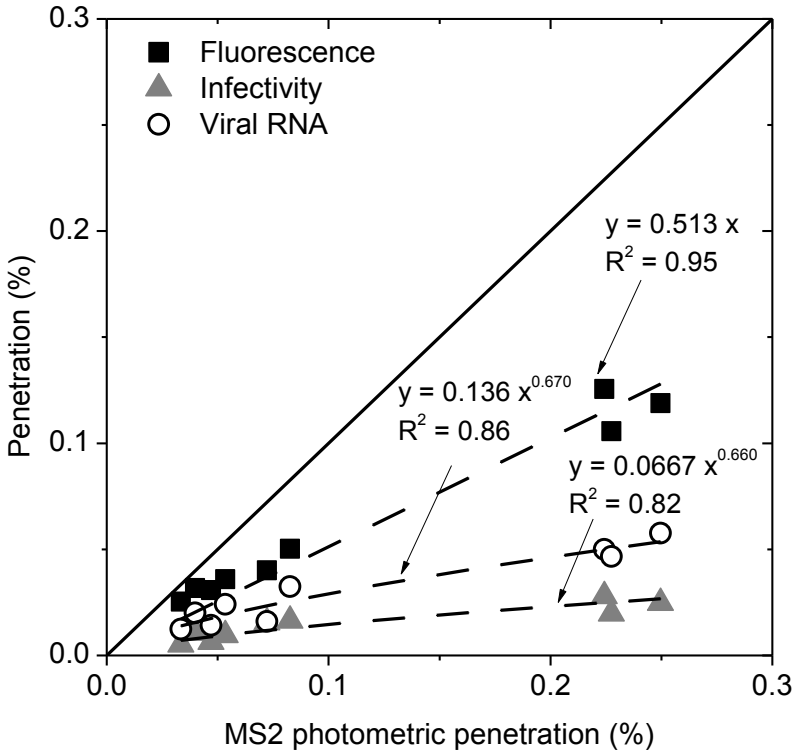

Figure 5.3 Correlations between photometric penetration and fluorescence, infectivity, and viral RNA penetration. The solid line indicates a 1:1 correspondence between the two axes.

5.4 Discussion

The virus content in aerosols produced by Collison nebulizers generally follows a particle volume distribution, not a particle number distribution (Zuo et al. 2013c; Zuo et al. 2014), which made us hypothesize that particle volume and photometric penetration might better represent infectivity penetration through respirators than particle number penetration. The above hypothesis was verified in this study (Table 5.1). However, infectivity penetration was still significantly different from fluorescence and photometric penetration, two particle volume-based penetration measurements. This difference may be partially

explained by the different survivability of airborne MS2 between upstream and downstream aerosol samples. Namely, the virus aerosol upstream better maintained its infectivity and was therefore recovered more efficiently than downstream, as indicated by the higher upstream RR_{IV} and RR_{TV} values than downstream. Aerosol upstream had a larger CMD than downstream, which possibly enhanced virus survival upstream due to the shielding effect offered by large particle size (Zuo et al. 2013c; Zuo et al. 2014). A similar situation existed for viral RNA, but because it is more stable than virus infectivity in air (Zuo et al. 2013c; Zuo et al. 2014), viral RNA penetration was higher than infectivity penetration. Since survival of airborne viruses affects the measured infectivity penetration, the test protocol such as particle size distribution, environmental conditions (Lore et al. 2013), and nebulizer suspension (Zuo et al. 2014) for respirators challenged with virus aerosols should be documented and standardized.

Similar to particle number penetration (Eninger et al. 2008b; Lore et al. 2013), photometric penetration of MS2 was also well predicted by that of NaCl aerosol, indicating that physical penetration of virus aerosols through respirators can be simulated using NaCl aerosol of similar sizes. However, infectivity penetration can only be determined using virus as a challenge aerosol. Infectivity penetration was lower than photometric penetration (Table 5.1), suggesting that the current NIOSH (photometer-based) certification method provides a conservative estimate for respirator performance against virus aerosols.

The correlation been photometric and infectivity penetration has been little studied. In this study, photometer-based and virus infectivity-based tests were found to rank respirators in a similar and predictable manner (Figure 5.3), indicating that the current NIOSH certification method can be used as a quick test to prescreen respirators for hospital and healthcare applications. There has been concern that the current NIOSH certification method may not properly predict the performance of respirators against engineered nanoparticles, because photometers are insensitive to particles smaller than 100 nm (Eninger et al. 2008c; Rengasamy et al. 2011; Rengasamy and Eimer 2012). Although viruses causing common respiratory infection are also small in size (Flint et al. 2004), e.g., 80-120 nm for influenza A virus, 150-300 nm for respiratory syncytial virus, 150-250 nm for parainfluenza virus, and 70-90 nm for adenovirus, they are often aerosolized and carried by respiratory droplets/secretions of larger sizes (Reponen et al. 2005). Field measurements have shown that a majority of virus aerosols in the ambient is micrometer-sized (Blachere et al. 2009; Lindsley et al. 2010b; Yang and Marr 2011), which can be efficiently removed by filtering facepiece respirators.

In general, penetration of virus aerosol through respirators depends on not only the challenge aerosol size distribution, the particle size dependent penetration of the respirator, and how each instrument measures aerosol/virus (Biermann and Bergman 1988; Li et al. 2012), but also virus survival and virus content distribution in the challenge aerosol particles. These parameters have to be fully understood in order to predict infectivity penetration based on physical penetration measurements. For example,

contrary to Collison nebulizers, virus aerosols generated using electrosprays contain almost no residual particles with the virus size distribution similar to particle number distribution (Thomas et al. 2004; Eninger et al. 2009; Jung et al. 2009). Consequently, in this case, the infectivity penetration would be expected to be particle number-based instead of particle volume-based.

Chapter 6: Conclusions and Future Work

6.1 Summary and conclusions

Focusing on the measurement and filtration of laboratory-generated virus aerosols, this dissertation contributes to the field of virus aerosol research in several important ways, helping to better understand and better control the transmission of viral diseases via the aerosol route.

First, a size-segregated aerosol to hydrosol sampling method was developed for airborne viruses (Chapter 2). Compared with traditional samplers, the use of a differential mobility analyzer and a gelatin filter in series provides high size resolution, high physical collection efficiency, high biological collection efficiency, and easy recovery for airborne viruses. This method is particularly useful for sampling laboratory-generated virus aerosol particles at high concentrations in the sub-micrometer size range.

Second, the infectivity and survivability of laboratory-generated viruses were determined and successfully associated with particle size, which has been often overlooked in previous studies. By using the sampling method described above in combination with virus infectivity assay, qRT-PCR analysis, spectrofluorometry, and a scanning mobility particle sizer, virus infectivity, virus survival, and particle concentration were measured as a function of particle size between 100-450 nm for airborne MS2 bacteriophage and three animal viruses (transmissible gastroenteritis virus [TGEV], swine influenza virus

[SIV], and avian influenza virus [AIV]) generated from cell culture media (Chapter 2). Virus aerosol content distributions of the four viruses were found to generally follow their particle volume distributions. Only a small fraction of the particles generated actually carried virus and the amount of virus carried per particle increased with the particle volume. In addition, survival of the three animal viruses in particles that ranged from 300-450 nm was observed to be much higher than that at smaller sizes. These results demonstrate that particle size has a significant effect on infectivity and survivability of airborne viruses, which emphasizes the importance of particle size in the airborne transmission of viral diseases.

Third, the survival of airborne MS2 bacteriophage, which is frequently used as a model virus in laboratory aerosol studies, has been systematically compared with that of the three animal viruses (Chapter 2). Particle size (100-450 nm) had little effect on the survival of airborne MS2, but it played a significant role in the survival of the three animal viruses. In addition, airborne MS2 was found to be inactivated mainly due to the loss of its viral RNA, whereas the decay of three airborne animal viruses generally resulted from the damage of their virus envelop or capsid. Such differences in the airborne behavior between MS2 bacteriophage and TGEV, SIV, and AIV calls into question use of MS2 bacteriophage as a general surrogate for animal and human viruses in aerosol studies.

Fourth, in view of the situation that most laboratory studies generate virus aerosols from artificial nebulizer suspensions, we measured airborne MS2 bacteriophage generated from human saliva, artificial saliva, and cell culture medium (Chapter 3). The survival of MS2 bacteriophage was independent of particle size, but heavily depended on the type of nebulizer suspension, with cell culture medium and artificial saliva giving much higher virus recovery than human saliva. In addition, incubation experiments showed that human saliva exhibited antiviral properties when mixed with TGEV, SIV, and AIV in the liquid phase, which may potentially contribute to the inactivation of these viruses in the aerosol phase. These results highlight the need for using natural nebulizer suspensions such as human saliva and respiratory secretions in order to increase the epidemiological values of laboratory studies.

Fifth, the performance of filtering facepiece respirators was evaluated using human adenovirus and SIV as challenge aerosols, whose characteristics are closer to human pathogenic viruses than the widely used MS2 bacteriophage reported in the literature (Chapter 4). Due to the high concentration of virus-free residual particles generated by Collison nebulizers, particle number penetration was found to be much higher than infectivity penetration, suggesting the former provides a conservative estimate for respirator performance against airborne viruses.

Sixth, in addition to particle number penetration, other forms of physical penetration were measured and compared with infectivity penetration through respirators for the first time

(Chapter 5). Compared with particle number penetration, infectivity penetration was better represented by photometric and particle volume penetration, which indicates that the current (photometer-based) NIOSH certification method can be used to prescreen respirators for infection control applications. Factors such as virus survival (e.g., higher survival upstream of the respirator than downstream) and virus size distribution in the challenge aerosol affect the determination of infectivity penetration, which have to be fully understood in order to predict infectivity penetration based on physical penetration measurement.

6.2 Directions for future work

The study of measuring laboratory generated virus aerosols presented in this dissertation (Chapter 2 and 3) can be improved in a few ways. First, this study used only one level of relative humidity (~50%). Multiple levels of relative humidity and their effect on the survival of airborne viruses should be investigated. Although similar information may be available in the literature (e.g., Table 1.1), relative humidity and the composition of nebulizer suspension may play a combined role in the airborne behavior of airborne viruses. Second, the measurement of laboratory generated virus aerosols can be extended to particle sizes larger than 450 nm. A differential mobility analyzer may only select virus aerosol particles up to 1 μm, but a vibrating orifice aerosol generator can produce monodisperse aerosols of much larger sizes. Survival of airborne viruses in the micrometer size range is an important piece of information to the understanding of the airborne transmission of viral diseases. Third, viruses were sampled right after they were

aerosolized with a residence time in the aerosol phase of only ~1 min. In the future, viruses may be kept airborne for a longer time and several residence time points should be tested so that their inactivation rate can be determined.

This study evaluated only the filtration efficiency of filtering facepiece respirators against virus aerosols (Chapter 4 and 5). Other important issues such as respirator face seal/fit, breathing-like cyclic flow, reuse, virus survival and transfer from respirators, cross-contamination, respirator decontamination, antimicrobial coated filter media, stockpiling, and storage for prolonged time periods should be addressed in the future in order to better assess filtering facepiece respirators as a control measure for airborne transmission of viral diseases.

In addition to improvements closely related to this thesis work, several possible directions for future work in the broad field of virus aerosol research have also been identified.

First, the exact inactivation mechanisms for airborne viruses remain unknown. Although numerous inactivation mechanisms have been proposed and reviewed (De Jong and Winkler 1968; Satter et al. 1987; Cox 1989; Sobsey and Meschke 2003; Yang and Marr 2012), most of them are speculative and qualitative. A method used by Wigginton et al. (2012), which includes virus infectivity assay (to quantify virus infectiousness), virus functionality assays (to quantify the virus capability of binding to cells and injecting its

genome), virus integrity assays (to quantify the integrity of viral genome and its capsid proteins) might be promising to explore the exact virus inactivation mechanisms in the aerosol phase. Other possible methods to consider include virus image analysis by transmission electron microscopy and virus integrity analysis by electrospray (Bacher et al. 2001).

Second, numerical models to describe the survival of airborne viruses are needed. Ideally, the models may collapse virus survival data obtained from different studies along a single curve, governed by parameters such as relative humidity, ambient temperature, nebulizer suspension, etc. However, due to the use of different viruses, nebulizer suspension, samplers, test conditions, the development of such models is difficult and large uncertainty is expected. One example is given by Posada et al. (2010).

Third, in order to quantify the contribution of the aerosol mode to the transmission of viral diseases relative to other modes, field measurement and human subject studies are eventually needed. However, due to the extremely low concentration of virus aerosols in the natural environment and other issues (see Section 1.2), a better virus aerosol sampler is needed. The ideal sampler should operate at a large sampling flow rate with high concentration factor, provide particle size fractionation, and preserve infectivity of the collected virus aerosols. Work is currently underway in the lab to design, prototype, calibrate, and evaluate such a sampler.

Bibliography

Adams, D.J. et al., 1982. Aerosol stability of infectious and potentially infectious reovirus particles. *Applied and Environmental Microbiology*, 44(4), pp.903-8.

Alvarez, A.J., Buttner, M.P. & Stetzenbach, L.D., 1995. PCR for bioaerosol monitoring : sensitivity and environmental interference. *Applied and Environmental Microbiology*, 61(10), pp.3639-3644.

Agranovski, I.E. et al., 2004. Inactivation of viruses in bubbling processes utilized for personal bioaerosol monitoring. *Applied and Environmental Microbiology*, 70(12), pp.6963-6967.

Agranovski, I.E. et al., 2005. Long-Term sampling of viable airborne viruses. *Aerosol Science and Technology*, 39(9), pp.912–918.

Aiello, A.E. et al., 2010. Research findings from nonpharmaceutical intervention studies for pandemic influenza and current gaps in the research. *American Journal of Infection Control*, 38(4), pp.251–8.

Akers, T.G. & Hatch, M.T., 1968. Survival of a picornavirus and its infectious ribonucleic acid after aerosolization. *Applied Microbiology*, 16(11), pp.1811–3.

Alexandersen, S., Brotherhood, I. & Donaldson, A.I., 2002. Natural aerosol transmission of foot-and-mouth disease virus to pigs: minimal infectious dose for strain O1 Lausanne. *Epidemiology and Infection*, 128(2), pp.301-12.

Alford, R.H. et al., 1966. Human influenza resulting from aerosol inhalation. *Proceedings of the Society for Experimental Biology and Medicine*, 122, pp.800–804.

Aller, J. et al., 2005. The sea surface microlayer as a source of viral and bacterial enrichment in marine aerosols. *Journal of Aerosol Science*, 36(5-6), pp.801-812.

Appert, J. et al., 2012. Influence of suspending liquid, impactor type, and substrate on size-selective sampling of MS2 and adenovirus aerosols. *Aerosol Science and Technology*, 46(3), pp.249-257.

ASTM, 2011. Standard test method for evaluation of effectiveness of decontamination procedures for surfaces when challenged with droplets containing human pathogenic viruses. ASTM Standard E2721 – 10.

ASTM, 2011. Standard test method for evaluation of effectiveness of decontamination procedures for air-permeable materials when challenged with biological aerosols containing human pathogenic viruses. ASTM Standard E2720 – 10.

Bacher, G. et al., 2001. Charge-reduced nano electrospray ionization combined with differential mobility analysis of peptides, proteins, glycoproteins, noncovalent protein complexes and viruses. *Journal of Mass Spectrometry : JMS*, 36(9), pp.1038–52.

Balazy, A. et al., 2006. Do N95 respirators provide 95% protection level against airborne viruses, and how adequate are surgical masks? *American Journal of Infection Control*, 34(2), pp.51–7.

Bansil, R. & Turner, B.S., 2006. Mucin structure, aggregation, physiological functions and biomedical applications. *Current Opinion in Colloid & Interface Science*, 11(2-3), pp.164–170.

Barker, J. & Jones, M.V., 2005. The potential spread of infection caused by aerosol contamination of surfaces after flushing a domestic toilet. *Journal of Applied Microbiology*, 99(2), pp.339-47.

Barlow, D.F. and Donaldson, A.I. (1973) Comparison of the aerosol stabilities of foot-and- mouth disease virus suspended in cell culture fluid or natural fluids. *Journal of General Virology*, 20, pp.311- 318.

Blachere, F.M. et al., 2009. Measurement of airborne influenza virus in a hospital emergency department. *Clinical Infectious Diseases*, 48(4), pp.438–40.

Benbough, J.E., 1971. Some factors affecting the survival of airborne viruses. *Journal of General Virology*, 10(3), pp.209-20.

Berendt, R.F.& Dorsey, E.L., 1971. Effect of simulated solar radiation and sodium fluorescein on the recovery of Venezuelan equine encephalomyelitis virus from aerosols. *Applied Microbiology*, 21, pp.447–450.

Biermann, A. & Bergman, W., 1988. Filter penetration measurements using a condensation nuclei counter and an aerosol photometer. *Journal of Aerosol Science*, 19(4), pp.471–483.

Booth, C.M. et al., 2013. Effectiveness of surgical masks against influenza bioaerosols. *Journal of Hospital Infection*, 84(1), pp.22–6.

Borkow, G. et al., 2010. A novel anti-influenza copper oxide containing

respiratory face mask. *PLoS ONE,* 5(6), p.e11295.

Bourgueil, E. et al., 1992. Air sampling procedure for evaluation of viral excretion level by vaccinated pigs infected with Aujeszky's disease (pseudorabies) virus. *Research in Veterinary Science*, 52(2), pp.182-186.

Brankston, G. et al., 2007. Transmission of influenza A in human beings. *The Lancet Infectious Diseases*, 7(4), pp.257-265.

Buckland, F.E. & Tyrrell, D.A., 1962. Loss of infectivity on drying various viruses. *Nature*, 195, pp.1063–1064.

Burton, N.C., Grinshpun, S.A., & Reponen, T., 2007. Physical collection efficiency of filter materials for bacteria and viruses. *Annals of Occupational Hygiene,* 51(2), pp.143–51.

Carducci, A, Arrighi, S. & Ruschi, A, 1995. Detection of coliphages and enteroviruses in sewage and aerosol from an activated sludge wastewater treatment plant. *Letters in Applied Microbiology*, 21(3), pp.207-9.

Casanova, L.M. et al., 2010. Effects of air temperature and relative humidity on coronavirus survival on surfaces. *Applied and Environmental Microbiology*, 76(9), pp.2712–7.

CDC, 2009. Interim Recommendations for Facemask and Respirator Use to Reduce 2009 Influenza A (H1N1) Virus Transmission. Available at http://www.cdc.gov/h1n1flu/masks.htm

Chan, C., Kwok, C. & Chow, A., 1997. Study of hygroscopic properties of aqueous mixtures of disodium fluorescein and sodium chloride using an electrodynamic balance. *Pharmaceutical Research*, 14, pp.1171–1175.

Chan, K.H. et al., 2011. The effects of temperature and relative humidity on the viability of the SARS coronavirus. *Advances in Virology*, 2011, pp.1–7.

Chao, C. et al., 2009. Characterization of expiration air jets and droplet size distributions immediately at the mouth opening. *Journal of Aerosol Science*, 40(2), pp.122-133.

Cox, C.S. & Wathes C.M., 1995. Bioaerosol Handbook. New York, CRC Press.

Cox, C. S. (1989) Airborne bacteria and viruses. *Science Progress Oxford,* 73, pp.469-500.

Davis, G.W. et al., 1971. Effect of relative humidity on dynamic aerosols of adenovirus 12. *Applied Microbiology*, 21(4), pp.676–9.

De Jong, J.C. & Winkler, K.C., 1968. The inactivation of poliovirus in aerosols. *Journal of Hygiene*, 66(4), pp.557–65.

De Jong, J.C., Harmsen, M. & Trouwborst, T., 1975. Factors in the inactivation of Encephalomyocarditis virus in aerosols. *Infection and Immunity*, 12(1), pp.29–35.

Detmer, S.E. et al., 2011. Detection of influenza a virus in porcine oral fluid samples. *Journal of Veterinary Diagnostic Investigation*, 23(2), pp.241–247.

DHHS, 1995. 42 CFR 84 Respiratory protective devices; Final rules and notice. Federal Register 60:110. Public Health Service. Morgantown, WV: Department of Health and Human Services (DHHS)

Douglas, R.G., 1975. Influenza in man. The Influenza Viruses and Influenza. Kilbourne E.D. ed, Academic Press, New York.

Donaldson, A.I., 1972. The influence of relative humidity on the aerosol stability of different strains of foot-and-mouth disease virus suspended in saliva. *Journal of General Virology*, 15, pp.25–33.

Donaldson, A.I. & Alexandersen, S., 2002. Predicting the spread of foot and mouth disease by airborne virus. *Revue scientifique et technique (International Office of Epizootics)*, 21(3), pp.569-75.

Dubovi, E.J. & Akers, T.G., 1970. Airborne stability of tailless bacterial viruses S-13 and MS-2. *Applied Microbiology*, 19(4), pp.624–628.

Ehrlich, R. & Miller, S., 1971. Effect of relative humidity and temperature on airborne Venezuelan equine encephalitis virus. *Applied Microbiology*, 22(2), pp.194-9.

Elazhary, M.A. & Derbyshire, J.B., 1979a. Aerosol stability of bovine adenovirus type 3. *Canadian Journal of Comparative Medicine*, 43, pp.305–312.

Elazhary, M.A. & Derbyshire, J.B., 1979b. Aerosol stability of bovine parainfluenza type 3 virus. *Canadian Journal of Comparative Medicine. Revue canadienne de médecine comparée*, 43(3), pp.295–304.

Elazhary, M.A. & Derbyshire, J.B., 1979c. Effect of temperature, relative humidity and medium on the aerosol stability of infectious bovine rhinotracheitis virus. *Canadian Journal of Comparative Medicine*, 43(2), pp.158–67.

Eninger, R.M. et al., 2008a. Differentiating between physical and viable penetrations when challenging respirator filters with bioaerosols. *CLEAN - Soil, Air, Water*, 36(7), pp.615–621.

Eninger, R.M. et al., 2008b. Filter performance of N99 and N95 facepiece respirators against viruses and ultrafine particles. A*nnals of Occupational Hygiene*, 52(5), pp.385–96.

Eninger, R.M. et al., 2008c. What does respirator certification tell us about filtration of ultrafine particles? *Journal of Occupational and Environmental Hygiene*, 5(5), pp.286–95.

Eninger, R.M. et al., 2009. Electrospray versus nebulization for aerosolization and filter testing with bacteriophage particles. *Aerosol Science and Technology*, 43(4), pp.298–304.

Fabian, P. et al., 2008. Influenza virus in human exhaled breath: an observational study. *PloS one*, 3(7), p.e2691.

Fabian, P. et al., 2009. Airborne influenza virus detection with four aerosol samplers using molecular and infectivity assays: considerations for a new infectious virus aerosol sampler. *Indoor Air*, 19(5), pp.433–41.

Fabian, P. et al., 2011. Origin of exhaled breath particles from healthy and human rhinovirus-infected subjects. *Journal of Aerosol Medicine and Pulmonary Drug Delivery*, 24(3), pp.137-47.

Flint, J.S. et al., 2004. Principles of Virology: Molecular Biology, Pathogenesis, and Control. Washington DC, ASM Press.

Gardner, P.D. et al., 2013. Viable viral efficiency of N95 and P100 respirator filters at constant and cyclic flow. *Journal of Occupational and Environmental Hygiene*, 10(10), pp.564–72.

Gerone, P.J. et al., 1966. Assessment of experimental and natural viral aerosols. *Bacteriological Reviews*, 30(3), pp.576–88.

Gloster, J. & Alexandersen, S., 2004. New Directions : Airborne Transmission of Foot-and-Mouth Disease Virus. *Atmospheric Environment*, 38, pp.503-505.

Gloster, J. et al., 2005. Re-assessing the likelihood of airborne spread of foot-and-mouth disease at the start of the 1967-1968 UK foot-and-mouth disease epidemic. *Epidemiology and Infection*, 133(5), pp.767-83.

Gloster, J. et al., 2007. Foot-and-mouth disease - quantification and size distribution of airborne particles emitted by healthy and infected pigs. *Veterinary Journal*, 174(1), pp.42-53.

Gralton, J. et al., 2011. The role of particle size in aerosolised pathogen transmission: a review. *Journal of Infection*, 62(1), pp.1–13.

Griffiths, W.D. & DeCosemo, G.A.L., 1994. The assessment of bioaerosols: a critical review. *Journal of Aerosol Science*, 25(8), pp.1425–1458.

Grinshpun, S. A. et al., 1997. Effect of impaction, bounce and reaerosolization on the collection efficiency of impingers. *Aerosol Science and Technology*, 26(4), pp.326-342.

Grinshpun, S.A. et al., 2007. Control of aerosol contaminants in indoor air: combining the particle concentration reduction with microbial inactivation. *Environmental Science and Technology*, 41(2), pp.606–12.

Hamory, B.H. et al., 1972. Characterization of the infectious unit for man of two respiratory viruses. *Proceedings of the Society for Experimental Biology and Medicine*, 139, pp.890–893.

Harnish, D.A. et al., 2013. Challenge of N95 filtering facepiece respirators with viable H1N1 influenza aerosols. *Infection Control and Hospital Epidemiology* , 34(5), pp.494–9.

Harper, G.J., 1961. Airborne micro-organisms: survival tests with four viruses. *Journal of Hygiene*, 59, pp.479–86.

Harper, G.J., 1963. The influence of environment on the survival of airborne virus particles in the laboratory. *Archiv für die gesamte Virusforschung*, 13, pp.64–71.

Haslbeck, K. et al., 2010. Submicron droplet formation in the human lung. *Journal of Aerosol Science*, 41(5), pp.429–438.

Hemmes, J.H., Winkler, K.C. & Kool, S.M., 1960. Virus survival as a seasonal factor in influenza and poliomyelitis. *Nature*, 188, pp.430–431.

Hietala, S.K. et al., 2005. Environmental air sampling to detect exotic Newcastle disease virus in two California commercial poultry flocks. *Journal of Veterinary Diagnostic Investigation*, 17(2), pp.198-200.

Hogan, C.J. et al., 2005. Sampling methodologies and dosage assessment techniques for submicrometre and ultrafine virus aerosol particles. *Journal of Applied Microbiology*, 99(6), pp.1422-34.

Hogan, C., Lee, M.-H. & Biswas, P., 2004. Capture of viral particles in soft x-ray-enhanced corona systems: charge distribution and transport characteristics. *Aerosol Science and Technology*, 38(5), pp.475–486.

Holmgren, H. et al., 2010. Size distribution of exhaled particles in the range from 0.01 to 2.0μm. *Journal of Aerosol Science*, 41(5), pp.439–446.

Hood, A.M., 1963. Infectivity of influenza virus aerosols. *Journal of Hygiene*, 61, pp.331–5.

Hornung R.W. & Reed L.D., 1990. Estimation of average concentration in the presence of nondetectable values. *Applied Occupational Environmental Hyg*iene, 5:pp.46–51.

Humphrey, S.P. & Williamson, R.T., 2001. A review of saliva: normal composition, flow, and function. *The Journal of Prosthetic Dentistry*, 85(2), pp.162–9.

Huynh, K.N. et al., 2008. A new method for sampling and detection of exhaled respiratory virus aerosols. *Clinical Infectious Diseases*, 46(1), pp.93-5.

Ijaz, M.K. et al., 1985. Survival characteristics of airborne human coronavirus 229E. *Journal of General Virology*, 66 (12), pp.2743-8.

Ijaz, M.K. et al., 1987. Development of methods to study the survival of airborne viruses. *Journal of Virological Methods*, 18(2-3), pp.87-106.

Jackwood, M.W. 2006. The relationship of severe acute respiratory syndrome coronavirus with avian and other coronaviruses. *Avian Diseases*, 50:pp.315-320.

Jaschhof, H., 1992. Sampling virus aerosols using the gelatin membrane filter. *Bio Tech*, 6, (English translation).

Johnson, G.R. & Morawska, L., 2009. The Mechanism of Breath Aerosol Formation. *Journal of Aerosol Medicine*, 22(3), pp.229-237.

Johnson, G.R. et al., 2011. Modality of human expired aerosol size distributions. *Journal of Aerosol Science*, 42(12), pp.839-851.

Jung, J.H., Lee, J.E. & Kim, S.S., 2009. Generation of nonagglomerated airborne bacteriophage particles using an electrospray technique. *Analytical Chemistry*, 81(8), pp.2985–90.

Karber, G., 1931. Fifty percent endpoint calculation. *Arch. Exp. Path. Pharmak.*, 162, pp.480-487.

Karim, Y.G. et al., 1985. Effect of relative humidity on the airborne survival of rhinovirus-14. *Canadian Journal of Microbiology*, 31(11), pp.1058–1061.

Kim, S.W. et al., 2007. Effects of humidity and other factors on the generation and sampling of a coronavirus aerosol. *Aerobiologia*, 23(4), pp.239-248.

Lamb, R.A. & Choppin, P.W., 1983. The gene structure and replication of influenza virus. *Annual Review of Biochemistry*, 52, pp.467–506.

Lee, S.A., Grinshpun, S.A. & Reponen, T., 2008. Respiratory performance offered by N95 respirators and surgical masks: human subject evaluation with NaCl aerosol representing bacterial and viral particle size range. *Annuals of Occupational Hygiene*, 52(3), pp.177-85.

Lee, J. H., 2009. *Assessment of the performance of iodine-treated biocidal filters and characterization of virus aerosols*. Ph.D. Thesis, University of Florida-Gainesville.

Lester, W., 1948. The influence of relative humidity on the infectivity of air-borne influenza A virus (PR8 strain). *Journal of Experimental Medicine*, 88(3), pp.361–368.

Li, L. et al., 2012. Evaluation of filter media for particle number , surface area and mass penetrations. *Annals of Occupational Hygiene*, 56(5), pp.581–594.

Li, X. et al., 2008. An in vitro model to evaluate virus aerosol characteristics using a GFP-expressing adenovirus. *Journal of Medical Microbiology*, 57(11), pp.1335–9.

Lin, X. et al., 1997. Effect of sampling time on the collection efficiency of all-glass impingers. American Industrial Hygiene Association Journal, 58(7), pp.480-488.

Lindsley, W.G. et al., 2010a. Measurements of airborne influenza virus in aerosol particles from human coughs. *PLoS ONE*, 5(11), p.e15100.

Lindsley, W.G. et al., 2010b. Distribution of airborne influenza virus and respiratory syncytial virus in an urgent care medical clinic. *Clinical Infectious Diseases*, 50(5), pp.693-8.

Loosli, C.G. et al., 1943. Experimental air-borne influenza infection. I. Influence of humidity on survival of virus in air. *Proceedings of the Society for Experimental Biology and Medicine*, 53, pp.205–206.

Lore, M.B. et al., 2012. Performance of conventional and antimicrobial-treated filtering facepiece respirators challenged with biological aerosols. *Journal of Occupational and Environmental Hygiene*, 9(2), pp.69–80.

Mackay, I.M., Arden, K.E. & Nitsche, A., 2002. Real-time PCR in virology. *Nucleic Acids Research*, 30(6), pp.1292-305.

Mackay, I.M., 2004. Real-time PCR in the microbiology laboratory. *Clinical Microbiology and Infection*, 10(3), pp.190-212.

Malamud, D. et al., 2011. Antiviral activities in human saliva. *Advances in Dental Research*, 23(1), pp.34–7.

Marks, P.J. et al., 2003. A school outbreak of Norwalk-like virus: evidence for airborne transmission. *Epidemiology and Infection*, 131(1), pp.727-736.

Marthi, B. et al., 1990. Survival of bacteria during aerosolization. *Applied Environmental Microbiology*, 56(11), pp.3463-3467.

May, K., 1973. The Collison nebulizer, description, performance and applications. *Journal of Aerosol Science*, 4, pp.235-243.

Mayhew, C.J., Zimmerman, W.D. & Hahon, N., 1968. Assessment of aerosol stability of yellow fever virus by fluorescent-cell counting. *Applied Microbiology*, 16(2), pp.263-6.

McDevitt, J.J. et al., 2013. Development and performance evaluation of an exhaled-breath bioaerosol collector for influenza virus. *Aerosol Science and Technology*, 47(4), pp.444–451.

McGarrity, G.J. & Dion, A.S., 1978. Detection of airborne polyoma virus. *Journal of Hygiene*, 81(1), pp.9-13.

Miller, W.S. & Artenstein, M.S., 1967. Aerosol stability of three acute respiratory disease viruses. *Proceedings of The Society for Experimental Biology and Medicine*, 125, pp.222–227.

Moore, B.E., Sagik, B.P. & Sorber, C. a, 1979. Procedure for the recovery of airborne human enteric viruses during spray irrigation of treated wastewater. *Applied and Environmental Microbiology*, 38(4), pp.688-93.

Morawska, L., 2006. Droplet fate in indoor environments , or can we prevent the spread of infection? *Indoor Air*, 16, pp.335-347.

Morawska, L. et al., 2009. Size distribution and sites of origin of droplets expelled from the human respiratory tract during expiratory activities. *Journal of Aerosol Science*, 40, pp.256-269.

Navazesh, M., 1993. Methods for collecting saliva. *Annals of the New York Academy of Sciences*, 694, pp.72–77.

O'Connell, K.P. et al., 2006. Real-Time fluorogenic reverse transcription-PCR assays for detection of bacteriophage MS2. *Applied and Environmental Microbiology*, 72(1), pp.478–483.

Otake, S., et al., 2002. Evaluation of aerosol transmission of porcine reproductive and respiratory syndrome virus under controlled field conditions. *Veterinary Record*, 150(26), pp.804-808.

Peirson, S.N., Butler, J.N. & Foster, R.G., 2003. Experimental validation of novel and conventional approaches to quantitative real-time PCR data analysis. *Nucleic Acids Research*, 31(14), p.73e–73.

Posada, J.A, Redrow, J. & Celik, I., 2010. A mathematical model for predicting the viability of airborne viruses. *Journal of Virological Methods*, 164(1-2), pp.88–95.

Pyankov, O. V., Pyankova, O.G. & Agranovski, I.E., 2012. Inactivation of airborne influenza virus in the ambient air. *Journal of Aerosol Science*, 53, pp.21–28.

Richardson A. & Hofacre K., 2010. Comparison of filtration efficiency of a N95 filtering facepiece respirator and surgical mask against viral aerosols. *American Journal of Infection Control*,38(5), pp.e20.

Reineking, A. & Porstendörfer, J., 1986. Measurements of particle loss functions in a differential mobility analyzer (TSI, Model 3071) for different flow rates. *Aerosol Science and Technology*, 5(4), pp.483–486.

Rengasamy, S., Miller, A. & Eimer, B.C., 2011. Evaluation of the filtration performance of NIOSH-approved N95 filtering facepiece respirators by photometric and number-based test methods. *Journal of Occupational and Environmental Hygiene*, 8(1), pp.23–30.

Rengasamy, S. & Eimer, B.C., 2012. Nanoparticle filtration performance of NIOSH-certified particulate air-purifying filtering facepiece respirators: evaluation by light scattering photometric and particle number-based test methods. *Journal of Occupational and Environmental Hygiene*, 9(2), pp.99–109.

Reponen, T. et al., 1997. Techniques for dispersion of microorganisms into air. *Aerosol Science and Technology*, 27(3), pp.405–421.

Reponen T. et al., 2005. Biological Particle Sampling, in Aerosol Measurement: Principles, Techniques and Applications 2nd Edition, Baron, P., & Willeke, K., Eds., New York, van Nostrand Reinhold.

Riemenschneider, L. et al., 2010. Characterization of reaerosolization from impingers in an effort to improve airborne virus sampling. *Journal of Applied Microbiology*, 108(1), pp.315-24.

Robinson, J. et al., 2008. Use of throat swab or saliva specimens for detection of respiratory viruses in children. *Clinical Infectious Diseases*, 46, pp.e61–64.

Rykke, M. et al., 1995. Micelle-like structures in human saliva. *Colloids and Surfaces B*, 4, pp.33–44.

Sattar, S., Ijaz, M.K. & Gerba, C., 1987. Spread of viral infections by aerosols. *Critical Reviews in Environmental Science and Technology*, 17(2), pp.89-131.

Schaffer, F.L., Soergel, M.E. & Straube, D.C., 1976. Survival of airborne influenza virus : effects of propagating host , relative humidity , and composition of spray fluids. *Archives of Virology*, 273(51), pp.263-273.

Schipper, R.G., Silletti, E. & Vingerhoeds, M.H., 2007. Saliva as research material: biochemical, physicochemical and practical aspects. *Archives of Oral Biology*, 52(12), pp.1114–35.

Schoenbaum, M. et al., 1990. Survival of pseudorabies virus in aerosol. *American Journal of Veterinary Research*, 51(3), pp.331–333.

Scott, G.H. & Sydiskis, R.J., 1976. Responses of mice immunized with influenza virus by aerosol and parenteral routes. *Infection and Immunity*, 13(3), pp.696–703.

Shechmeister, I.L., 1950. Studies on the experimental epidemiology of respiratory infections : III . Certain aspects of the behavior of type A influenza virus as an air-borne cloud. *Journal of Infectious Diseases*, 87(2), pp.128–132.

Sinclair, R.G. et al., 2012. Criteria for selection of surrogates used to study the fate and control of pathogens in the environment. *Applied and Environmental Microbiology*, 78(6), pp.1969–77.

Slots, J. & Slots, H., 2011. Bacterial and viral pathogens in saliva: disease relationship and infectious risk. *Periodontology 2000*, 55(1), pp.48–69.

Snider, D.E., Bridges, C.B. & Weissman, D.N., 2010. *Meeting Summary of the Workshop "Approaches to Better Understand Human Influenza Transmission,"* Available at http://www.cdc.gov/influenzatransmissionworkshop2010/pdf/Influenza_Transmission_Workshop_Summary_508.pdf.

Soares, R. V et al., 2004. Salivary micelles: identification of complexes containing MG2, sIgA, lactoferrin, amylase, glycosylated proline-rich protein and lysozyme. *Archives of Oral Biology*, 49(5), pp.337–43.

Sobsey, M.D., and Meschke, J.S., 2003. Virus survival in the environment with special attention to survival in sewage droplets and other environmental media of fecal or respiratory origin. Report for the World Health Organization, Geneva, Switzerland.

Songer, J.R., 1967. Influence of relative humidity on the survival of some airborne viruses. *Applied Microbiology*, 15(1), pp.35-42.

Spackman E., et al., 2002. Development of a real-time reverse transcriptase PCR assay for type A influenza virus and the avian H5 and H7 hemagglutinin subtypes. *Journal of Clinical Microbiology*, 40:3256–3260.

Srikanth, P., Sudharsanam, S. & Steinberg, R., 2008. Bio-aerosols in indoor environment: composition, health effects and analysis. *Indian Journal of Medical Microbiology*, 26(4), pp.302–12.

Stelzer-Braid, S. et al., 2009. Exhalation of respiratory viruses by breathing , coughing , and talking. *Journal of Medical Virology*, 81, pp.1674-1679.

Tajima, M., 1970. Morphology of transmissible gastroenteritis virus of pigs. *Archives of Virology*, 29(1), pp.105–108.

Tang, J.W., 2009. The effect of environmental parameters on the survival of airborne infectious agents. *Journal of the Royal Society, Interface*, pp.S737-46.

Tellier, R., 2006. Review of aerosol transmission of influenza A virus. *Emerging Infectious Diseases*, 12(11), pp.1657-1662.

Tellier, R., 2009. Aerosol transmission of influenza A virus: a review of new studies. *Journal of the Royal Society, Interface*, 6, pp.S783-90.

Teunis, P.F.M. et al., 2005. Mixed plaques statistical evidence how plaque assays may underestimate virus concentrations. *Water Research*, 39, pp.4240–4250.

Thomas, G., 1970. Sampling rabbit pox aerosols of natural origin. *Journal of Hygiene*, 68(04), p.511.

Thompson, S.S. & Yates, M. V, 1999. Bacteriophage inactivation at the air-water-solid interface in dynamic batch systems. *Applied Environmental Microbiology*, 65(3), pp.1186–1190.

Trouwborst, T. and De Jong, J. C., 1973. Interaction of some factors in mechanism of inactivation of bacteriophage-MS2 in aerosols. *Applied Microbiology*, 26 (3), pp.252-257.

Trouwborst, T. et al., 1974. Inactivation of some bacterial and animal viruses by exposure to liquid-air interfaces. *Journal of General Virology*, 24(1), pp.155-65.

Trouwborst, T. & Kuyper, S., 1974. Inactivation of bacteriophage T3 in aerosols: effect of prehumidification on survival after spraying from solutions of salt, peptone, and saliva. *Applied Microbiology*, 27(5), pp.834–7.

Tseng, C.C. & Li, C.S., 2005a. Collection efficiencies of aerosol samplers for virus-containing aerosols. *Journal of Aerosol Science*, 36, pp.593–607.

Tseng, C.C. & Li, C.S., 2005b. Inactivation of virus-containing aerosols by ultraviolet germicidal irradiation. *Aerosol Science and Technology*, 39(12), pp.1136–1142.

Tyrrell, D.A., 1967. The spread of viruses of the respiratory tract by the airborne route. *Symposium of the Society for General Microbiology*, 17, pp.286–306.

U.S. Environmental Protection Agency. 2001. Method 1601: male specific (F1) and somatic coliphage in water by two-step enrichment procedure.

Valegard, K. et al., 1990. The three-dimensional structure of the bacterial virus MS2. *Nature*, 345, pp.36–41.

Verreault, D., Moineau, S. & Duchaine, C., 2008. Methods for sampling of airborne viruses. *Microbiology and Molecular Biology Reviews*, 72(3), pp.413-44.

Wang, W., Chen, S. & Liu, I., 2004. Detection of SARS-associated coronavirus in throat wash and saliva in early diagnosis. *Emerging Infectious Diseases*, 10(7), pp.1213–1219.

Wang, Z. et al., 1999. Survival of bacteria on respirator filters. *Aerosol Science and Technology*, 30(3), pp.300-308.

Warren, J.C. & Hatch, M.T., 1969. Survival of T3 coliphage in varied extracellular environments. I. Viability of the coliphage during storage and in aerosols. *Applied Microbiology*, 17(2), pp.256-61.

Weber, T.P. & Stilianakis, N.I., 2008. Inactivation of influenza A viruses in the environment and modes of transmission A critical review. *Journal of Infection*, 57, pp.361-373.

Wei, Z. et al., 2007. Biophysical characterization of influenza virus subpopulations using field flow fractionation and multiangle light scattering: correlation of particle counts, size distribution and infectivity. *Journal of Virological Methods*, 144(1-2), pp.122–32.

Wiedensohler, A., 1988. An approximation of the bipolar charge distribution for particles in the submicron size range. *Journal of Aerosol Science*, 19(3), pp.387–389.

Wigginton, K.R. et al., 2012. Virus inactivation mechanisms: impact of disinfectants on virus function and structural integrity. *Environmental Science and Technology*, 46(21), pp.12069–78.

Winkler, W.G., 1968. Airborne rabies virus isolation. *Wildlife Disease Association*, 4, pp.37-40.

White, M.R. et al., 2009. Multiple components contribute to ability of saliva to inhibit influenza viruses. *Oral Microbiology and Immunology*, 24(1), pp.18–24.

Woo, M.H., 2009. Improving Protection Against Viral Aerosols through Development of Novel Decontamination Methods and Characterization of Viral Aerosol. Ph.D. Thesis, University of Florida-Gainesville.

Woo, M.-H. et al., 2010. Method for contamination of filtering facepiece respirators by deposition of MS2 viral aerosols. *Journal of Aerosol Science*, 41(10), pp.944–952.

Woo, M.H. et al., 2012. Effects of relative humidity and spraying medium on UV decontamination of filters loaded with viral aerosols. *Applied and Environmental Microbiology*, 78(16), pp.5781–7.

Xu, Z. et al., 2011. Bioaerosol science, technology, and engineering: past, present, and future. *Aerosol Science and Technology*, 45(11), pp.1337–1349.

Yang, W., Elankumaran, S. & Marr, L.C., 2011. Concentrations and size distributions of airborne influenza A viruses measured indoors at a health centre, a day-care centre and on aeroplanes. *Journal of the Royal Society, Interface*, 8(61), pp.1176–1184.

Yang, W. & Marr, L.C., 2012. Mechanisms by which ambient humidity may affect viruses in aerosols. *Applied and Environmental Microbiology*, 78(19), pp.6781–8.

Yu, I.T. et al. 2004. Evidence of airborne transmission of the severe acute respiratory syndrome virus. *New England Journal of Medicine*, 350(17), pp.1731-1739.

Yu, L. et al., 2009. Effects of different sampling solutions on the survival of bacteriophages in bubbling aeration. *Aerobiologia*, 26(1), pp.75-82.

Zuo, Z. et al., 2013a. Comparison of spike and aerosol challenge tests for the recovery of viable influenza virus from non-woven fabrics. *Influenza and Other Respiratory Viruses*, 7(5), pp.637–644.

Zuo, Z., Kuehn, T.H. & Pui, D.Y.H., 2013b. Performance evaluation of filtering facepiece respirators using virus aerosols. *American Journal of Infection Control*, 41(1), pp.80–82.

Zuo, Z. et al., 2013c. Association of airborne virus infectivity and survivability with its carrier particle size. *Aerosol Science and Technology*, 47(4), pp.373–382.

Zuo, Z. et al., 2014. Survival of airborne MS2 bacteriophage generated from human saliva, artificial saliva, and cell culture medium. *Applied and Environmental Microbiology*, 80(9), pp.2796-2803.

Appendix

This appendix contains copies of copyright permissions granted by the owners of the journals where the work is published.

Order Completed

Thank you very much for your order.

This is a License Agreement between Zhili Zuo ("You") and Elsevier ("Elsevier"). The license consists of your order details, the terms and conditions provided by Elsevier, and the payment terms and conditions.

Get the printable license.

License Number	3418921256159
License date	Jun 30, 2014
Licensed content publisher	Elsevier
Licensed content publication	American Journal of Infection Control
Licensed content title	Performance evaluation of filtering facepiece respirators using virus aerosols
Licensed content author	Zhili Zuo,Thomas H. Kuehn,David Y.H. Pui
Licensed content date	January 2013
Licensed content volume number	41
Licensed content issue number	1
Number of pages	3
Type of Use	reuse in a thesis/dissertation
Portion	full article
Format	both print and electronic
Are you the author of this Elsevier article?	Yes
Will you be translating?	No
Title of your thesis/dissertation	Measurement and Filtration of Virus Aerosols
Expected completion date	Jul 2014
Estimated size (number of pages)	130
Elsevier VAT number	GB 494 6272 12
Permissions price	0.00 USD
VAT/Local Sales Tax	0.00 USD / 0.00 GBP
Total	0.00 USD

ORDER MORE... CLOSE WINDOW